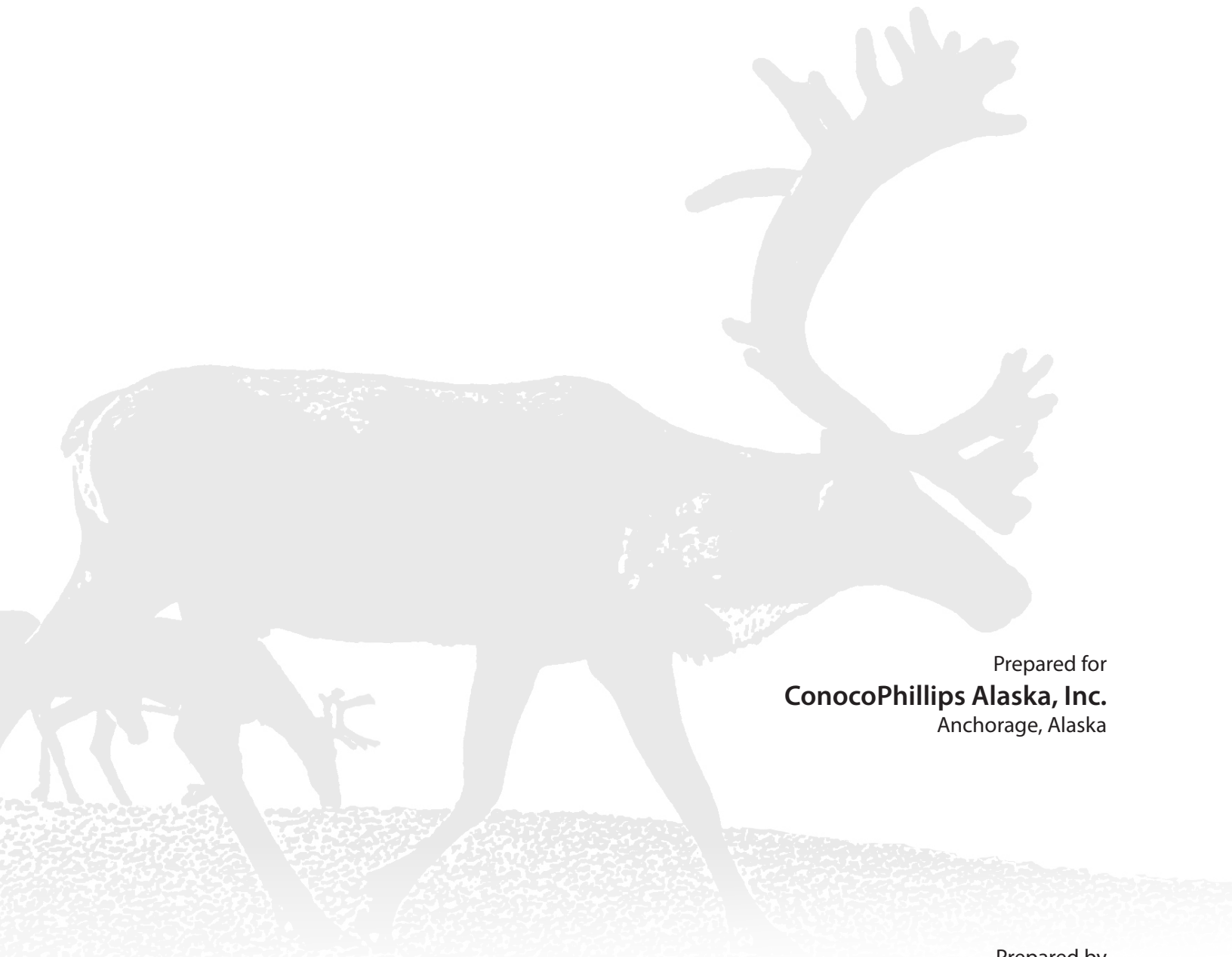


CARIBOU MONITORING STUDY FOR THE BEAR TOOTH UNIT PROGRAM,
ARCTIC COASTAL PLAIN, ALASKA, 2018

Alexander K. Prichard
Joseph H. Welch
Matthew J. Macander
Brian E. Lawhead



Prepared for
ConocoPhillips Alaska, Inc.
Anchorage, Alaska

Prepared by
ABR, Inc.—Environmental Research & Services
Fairbanks, Alaska

**CARIBOU MONITORING STUDY FOR THE BEAR TOOTH UNIT
PROGRAM, ARCTIC COASTAL PLAIN, ALASKA, 2018**

Prepared for

ConocoPhillips Alaska, Inc.
P.O. Box 100360
Anchorage, Alaska 99510-0360

Prepared by

Alexander K. Prichard
Joseph H. Welch
Matthew J. Macander
Brian E. Lawhead

ABR, Inc.—Environmental Research & Services
P.O. Box 80410
Fairbanks, Alaska 99708-0410

April 2019

TABLE OF CONTENTS

| | |
|--|-----|
| List of Figures..... | iii |
| List of Tables | v |
| List of Appendices..... | v |
| Acknowledgments | vi |
| Introduction..... | 1 |
| Background | 1 |
| Study Objectives | 2 |
| Study Area | 3 |
| Methods | 5 |
| Weather And Insect Conditions | 5 |
| Caribou Distribution and Movements..... | 5 |
| Aerial Transect Surveys..... | 5 |
| Density Mapping..... | 6 |
| Radio Telemetry | 6 |
| Seasonal Occurrence in the Study Area..... | 8 |
| Aerial Photography | 8 |
| Remote Sensing..... | 9 |
| Snow Cover..... | 9 |
| Vegetative Biomass | 9 |
| Forage Modeling..... | 10 |
| Habitat Classification..... | 10 |
| Resource Selection Analysis..... | 11 |
| Results..... | 13 |
| Weather Conditions | 13 |
| Caribou Distribution and Movements..... | 13 |
| Aerial Transect Surveys..... | 13 |
| Radio Telemetry | 18 |
| Aerial Photography | 30 |
| Remote Sensing..... | 32 |
| Vegetative Biomass..... | 35 |
| Resource Selection Analysis..... | 41 |
| Discussion..... | 47 |
| Weather, Snow, and Insect Conditions | 47 |
| Caribou Distribution and Movements..... | 47 |
| Resource Selection..... | 48 |
| Literature Cited..... | 52 |

LIST OF FIGURES

| | | |
|-----------|---|---|
| Figure 1. | Population size of the Teshekpuk and Central Arctic caribou herds, 1975–2017, based on Alaska Department of Fish and Game census estimates. | 1 |
| Figure 2. | Location of the caribou monitoring study area on the central North Slope of Alaska and detailed view showing locations of the Bear Tooth North and Bear Tooth South survey areas, 2001–2018 | 4 |

| | | |
|------------|---|----|
| Figure 3. | Habitat types used for caribou habitat-selection analysis in the NPRA | 12 |
| Figure 4. | Snow depth, long-term mean, and 95% confidence interval at the Kuparuk airstrip, May–June 2018 and daily average air temperature, long-term mean, and 95% confidence interval at Kuparuk, May–September 2018..... | 14 |
| Figure 5. | Hourly air temperature, wind speed, mosquito probability index, and oestrid fly probability index at Nuiqsut, 15 June–7 September 2018..... | 15 |
| Figure 6. | Distribution and size of caribou groups during each of seven seasons in the Bear Tooth North and Bear Tooth South survey areas, April–September 2018 | 16 |
| Figure 7. | Seasonal density of caribou observed on 137 surveys in the NPRA, April–October 2001–2018 | 17 |
| Figure 8. | Mean seasonal densities of caribou in the NPRA caribou survey areas based on IDW interpolation of aerial survey results, 2002–2018..... | 19 |
| Figure 9. | Distribution of other large mammals observed during aerial and ground surveys in the northeastern NPRA, June–September 2018 | 20 |
| Figure 10. | Ranges of TH and CAH caribou in northern Alaska in relation to the study areas, based on VHF, satellite, and GPS radio-telemetry, 1980–2018 | 22 |
| Figure 11. | Movements of satellite-collared caribou from the TH and CAH in the Bear Tooth North and South study areas during each of eight seasons..... | 23 |
| Figure 12. | Movements of GPS-collared caribou from the TH and CAH in the Bear Tooth North and South study areas during each of eight seasons | 24 |
| Figure 13. | Seasonal distribution of CAH females based on fixed-kernel density estimation of telemetry locations, 2001–2018..... | 25 |
| Figure 14. | Seasonal distribution of TH females based on fixed-kernel density estimation of telemetry locations, 1990–2018..... | 26 |
| Figure 15. | Seasonal distribution of TH males based on fixed-kernel density estimation of telemetry locations, 1997–2018..... | 27 |
| Figure 16. | Distribution of parturient females of the Teshekpuk Herd during calving based on fixed-kernel density estimation of telemetry locations, 1990–2018..... | 28 |
| Figure 17. | Proportion of CAH and TH caribou within the BTN and BTS survey areas, based on fixed-kernel density estimation, 1990–2018..... | 29 |
| Figure 18. | Movements of GPS-collared TH caribou based on 95% isopleths of dynamic Brownian Bridge movement models | 31 |
| Figure 19. | Movements of GPS-collared caribou from the TH and CAH in the vicinity of the proposed Willow development during each of 8 seasons..... | 33 |
| Figure 20. | Proportion of TH caribou within 4 km of the proposed Willow development alignments, based on fixed-kernel density estimation, 1990–2018 | 35 |
| Figure 21. | Extent of snow cover between early May and mid-June on the central Arctic Coastal Plain of Alaska in 2018, as estimated from MODIS satellite imagery..... | 37 |
| Figure 22. | Median snowmelt date and vegetation index metrics, as estimated from MODIS satellite imagery time series, on the central Arctic Coastal Plain of Alaska, 2000–2018..... | 38 |
| Figure 23. | Departure of 2018 values from median snowmelt date and vegetation index metrics, as estimated from MODIS satellite imagery time series, on the central Arctic Coastal Plain of Alaska..... | 39 |

| | | |
|------------|--|----|
| Figure 24. | Metrics of relative vegetation biomass during the 2018 growing season on the central North Slope of Alaska, as estimated from NDVI calculated from MODIS satellite imagery. | 40 |
| Figure 25. | Predicted relative probability of use of the NPRA study area by caribou during each of eight seasons, 2002–2018, based on RSF analysis..... | 46 |

LIST OF TABLES

| | | |
|----------|--|----|
| Table 1. | Number of TH and CAH radio-collar deployments and total number of collared animals that provided movement data for the Bear Tooth caribou study. | 7 |
| Table 2. | Number and density of caribou in the Bear Tooth North and Bear Tooth South survey areas, April–September 2018..... | 17 |
| Table 3. | Location and number of other large mammals observed during aerial and ground wildlife surveys for CPAI, April–September 2018 | 21 |
| Table 4. | Proportion of collared Teshekpuk Herd caribou that crossed the proposed Willow alignment at least once in each season, 2000–2018 | 32 |
| Table 5. | Number of aerial surveys, radio collars, and locations for each sample type used in RSF analysis for the NPRA survey area, 2002–2018..... | 41 |
| Table 6. | Three top-performing seasonal RSF models, AICc scores, and the probability that each model was the best model in the candidate set for the NPRA survey area, 2002–2018 | 42 |
| Table 7. | Mean Pearson’s rank correlation coefficient of seasonal RSF model fit using k-fold cross-validation for the NPRA survey area, 2002–2018 | 43 |
| Table 8. | Independent variables and their probability of being in the best RSF model for the NPRA survey area during eight seasons, 2002–2018..... | 44 |
| Table 9. | Model-weighted parameter estimates for RSF models for the NPRA survey area during eight seasons, 2002–2018..... | 45 |

LIST OF APPENDICES

| | | |
|-------------|---|----|
| Appendix A. | Cover-class descriptions of the NPRA earth-cover classification | 60 |
| Appendix B. | Snow depth and cumulative thawing degree-days at the Kuparuk airstrip, 1983–2018 | 62 |
| Appendix C. | 2018 North Slope caribou aerial imagery survey. Survey report submitted by TerraSond, Inc..... | 65 |
| Appendix D. | Timing of annual snowmelt, compared with median date of snowmelt, on the central North Slope of Alaska during 2000–2018, as estimated from MODIS imagery | 85 |
| Appendix E. | Differences between annual relative vegetative biomass values and the 2000–2018 median during the caribou calving season on the central North Slope of Alaska, as estimated from NDVI calculated from MODIS satellite imagery | 86 |

| | | |
|-------------|---|----|
| Appendix F. | Differences between annual relative vegetative biomass values and the 2000–2018 median at estimated peak lactation for caribou on the central North Slope of Alaska, as estimated from NDVI calculated from MODIS satellite imagery | 87 |
| Appendix G. | Differences between annual relative vegetative biomass values and the 2000–2018 median at estimated peak biomass on the central North Slope of Alaska, as estimated from NDVI calculated from MODIS satellite imagery | 88 |

ACKNOWLEDGMENTS

This study was funded by ConocoPhillips Alaska, Inc., (CPAI) and was administered by Robyn McGhee, CPAI Environmental Studies Coordinator, for whose support we are grateful. Valuable assistance with field logistics was provided by Justin Blank, Zac Hobbs, and Krista Kenny. Alaska Department of Fish and Game (ADFG) biologists played crucial collaborative roles in this study by capturing caribou, deploying radio collars, and providing telemetry data under a cooperative agreement among ADFG, CPAI, and ABR. We thank ADFG biologists Lincoln Parrett, Elizabeth Lenart, and Jason Caikoski for their professional cooperation and assistance. Brian Person of the North Slope Borough Department of Wildlife Management (NSB) provided GPS and satellite telemetry data, valuable information, and advice. Jesse Cummings of Golden Eagle Outfitters, and Bob Gill and Tracy Kraun of 70 North LLC provided safe and efficient piloting of survey airplanes under flying conditions that often were less than optimal. Assistance in the field was provided by ABR employees Katie Hayden, Robert McNown, Tim Obritschkewitsch, Julie Parrett, and Pam Seiser as well as Tim Vosburgh from BLM. Frederick Tuckley, Jr., provided expert assistance retrieving time-lapse cameras by snowmobile. Support during data collection, analysis, and report production was provided by Christopher Swingley, Dorte Dissing, Will Lentz, Pamela Odom, and Tony LaCortiglia. Review by Robert Burgess of ABR improved this report.

INTRODUCTION

BACKGROUND

The caribou monitoring study for the Bear Tooth Unit (BTU) area is being conducted on the Arctic Coastal Plain of northern Alaska in the northeastern portion of the National Petroleum Reserve–Alaska (NPRA). This region is used primarily by one herd of barren-ground caribou (*Rangifer tarandus granti*)—the Teshekpuk Herd (TH). The TH generally ranges from the Colville River to the Chukchi Sea north of the Brooks range (Person et al. 2007, Arthur and Del Vecchio 2009, Wilson et al. 2012, Lawhead et al. 2015, Parrett 2015a, Lenart 2015, Nicholson et al. 2016).

The TH tends to remain on the coastal plain year-round. The area of most concentrated calving typically is located around Teshekpuk Lake and the primary area of insect-relief habitat in midsummer is the swath of land between Teshekpuk Lake and the Beaufort Sea coast (Kelleyhouse 2001; Carroll et al. 2005; Parrett 2007, 2015a; Person et al. 2007; Yokel et al. 2009; Wilson et al. 2012). Since 2010,

the calving distribution of the TH has expanded, with some calving occurring as far west as the Ikpikpuk River and Atqasuk and a few females calving east of the Colville River with the CAH (Parrett 2015a; L. Parrett, Alaska Department of Fish and Game [ADFG], pers. comm.).

Most TH caribou winter on the coastal plain, generally west of the Colville River, although some caribou occasionally overwinter south of the Brooks Range with the Western Arctic Herd (WAH) (Carroll et al. 2005, Person et al. 2007). In the last 15–20 years, substantial portions of the TH wintered in areas outside the previous range of the herd, both southeast near the winter range of the CAH since 2004–2005 (Lawhead et al. 2015, Lenart 2015, Parrett 2015a) and, in a highly unusual movement, far east in the Arctic National Wildlife Refuge (ANWR) in 2003–2004 (Carroll et al. 2004, Parrett 2009).

The TH increased substantially in size from the mid-1970s to the early 1990s (Parrett 2015a; Figure 1). The TH experienced a dip in numbers in the early 1990s, but increased steadily from 1995

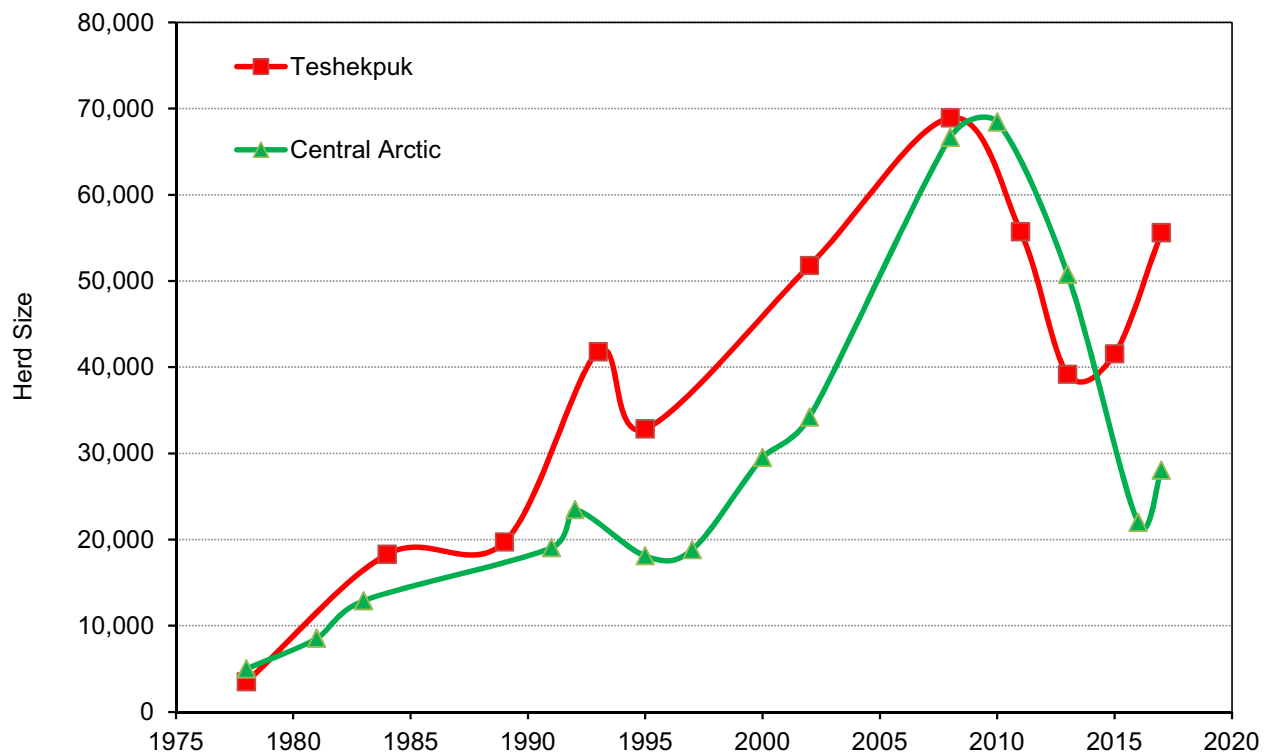


Figure 1. Population size of the Teshekpuk and Central Arctic caribou herds, 1975–2017, based on Alaska Department of Fish and Game census estimates.

to its peak estimated population size of 68,932 animals in July 2008 (Parrett 2015a). The herd subsequently declined. A photocensus in July 2011 produced a population estimate of 55,704 animals (Parrett 2015a), a decline of at least 19% from the 2008 estimate. A photocensus in July 2013 produced an estimate of 39,172 animals (including ~7,000 animals that were mixed with the WAH at the time of the census; Parrett 2015a), a further decrease of at least 30% since 2011. A photocensus in July 2015 produced a minimum count of 35,181 caribou and an accompanying estimate, using a homogeneity model for missing radio-collars, of 41,542 animals (SE = 3,486; Parrett 2015b), indicating the population had stabilized. A photocensus in July 2017 resulted in a minimum population count of 56,255 animals (Klimstra 2018). Although a portion of the higher population number since 2015 can be explained by the new higher-resolution digital photography used in 2017, the large difference in herd counts indicates that the TH has increased since 2015.

The Central Arctic Herd (CAH) of caribou is also located nearby to the east, and individuals sometimes cross over to the west of the Colville River. CAH caribou tend to calve between the Colville and Canning rivers (Wolfe 2000, Arthur and Del Vecchio 2009, Lenart 2015), move to the Beaufort Sea coast during periods of mosquito harassment (White et al. 1975, Dau 1986, Lawhead 1988), and generally winter south of the Brooks Range, usually east of the Dalton Highway/Trans-Alaska Pipeline (TAPS) corridor (Arthur and Del Vecchio 2009, Lawhead et al. 2015, Lenart 2015, Nicholson et al. 2016), although some animals have remained north of the Brooks Range on the coastal plain in recent years (Prichard et al. 2017; E. Lenart, ADFG, pers. comm.). Population trends of the CAH have closely mirrored those of the TH (Figure 1; Lenart 2009, 2015, 2017, 2018). The magnitude of the recent herd decline may have been affected by emigration of some CAH animals to the Porcupine Herd (PH) and TH, with which the CAH often intermixes on shared winter ranges (E. Lenart, ADFG, pers. comm.; ADFG 2017).

This monitoring study builds on prior research funded by ConocoPhillips Alaska, Inc., (CPAI, and its heritage companies Phillips Alaska, Inc., and ARCO Alaska, Inc.) that was conducted on the

Colville River delta and adjacent coastal plain east of the delta (Alpine transportation corridor) since 1992 and in the northeastern portion of the NPRA since 1999 (Johnson et al. 2015; Jorgenson et al. 1997, 2003, 2004). Since 1990, contemporaneous, collaborative telemetry studies of caribou distribution and movements have been conducted in the region west of the Colville River by ADFG, the North Slope Borough (NSB), and the Bureau of Land Management (BLM) (Philo et al. 1993, Carroll et al. 2005, Person et al. 2007, Wilson et al. 2012, Parrett 2015a, Prichard et al. 2017). Consultants working for BP Exploration (Alaska), Inc., conducted aerial transect surveys over much of the TH calving grounds during 1998–2001 (Noel 1999, 2000; Jensen and Noel 2002; Noel and George 2003).

STUDY OBJECTIVES

Evaluation of the natural and anthropogenic factors affecting caribou in the study area fall into two broad categories: those affecting movements and those affecting distribution. Clearly, these categories are linked and are not mutually exclusive, but the applicability of study methods differs between them. Information on the potential effects of development on caribou distribution can be collected using a variety of methods, including aerial transect surveys, radio telemetry, and other reported observations. Information about the potential effects on caribou movements, however, cannot be addressed adequately without employing methods such as radio telemetry that allow regular tracking of individually identifiable animals.

Several broad tasks were identified for study:

1. Evaluate the seasonal distribution, abundance, and movements of caribou in the study area, using a combination of historical and current data sets from aerial transect surveys and radio telemetry data obtained for this study and from ADFG under a cooperative agreement.
2. Characterize important habitat conditions, such as snow cover, spatial pattern and timing of snowmelt, seasonal flooding (if possible), and estimated biomass of new vegetative growth in the study area by applying remote-sensing techniques.

3. Compare caribou distribution with habitat mapping, remote-sensing data, and other landscape features to better understand seasonal distribution of caribou.
4. Conduct a pilot study to assess the feasibility of using high-resolution aerial photography to detect and enumerate caribou from a survey altitude higher than 500 feet.
5. Map the distribution and abundance of muskoxen, grizzly bears, and other large mammals encountered incidentally during aerial transect surveys.

STUDY AREA

CPAI began funding caribou surveys in the northeastern NPRA in 2001–2004 and continued these studies during 2005–2014 under the North Slope Borough (NSB) Amended Development Permit 04-117 stipulation for the CD-4 drill site project. Based on the earlier permit stipulations, the study area was specified as the area within a 48-km (30-mi) radius around the CD-4 drill site (Lawhead et al. 2015). During 2004–2017, aerial transect surveys were conducted in three survey areas, which encompassed most of that 48-km radius (Lawhead et al. 2015): the NPRA survey area (expanded from 988 km² in 2001 to 1,310 km² in 2002; 1,720 km² in 2005); the Colville River Delta survey area which encompasses CD-1 through CD-4 (494 km²); and the Colville East survey area (1,432–1,938 km², depending on the survey and year). Although 2014 was the tenth year of study, the NSB requested that annual monitoring be continued. In 2016, the study area was redefined to focus on the NPRA and Colville River Delta survey areas, so survey results for the Colville East survey area were reported elsewhere (Prichard et al. 2018b). In 2016 and 2017, the NPRA survey area was expanded westward by 1 and 2 transects, respectively (1,818 km² in 2016; 2,119 km² in 2017).

The NPRA survey area was again redefined in 2018 to focus on the two recently constructed drill sites (CD-5 and GMT-1, constructed in winter 2013–2014 and 2016–2017, respectively), and the proposed GMT-2 drill site, as well as their

connecting access roads and pipelines (Figure 2, bottom). This newly defined Greater Mooses Tooth (GMT) survey area (776.6 km²) also includes the Nuiqsut Spur Road that was constructed by the Kuukpik Corporation in winter 2013–2014 to connect the village of Nuiqsut to the CD-5 access road. Although that road is not part of CPAI's infrastructure, its presence in the study area warrants its inclusion in this analysis. The portion of the previous NPRA survey area west of GMT-2 was expanded west and south to focus on the Willow prospect and other potential future developments within the BTU. Results of studies within this new expanded study area are reported on here. For surveys and analysis, the BTU study area was split up into 2 survey areas, Bear Tooth Unit North (BTN) and Bear Tooth Unit South (BTS). To provide a wider context for analytical results and avoid duplication, some of the analyses in this report were conducted for all NPRA survey areas (GMT, BTN, and BTS) and those results are included in both this report and the GMT report (Prichard et al., *in prep.*).

The study area is located on the central Arctic Coastal Plain of northern Alaska (Figure 2, top). The climate in the region is arctic maritime (Walker and Morgan 1964). Winter lasts about eight months and is cold and windy. The summer thaw period lasts about three months (June–August) and the mean summer (June–August) air temperature in Nuiqsut is 7.6 °C (National Oceanic and Atmospheric Administration, unpublished records 1998–2017). Monthly mean air temperatures at Nuiqsut range from about –4.6 °C in May to 9.7 °C in July, with a strong regional gradient of summer temperatures increasing with distance inland from the coast (Brown et al. 1975). Mean summer precipitation is <8 cm, most of which falls as rain in August. The soils are underlain by permafrost and the temperature of the active layer of thawed soil above permafrost ranges from 0 to 10°C during the growing season.

Spring is brief, lasting about three weeks from late May to mid-June, and is characterized by the flooding and break-up of rivers and smaller tundra streams. In late May, water from melting snow flows both over and under the ice on the Colville River, resulting in flooding on the Colville River delta that typically peaks during late May or the

Study Area

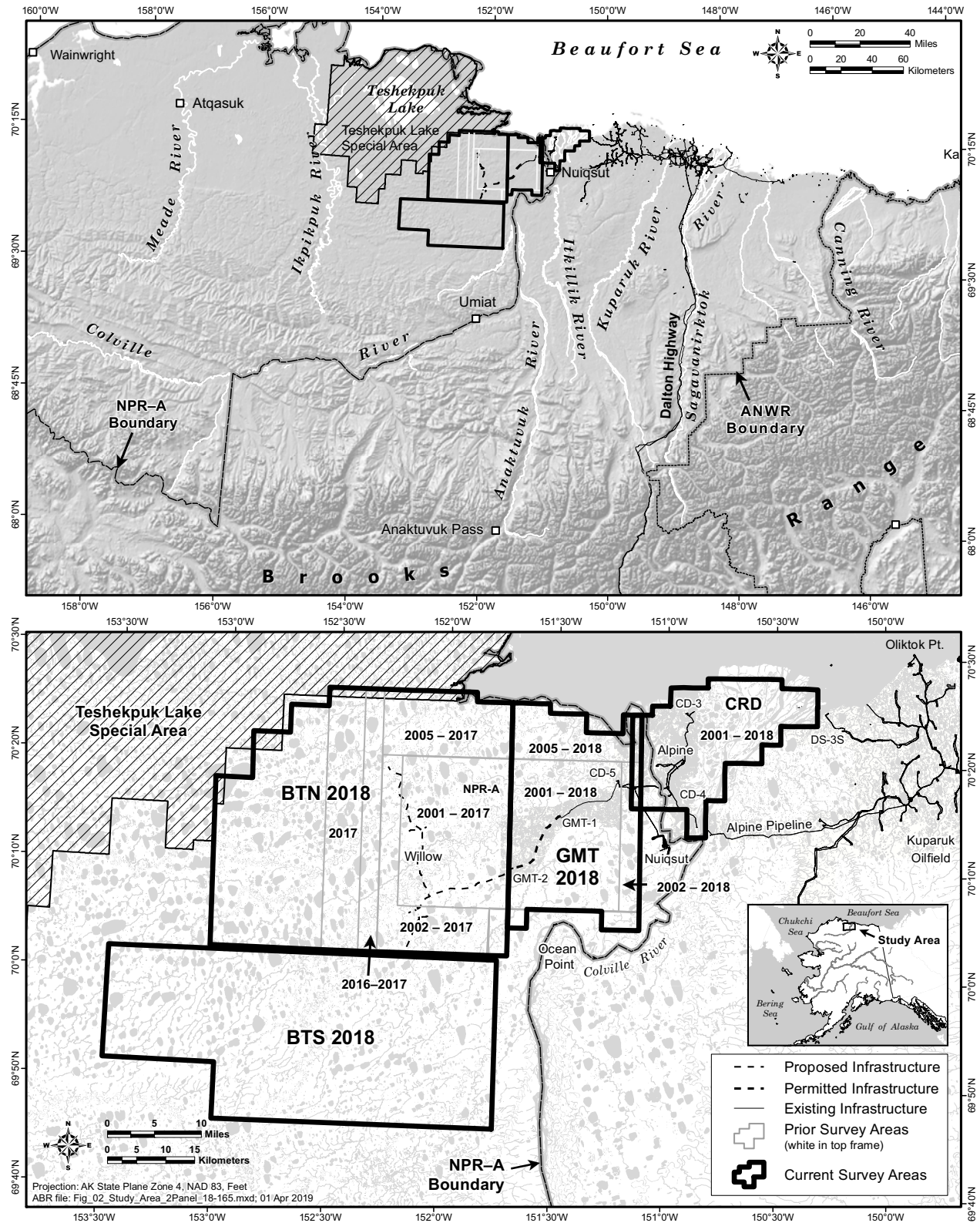


Figure 2. Location of the caribou monitoring study area on the central North Slope of Alaska and detailed view showing locations of the Bear Tooth North and Bear Tooth South survey areas, 2001–2018.

first week of June (Walker 1983; annual hydrology reports to CPAI by Michael Baker Jr., Inc.). Break-up of the river ice usually occurs when floodwaters are at maximal levels. Water levels subsequently decrease throughout the summer, with the lowest levels occurring in late summer and fall, just before freeze-up (Walker 1983; annual hydrology reports to CPAI by Michael Baker Jr., Inc.). Summer weather is characterized by low precipitation, overcast skies, fog, and persistent northeasterly winds. The less common westerly winds often bring storms that are accompanied by high wind-driven tides and rain (Walker and Morgan 1964). Summer fog occurs more commonly at the coast and on the delta than it does farther inland.

METHODS

To evaluate the distribution and movements of TH caribou in the study area, ABR biologists conducted aerial transect surveys in 2018 and analyzed existing telemetry data sets provided by ADFG, NSB, BLM, and the U.S. Geological Survey (USGS), and from GPS collars deployed specifically for this study annually in 2006–2010, 2013–2014, and 2016–2018.

Eight seasons were used for analysis of telemetry and aerial survey data, based on mean movement rates and observed timing of caribou life-history events (adapted from Russell et al. 1993 and Person et al. 2007): winter (1 December–30 April); spring migration (1–29 May); calving (30 May–15 June); postcalving (16–24 June); mosquito harassment (25 June–15 July); oestrid fly harassment (16 July–7 August, a period that also includes some mosquito harassment); late summer (8 August–15 September); and fall migration, a period that includes the breeding season, or rut (16 September–30 November).

WEATHER AND INSECT CONDITIONS

To estimate spring and summer weather conditions in the area during 2018, we used meteorological data from National Weather Service reporting stations at Kuparuk and Nuiqsut. Thawing degree-day sums (TDD; total daily degrees Celsius above zero) were calculated using average daily temperatures at the Kuparuk airstrip. Average index values of mosquito activity were

estimated based on hourly temperatures from Nuiqsut, using equations developed by Russell et al. (1993). The estimated probability of oestrid-fly activity was calculated from average hourly wind speeds and temperatures recorded at Nuiqsut, using equations developed by Mörschel (1999).

CARIBOU DISTRIBUTION AND MOVEMENTS

AERIAL TRANSECT SURVEYS

Transect surveys provided information on the seasonal distribution and density of caribou in the study area. Surveys of the BTN and BTS survey areas (Figure 2, bottom) were conducted periodically from April to September 2018 in a fixed-wing airplane (Cessna 206 or 207), following the same procedures used since 2001 in the NPRA survey area (Lawhead et al. 2015 and references therein).

In 2018, aerial transect surveys in the BTN and BTS survey areas were scheduled for mid-April (late winter), mid-May (spring migration), early June (calving), late June (postcalving), late July (oestrid fly), late August (late summer), and mid to late September (fall migration). Due to inclement weather, the BTN survey area was not surveyed in May.

Two observers looked out opposite sides of the airplane during all surveys and a third observer was present to record data on calving surveys. The pilot navigated the airplane along transect lines using a GPS receiver and maintained an altitude of ~150 m (500 ft) above ground level (agl) or ~90 m (300 ft) agl. Surveys were flown at 90 m agl only during the calving survey and only on the seven westernmost transects in the BTN survey area. The lower flight altitude was chosen due to the anticipated high levels of calving activity near Teshekpuk Lake.

Transect lines were spaced at intervals of 3.2 km (2 mi) in BTN and 4.8 km (3 mi) in BTU South, following section lines on USGS topographic maps (scale 1:63,360). Observers counted caribou within an 800-m-wide strip on each side of the airplane when flying at 150 m agl or a 400-m-wide strip when flying at 90 m agl. Therefore, we sampled ~50% of the BTN survey area when flying 150 m agl, 25% of the western portion of BTN when flying 90 m agl during the

calving survey, and 33% of the BTS survey area while flying 150 m agl. The number of caribou observed in the transect strips was adjusted for survey coverage to estimate the total number of caribou in the survey area on each survey. The strip width was delimited visually for the observers by placing tape markers on the struts and windows of the aircraft, as recommended by Pennycuick and Western (1972), or by measuring distances to recognizable landscape features displayed on maps in GPS receivers.

When caribou were observed within the transect strip, a GPS location was recorded when the plane was perpendicular to the animal or herd, the numbers of “large” caribou (adults and yearlings) and calves were recorded, and the perpendicular distance from the transect centerline was assigned to one of four 100-m or 200-m intervals, depending on the strip width. For plotting on maps, the midpoint of the distance interval was used (e.g., 300 m for the 200–400-m interval). Thus, the maximal mapping error was estimated to be ~100 m. Confidence intervals for estimates of total caribou and calves were calculated with a standard error formula modified from Gasaway et al. (1986), using 3.2-km segments of the transects as the sample units.

Observations of other large mammals were recorded during field surveys (both aerial and ground-based) for this and other wildlife studies conducted for CPAI and are reported upon in this report.

DENSITY MAPPING

To summarize aerial survey data in the BTN and BTS survey areas for the period 2002–2018, we used the inverse distance-weighted (IDW) interpolation technique of the *gstat* package in *R* (Pebesma 2004) to map seasonal densities of caribou. Transect strips in the BTN and BTS survey areas were subdivided into 208 and 114 grid cells, respectively. Each grid cell was 1.6 km wide by 1.6 or 3.2 km long, depending on the transect length. The IDW technique used mean seasonal density of caribou in each of the grid cells. Density was calculated by dividing the total number of caribou observed on each survey by the land area in the grid cell. The best power (from 1 to 1.2) and the best number of adjacent centroids (from 10 to 24) to use in the calculations were selected, based

on the values that minimized the residual mean square error. This analysis produced color maps showing surface models of the estimated density of all caribou (large caribou plus calves) observed over the entire survey area for each season.

RADIO TELEMETRY

VHF Collars

Location data were provided by ADFG for all VHF collars in the CAH and TH during the years 1980–2005 (Table 1). Radio-collared caribou (primarily adult females) were tracked by ADFG biologists from fixed-wing aircraft using strut-mounted antennas and a scanning radio receiver. Although VHF telemetry does not provide detailed movement data, this method provided data on group size and behavior when the collared caribou could be observed (Cameron et al. 1995, Arthur and Del Vecchio 2009).

Satellite Collars

Satellite (Platform Transmitter Terminal; PTT) telemetry used the Argos system (operated by CLS America, Inc.; CLS 2016) and locations were transferred monthly to the NSB for data archiving. Locations were transmitted either at 6 h/day for a month after deployment and then 6 h every other day throughout the year, or once every 6 days in winter and every other day during summer (Lawhead et al. 2015). The CAH satellite collars were programmed to operate 6 h/day or 6 h every 2 days (Fancy et al. 1992, Lawhead et al. 2015).

Satellite-collar data were obtained from ADFG, NSB, and BLM for TH animals during the period July 1990–November 2018 (Lawhead et al. 2006, 2007, 2008, 2009, 2010, 2011, 2012, 2013, 2014, 2015; Person et al. 2007; Prichard et al. 2017, 2018a, 2018b, this study) and for CAH caribou during the periods October 1986–July 1990 (from USGS), July 2001–September 2004, and April 2012–September 2016 (Cameron et al. 1989, Fancy et al. 1992, Lawhead et al. 2006, Lenart 2015; Table 1). In the TH sample (based on herd affiliation at capture), 185 collars deployed on 165 different caribou (87 females, 78 males) transmitted signals for a mean duration of 546 days per collar. The CAH 1986–1990 sample included 17 caribou (16 females, 1 male). The CAH 2001–2004 and 2012–2018 deployment samples

Table 1. Number of TH and CAH radio-collar deployments and total number of collared animals that provided movement data for the Bear Tooth caribou study.

| Herd ^a / Collar Type | Years | Female | | Male | | Total Deployments |
|------------------------------------|-----------|-------------|-------------|-------------|-------------|----------------------|
| | | Deployments | Individuals | Deployments | Individuals | |
| Teshekpuk Herd | | | | | | |
| VHF collars ^b | 1980–2005 | n/a | | n/a | | 212 |
| Satellite collars | 1990–2018 | 98 | 87 | 87 | 78 | 185 |
| GPS collars | 2004–2018 | 254 | 182 | 6 | 6 | 260 |
| Central Arctic Herd | | | | | | |
| VHF collars ^b | 1980–2005 | n/a | | n/a | | 412 |
| Satellite collars | 1986–1990 | 16 | | 1 | | 17 |
| Satellite collars | 2001–2004 | 10 | 10 | 2 | 2 | 12 |
| Satellite collars | 2012–2018 | 6 | 6 | 6 | 6 | 12 |
| GPS collars | 2003–2018 | 173 | 119 | 0 | 0 | 173 |

^a Herd affiliation at time of capture.

^b n/a = not available, but most collared animals were females.

included 24 collars deployed on 24 caribou (16 females, 8 males), transmitting for a mean duration of 585 days per collar. Satellite telemetry locations are considered accurate to within 0.5–1 km of the true locations (CLS 2016), but the data require screening to remove spurious locations (Lawhead et al. 2015).

GPS Collars

GPS collars purchased by BLM, NSB, ADFG, and CPAI (TGW-3680 GEN-III or TGW-4680 GEN-IV store-on-board configurations with Argos satellite uplink, manufactured by Telonics, Inc., Mesa, AZ) were deployed 260 times by ADFG biologists on 188 different TH caribou (182 females, 6 males) during 2004 and 2006–2018, with a mean deployment duration of 524 days (Table 1). GPS collars (purchased by CPAI and ADFG) were deployed 173 times on 119 different female CAH caribou during 2003–2018, with a mean duration of 588 days. Collars were programmed to record locations at 2-, 3-, 5-, or 8-h

intervals, depending on the desired longevity of the collar (Arthur and Del Vecchio 2009, Lawhead et al. 2015).

GPS collars were deployed on female caribou, with the exception of six collars deployed on TH males. Females are preferred for GPS collar deployment because the collar models used are subject to antenna problems when using the expandable collars that are required for male caribou due to increased neck size during the rut (Dick et al. 2013; C. Reindel, Telonics, pers. comm.). Caribou were captured by ADFG personnel firing a handheld net-gun from a Robinson R-44 piston-engine helicopter. In keeping with ADFG procedures for the region, no immobilizing drugs were used.

Data reports from Argos satellite uplinks were downloaded daily from CLS America, Inc., (Largo, MD) and the full dataset was downloaded after the collars were retrieved. Data were screened to remove spurious locations using methods described in Lawhead et al. (2015).

SEASONAL OCCURRENCE IN THE STUDY AREA

Seasonal use of the BTN and BTS survey areas was evaluated using two methods. The first method was to calculate the proportion of each monthly utilization distribution from kernel density estimation within the survey areas, by sex and herd, after first removing the portion of each seasonal utilization distribution contour that overlapped the ocean. The second method was to examine GPS- and satellite-collar data to describe caribou movements in the immediate vicinity of existing and proposed infrastructure. Additionally, we calculated the proportion of each monthly utilization distribution within 4 km of the Alternative 1 road and pad alignments (GIS layers supplied to ABR on 20 December 2018). We also calculated to proportion of collared TH caribou that crossed the alignments at least once during a season for each year. We only included animals that had locations for >75% of the season and locations within 30 days of collaring were removed.

To calculate kernels, we first calculated the mean location of each caribou for every two-day period during the year. Using the *ks* package for *R* (Duong 2017), fixed-kernel density estimation was employed to create utilization distribution contours of caribou distribution for every two-day period throughout the year (all years combined). We then calculated an average utilization distribution for each combination of season, herd, and sex. By calculating the average of utilization distribution based on the mean location for each animal we were able to account for movements within a season while not biasing the calculation due to autocorrelation among locations for a single caribou or due to unequal sample sizes among caribou. The plug-in method was used to calculate the bandwidth of the smoothing parameter. Because caribou are sexually segregated during some seasons, kernels were analyzed separately for females and males, although the sample size for male CAH caribou was insufficient to allow kernel density analysis. We also calculated a separate kernel for parturient TH females during the calving season to delineate the calving range of the TH.

To visualize movements of caribou outfitted with GPS collars, we used dynamic Brownian

Bridge Movement Models (dBBMM) to create utilization distribution maps of movements based on the locations of collared individuals (Kranstauber et al. 2014). These dBBMM models, a modification of earlier Brownian bridge models (Horne et al. 2007), use an animal's speed of movement and trajectory calculated from intermittent GPS locations to create a probability map describing relative use of the area traversed. We computed the 95% isopleth of movements for each individual TH caribou outfitted with a GPS collar in the area and then overlaid the isopleth layers for each season to calculate the relative proportion of collared caribou using each 100-m pixel. This visualization displays the seasonal use of the area by TH caribou as a function of both caribou distribution and movements. The dBBMM models were computed using the *move* package in *R* (Kranstauber et al. 2017).

AERIAL PHOTOGRAPHY

High-resolution digital photography is increasingly being used for aerial surveys of wildlife due to the potential for more accurate counts, increased observer safety, higher flight altitudes with lower noise levels, and the potential for automating counts. Recent improvements in digital camera technology may provide a promising method to accurately quantify caribou presence while flying at higher altitudes (e.g., $\geq 1,000$ feet agl) than currently used for visual surveys (300 or 500 feet agl). Therefore, we conducted a pilot study in 2018 to test the feasibility of using cameras mounted on survey aircraft to identify caribou during five surveys, at different times of year and sampling under a variety of environmental conditions. ABR contracted TerraSond, Inc., based in Palmer, AK, to provide the high-resolution cameras and expertise in photo processing and digital photo interpretation. We used high-resolution cameras (RGB), as well as multispectral sensors, including near infrared (NIR), to assess whether caribou can be identified consistently in photographs and if the detection of potential caribou can be partially or fully automated. We used aerial photography in conjunction with our regular aerial strip transect surveys (at 500 ft agl) as well as dedicated flights for photography to capture images at multiple

angles and heights (300–2,000 feet agl) to develop and test the method.

REMOTE SENSING

We analyzed 2018 snow cover and 2000–2018 vegetation greenness using gridded, daily reflectance and snow-cover products from MODIS Terra and Aqua sensors. The snow-cover data were added to the data compiled for 2000–2017 (see Lawhead et al. 2015, Prichard et al. 2017, and Prichard et al. 2018a for detailed description of methods). The entire vegetation index record, based on atmospherically corrected surface reflectance data, was processed to ensure comparability of greenness metrics.

For data through 2015, we applied a revised cloud mask that incorporated snow-cover history to reduce false cloud detection during the active snowmelt season. However, the revised cloud mask did not work on the 2016–2018 imagery, probably due to changes in the data and data format from the aging MODIS sensors. For 2016–2018, we applied manual cloud masks for the snowmelt season and applied the standard cloud mask for images collected in June and later.

We analyzed and summarized the data using Google Earth Engine, a cloud computing service (Gorelick et al. 2017). For final analysis and visualization, we exported the results to the Alaska Albers coordinate system (WGS-84 horizontal datum) at 240-m resolution.

SNOW COVER

Snow cover was estimated using the fractional snow algorithm developed by Salomonson and Appel (2004). Only MODIS Terra data were used for snow mapping through 2016 because MODIS Band 6, which was used in the estimation of snow cover, was not functional on the MODIS Aqua sensor. However, a Quantitative Image Restoration algorithm has recently been applied to restore the missing Aqua Band 6 data to a scientifically usable state for snow mapping (Riggs and Hall 2015). At the same time, the aging Terra sensor was no longer reliable for snow mapping in 2017, so we used MODIS Aqua data for snow mapping in 2017–2018. The 2018 analysis was based on MYD10A1.006 data (MODIS/Aqua Snow Cover Daily L3 Global 500m Grid).

A time series of images covering the April–June period was analyzed for each year during 2000–2018. Pixels with >50% water (or ice) cover were excluded from the analysis. For each pixel in each year, we identified:

- The first date with 50% or lower snow cover;
- The closest prior date with >50% snow cover was then identified;
- The midpoint between the last observed date with >50% snow cover and the first observed date with <50% snow cover, which is an unbiased estimate of the actual snowmelt date (the first date with <50% snow cover);
- The duration between the dates of the two satellite images with the last observed “snow” date and the first observed “melted” date, providing information on the uncertainty in the estimate of snowmelt date. When the time elapsed between those two dates exceeded a week because of extensive cloud cover or satellite sensor malfunction, the pixel was assigned to the “unknown” category.

VEGETATIVE BIOMASS

The Normalized Difference Vegetation Index (NDVI; Rouse et al. 1973) is used to estimate the biomass of green vegetation within a pixel of satellite imagery at the time of image acquisition. The rate of increase in NDVI between two images acquired on different days during green-up has been hypothesized to represent the amount of new growth occurring during that time interval (Wolfe 2000, Kelleyhouse 2001, Griffith et al. 2002). NDVI is calculated as follows (Rouse et al. 1973; <http://modis-atmos.gsfc.nasa.gov/NDVI/index.html>):

$$\text{NDVI} = (\text{NIR} - \text{VIS}) \div (\text{NIR} + \text{VIS})$$

where:

NIR = near-infrared reflectance (wavelength 0.841–0.876 μm for MODIS), and

VIS = visible light reflectance (wavelength 0.62–0.67 μm for MODIS).

We derived constrained view-angle (sensor zenith angle $\leq 40^\circ$) maximum-value composites

from daily surface reflectance composites acquired over targeted portions of the growing season in 2000–2018. The data products used were MOD09GA.006 (Terra Surface Reflectance Daily Global 1 km and 500 m) and MYD09GA.006 (MYD09GA.006 Aqua Surface Reflectance Daily L2G Global 1 km and 500 m). NDVI during the calving period (NDVI_Calving) was calculated from a 10-day composite period (1–10 June) for each year during 2000–2018 (adequate cloud-free data were not available to calculate NDVI_Calving over the entire study area in some years). NDVI values near peak lactation (NDVI_621) were interpolated based on the linear change from two composite periods (15–21 June and 22–28 June) in each year. NDVI_Rate was calculated as the linear change in NDVI from NDVI_Calving to NDVI_621 for each year. Finally, NDVI_Peak was calculated from all imagery obtained between 21 June and 31 August each year during 2000–2018. Due to the availability of new forage models, NDVI_Calving, NDVI_621, NDVI_Rate, and NDVI_Peak were not included in analyses of caribou distribution in 2018, but we included summaries of these metrics in this report for comparison with previous reports.

FORAGE MODELING

We applied forage models from Johnson et al. (2018) that incorporate daily NDVI values as well as habitat type, distance to coast, and days from peak NDVI to predict biomass, nitrogen, and digestible energy for a given location on a given day. These models may provide metrics that are more directly related to caribou forage needs than NDVI alone.

We used the MCD43A4.Version 6 daily product at 500 m resolution (Schaaf and Wang 2015). This is the Nadir Bidirectional Reflectance Distribution Function Adjusted Reflectance (NBAR) product, and it provides 500 meter reflectance data that are adjusted using a bidirectional reflectance distribution function (BRDF) to model the reflectance values as if they were collected from a nadir view (i.e., viewed from directly overhead). The NBAR data are produced daily within 16-day retrieval periods using data from both MODIS platforms (i.e., the Terra and Aqua satellites). The product is developed using a single observation from each 16-day period for

each 500 m pixel, with priority given to the central day in each compositing period (i.e., the ninth day) to provide the most representative information possible for each period of the year. Other observations in the period are used to parameterize the BRDF model that is required to adjust the observation to nadir. Similar to other MODIS vegetation index products such as MOD13Q1, it has a 16-day composite period, but unlike other products it has a temporal frequency of one day, with the 16-day window shifting one day with each new image. Thus it avoids any artificial steps at the break between composite intervals, and is a good tool to assess daily phenology normals. It is more likely to provide an observation for a given day than true daily products such as the MOD09GA.006/MYD09GA.006 products used for the NDVI composite metrics (above).

Johnson et al. (2018) calibrated the forage models for four broad vegetation classes (tussock tundra, dwarf shrub, herbaceous mesic, and herbaceous wet). Following their approach, we used the Alaska Center for Conservation Science (ACCS) land cover map for Northern, Western, and Interior Alaska (Boggs et al. 2016), aggregated on the “Coarse_LC” attribute. This map is based on the North Slope Science Initiative (NSSI 2013) with the addition of the aggregation field. We calculated the modal land cover class for each 500-m pixel.

For each date from the start of the calving season through the end of the late summer season (30 May–15 September) and for each year with telemetry locations (2002–2018) we mapped daily NDVI (dNDVI), annual NDVIMax, and days to NDVIMax. Then, we applied the equations from Johnson et al. (2018) to calculate daily forage nitrogen content, and forage biomass for the four broad vegetation classes. We set the forage metrics to zero for water, snow/ice, and barren classes and set it to undefined for other vegetation classes that were not included in the Johnson et al. (2018) models. The areas with undefined forage metrics within the study area were primarily low and tall shrub which comprise a small proportion of the surface area.

HABITAT CLASSIFICATION

We used the NPRA earth-cover classification created by BLM and Ducks Unlimited (2002) for

habitat classification for analyses (Figure 3). The BTN and BTS survey areas contained 15 cover classes from the NPRA earth-cover classification (Appendix A), which we lumped into nine types to analyze caribou habitat use. The Barren Ground/Other, Dunes/Dry Sand, Low Shrub, and Sparsely Vegetated classes, which mostly occurred along Fish and Judy creeks, were combined into a single Riverine habitat type. The two flooded-tundra classes were combined as Flooded Tundra and the Clear-water, Turbid-water, and *Arctophila fulva* classes were combined into a single Water type; these largely aquatic types are used very little by caribou, so the Water type was excluded from the analysis of habitat preference.

RESOURCE SELECTION ANALYSIS

Caribou group locations were analyzed with respect to multiple factors including habitat, snow-cover classes, longitude, distance to coast, and estimated daily values of vegetative NDVI, estimated annual maximum values of vegetative NDVI, forage nitrogen content, and forage biomass to evaluate the relationship of those factors to caribou distribution by using resource selection function (RSF) models (Boyce and McDonald 1999, Manly et al. 2002). RSF models allow simultaneous comparison of selection for multiple variables and incorporation of caribou locations from both aerial surveys and radio telemetry. RSF models compare actual locations with random locations (use vs. availability) and can be a useful tool for quantifying important factors influencing habitat selection during different seasons and for assessing relative importance of different areas based on the spatial pattern of those factors.

We used group locations from aerial surveys and locations from GPS-collared individuals for the RSF analysis. Locations of satellite-collared animals were not used due to the lower accuracy of those locations. We used caribou locations from aerial transect surveys conducted during 2002–2018 in the BTN, BTS, and GMT combined survey areas, but the seasonal sample sizes for the Colville River Delta survey area were too small to support RSF analysis. The available telemetry data spanned the period 11 May 2003–31 December 2018 and were filtered to include only locations falling within the aerial survey area. To standardize

the time between GPS-collar locations, maintain an adequate sample size, and reduce the effect of autocorrelation on results, we subsampled GPS locations at 48-h intervals in all seasons. We assumed that 48 h was enough time for a caribou to move across the entire study area, so autocorrelation would be minimal (Lair 1987, McNay et al. 1994). We excluded caribou locations in waterbodies on the habitat map and in areas that were excluded from the NDVI calculations because they were predominantly water-covered.

To estimate resource selection, we used logistic regression (Manly et al. 2002). For each actual caribou or caribou group location, we generated 25 random locations in non-water habitats within the same survey area as the actual location. We were therefore testing for selection at the level of specific areas or attributes for animals that were within the survey area. For this analysis we use the terms “selection” and “avoidance” to refer to attributes that are used more or less than expected by caribou, when compared with random points.

We ran logistic regression models in *R* (*R* Core Team 2017) to compare actual caribou locations to random locations using the nine explanatory variables: habitat type (merged into the eight non-water categories; Figure 3); daily NDVI, daily nitrogen, daily biomass, and maximum NDVI for each respective day and year the group location was recorded (calculated across 500 m pixels); landscape ruggedness (Sappington et al. 2007; calculated over a 150-m by 150-m box centered at each 30-m pixel); the median snow-free date (date at which the pixel is typically snow-free; Macander et al. 2015); distance to coast; and west-to-east distribution. We used the natural logarithm of the landscape ruggedness variable to account for a skewed distribution (most values close to one) in that variable. The median snow-free date was used only for the winter, spring migration, and calving seasons, and daily NDVI, nitrogen, and biomass variables were used only for the calving, postcalving, mosquito, oestrid fly, and late summer seasons.

All locations were tested for collinearity between explanatory variables by calculating variance inflation factors (VIF) using the *corvif* function from the AED library in *R* (Zuur et al. 2009). In addition, continuous variables were

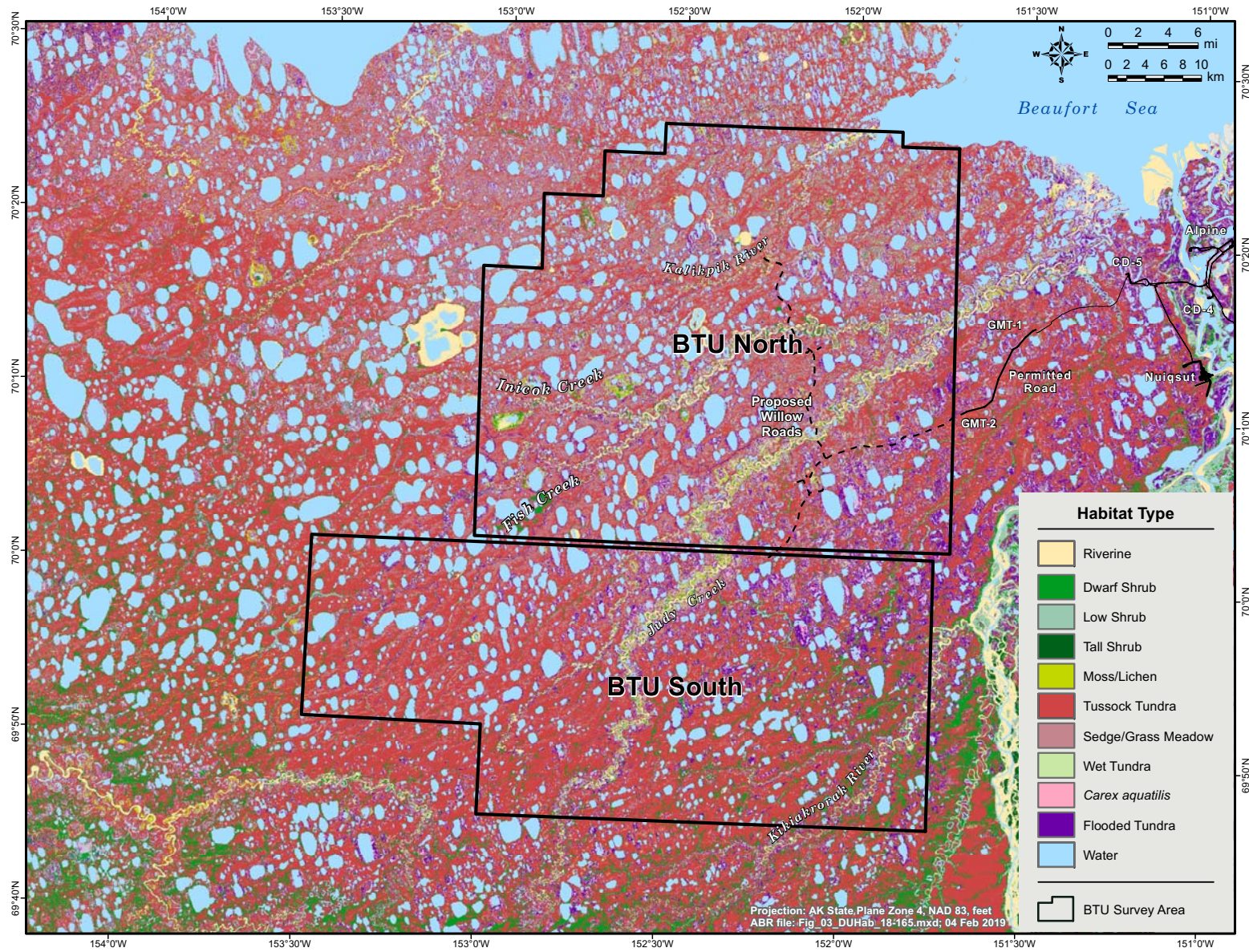


Figure 3. Habitat types used for caribou habitat-selection analysis in the NPRA.

scaled (subtracted the mean and divided by the standard deviation) to aid in model convergence and parameter interpretation (Zuur et al. 2009). Because aerial survey data had low spatial precision (estimated error 100–200 m) compared to the habitat map (30-m pixels), we calculated the most common habitat in a 210-m by 210-m area (7×7 pixels) centered on the estimated group location.

For each season, we tested all combinations of the variables (no interactions were included) using the *glmulti* package in *R* (Calcagno and de Mazancourt 2010) using Akaike's Information Criterion adjusted for small sample sizes (AICc) to compare models. We calculated the unconditional (model-weighted) coefficients and standard error (SE) of each parameter by calculating a weighted average of different models that was weighted by the probability that each model was the best model in the candidate set (Akaike's weight; Burnham and Anderson 2002).

We tested the fit of the best models for each season using *k*-fold cross-validation (Boyce et al. 2002). At each step, we withheld one-fifth of the caribou locations and calculated relative probabilities of use for locations used by those caribou (testing data) based on the remaining data (training data). We repeated this process five times; i.e., for each one-fifth of the caribou locations. We used the mean Pearson's rank correlation coefficient for the five testing data sets as a measure of model fit.

For each season, we created a map of the relative probability of use of the survey area based on the multi-year model output from the RSF models and landscape variable rasters. We used the model-weighted parameter estimates from all independent variables that had a 50% or greater probability of being in the best model (e.g., the sum of all Akaike weights for all models that included the variable was >0.5). We used daily NDVI, and calculated nitrogen and biomass for the midpoint of each season in 2018 and maximum NDVI in 2018.

RESULTS

WEATHER CONDITIONS

Snow was present and snow cover was much higher than average into early June, resulting in

patchy snow conditions for the early June calving survey which necessitated the use of a sightability correction factor to adjust the caribou count from that survey (Figure 4; Appendix B). Daily air temperatures at the Kuparuk Airstrip in 2018 were below average for most of May and June, above average for much of July, and below average for most of August (Figure 4; Appendix B).

Summer weather conditions can be used to predict the occurrence of harassment by mosquitoes (*Aedes* spp.) and oestrid flies (warble fly *Hypoderma tarandi* and nose bot fly *Cephenemyia trompe*) (White et al. 1975, Fancy 1983, Dau 1986, Russell et al. 1993, Mörschel 1999). Mosquitos in the study area usually emerge from the middle of June through early July. Conditions conducive to mosquito activity were not present until ~24–26 June and 2–3 July (Figure 5). ABR Biologists conducting ground-based surveys for other projects near the Colville River delta reported no noticeable mosquito activity before field work concluded on 26 June. Cool temperatures and winds >10 mph persisted until ~12 July yielding low estimated levels of insect harassment. However, weather data predicted elevated mosquito activity for much of the remainder of July. All of August was estimated to have low mosquito and fly activity due to a combination of high winds and below average temperatures

CARIBOU DISTRIBUTION AND MOVEMENTS

AERIAL TRANSECT SURVEYS

BTN Survey Area

Seven aerial surveys of the BTN survey area were attempted between 16 April and 25 September 2018 and six surveys were completed. The May spring migration survey could not be conducted in the BTN survey area due to persistent inclement weather, but all other surveys of the BTN survey area were completed as scheduled. The estimated density ranged from a high of 0.86 caribou/km² in September to a low of <0.01 caribou/km² on 31 July and 1 August (Table 2; Figures 6–7). A total of 625 caribou (0.59 caribou/km²) were observed on the late winter survey on 16–17 April (Table 2; Figures 6–7). The density of caribou had declined to 0.06 and 0.37

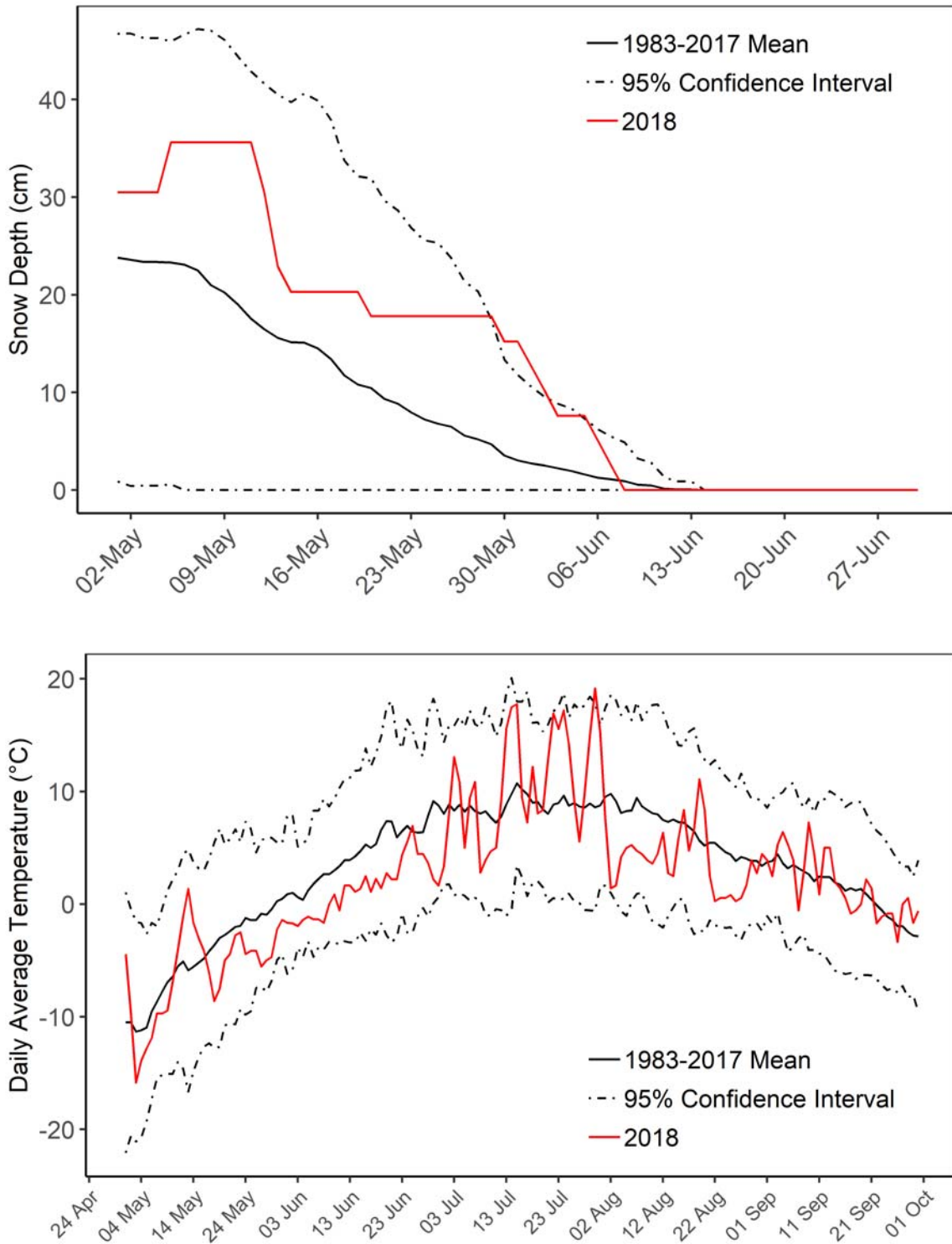


Figure 4. Snow depth, long-term mean, and 95% confidence interval at the Kuparuk airstrip, May–June 2018 (top) and daily average air temperature, long-term mean, and 95% confidence interval at Kuparuk, May–September 2018 (bottom).

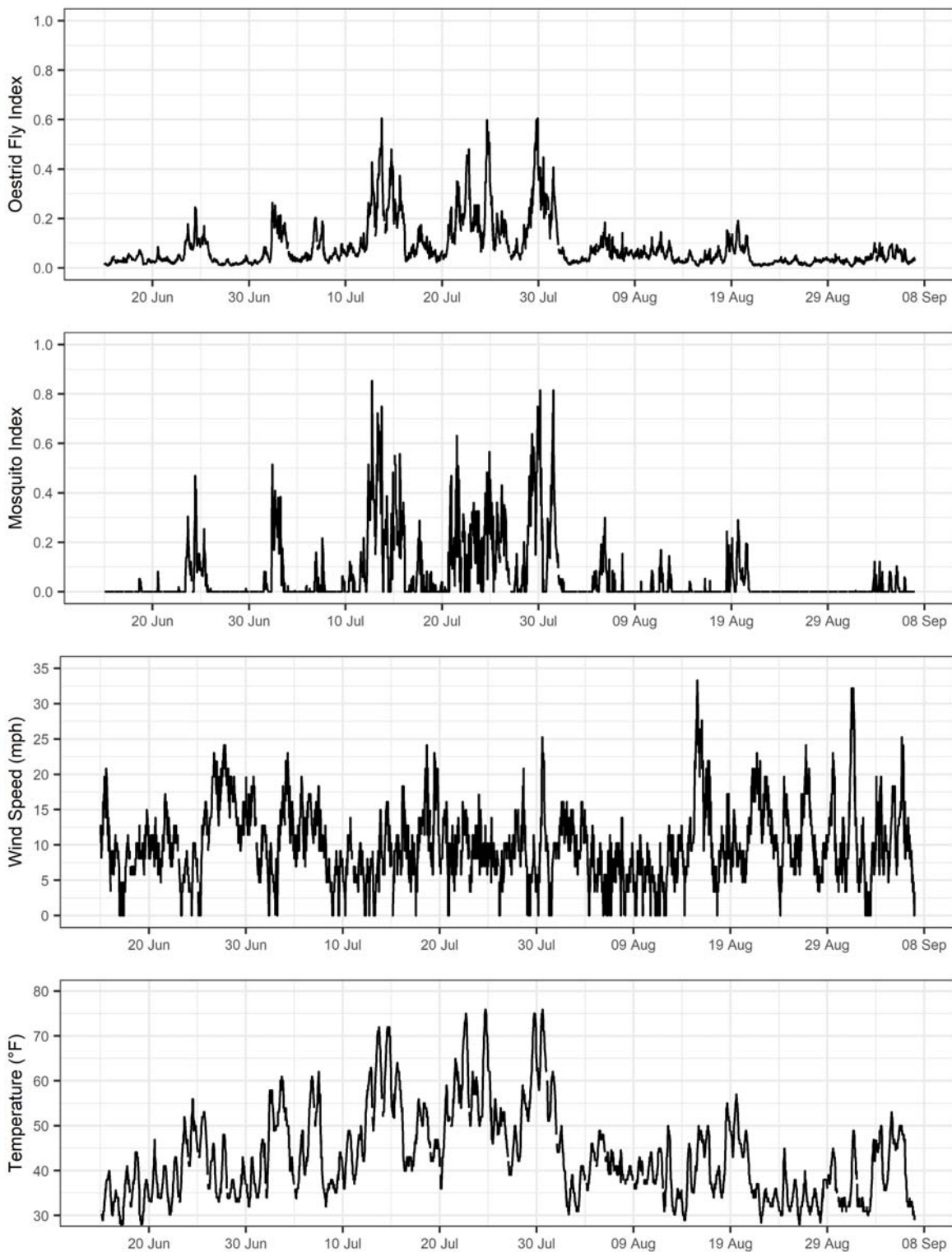


Figure 5. Hourly air temperature, wind speed, mosquito probability index, and oestrid fly probability index at Nuiqsut, 15 June–7 September 2018.

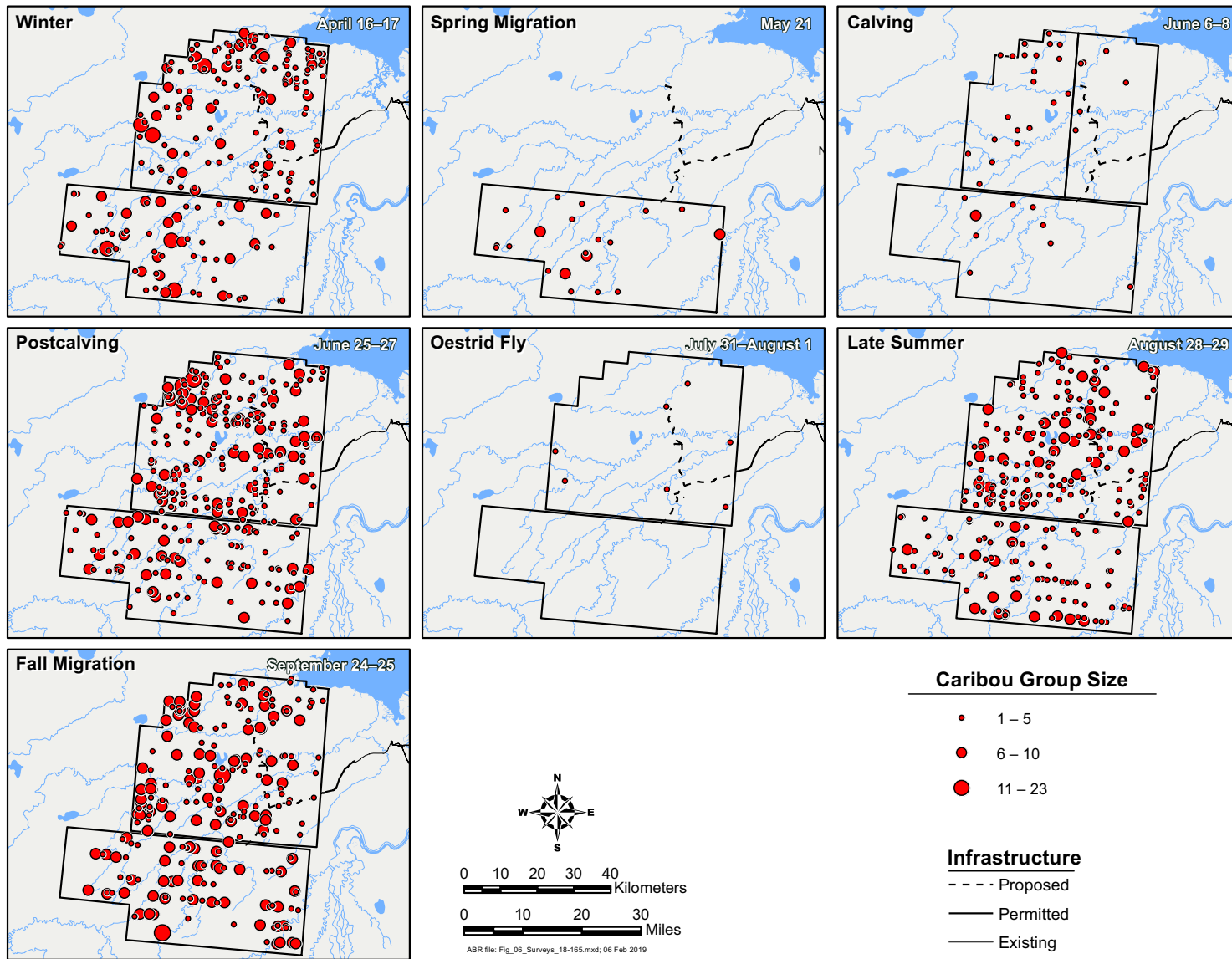


Figure 6. Distribution and size of caribou groups during each of seven seasons in the Bear Tooth North and Bear Tooth South survey areas, April-September 2018.

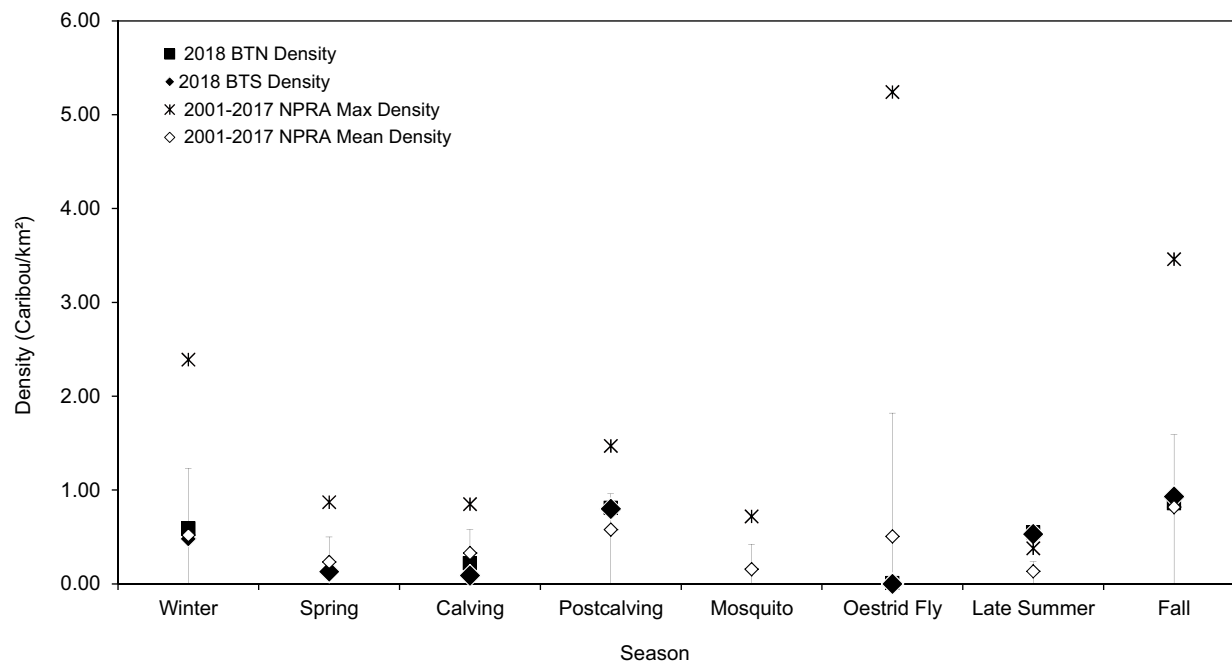


Figure 7. Seasonal density of caribou observed on 137 surveys in the NPRA, April–October 2001–2018. Error bars represent 95% confidence intervals.

Table 2. Number and density of caribou in the Bear Tooth North and Bear Tooth South survey areas, April–September 2018.

| Survey Area and Date | Total Area ^a | Observed Large Caribou ^b | Observed Calves ^c | Observed Total Caribou | Mean Group Size ^d | Estimated Total Caribou ^e | SE ^f | Density (caribou/km ²) ^g |
|----------------------|-------------------------|-------------------------------------|------------------------------|------------------------|------------------------------|--------------------------------------|-------------------|---|
| BTN | | | | | | | | |
| April 16–17 | 2,122 | 625 | nr | 625 | 4.0 | 1,250 | 81.9 | 0.59 |
| June 6–8 (East) | 999 | 16 | 0 | 16 | 2.7 | 60 ^h | 16.7 ^h | 0.06 ^h |
| June 6–8 (West) | 1,123 | 53 | 2 | 55 | 2.4 | 414 ^h | 87.9 ^h | 0.37 ^h |
| June 25–27 | 2,122 | 862 | 2 | 864 | 4.4 | 1,724 | 170.6 | 0.81 |
| July 31–August 1 | 2,122 | 8 | 0 | 8 | 1.1 | 16 | 4.1 | <0.01 |
| August 28 | 2,122 | 586 | nr | 586 | 3.3 | 1,172 | 91.6 | 0.55 |
| September 24–25 | 2,122 | 915 | nr | 915 | 6.2 | 1,830 | 147.5 | 0.86 |
| BTS | | | | | | | | |
| April 16–17 | 1,747 | 278 | nr | 278 | 4.4 | 834 | 167.2 | 0.48 |
| May 21 | 1,747 | 77 | nr | 77 | 3.2 | 231 | 26.4 | 0.13 |
| June 6 | 1,747 | 29 | 0 | 29 | 3.9 | 163 ^h | 39.1 ^h | 0.09 ^h |
| June 25 | 1,747 | 467 | 0 | 467 | 4.8 | 1,401 | 298.1 | 0.80 |
| July 31 | 1,747 | 0 | nr | 0 | - | 0 | - | 0.00 |
| August 28–29 | 1,747 | 306 | nr | 306 | 3.3 | 918 | 82.2 | 0.53 |
| September 24 | 1,747 | 539 | nr | 539 | 6.4 | 1,617 | 163.7 | 0.93 |

^a Survey coverage was 50% of this area in BTN, 25% in BTN West on June 6–8, and 33% in BTS.

^b Adults + yearlings.

^c nr = not recorded; calves not differentiated reliably due to larger size.

^d Mean Group Size = Observed Total Caribou ÷ number of caribou groups observed.

^e Estimated Total Caribou = Observed Total Caribou adjusted for survey coverage.

^f SE = Standard Error of Estimated Total Caribou, calculated following Gasaway et al. (1986), using transects as sample units.

^g Density = Estimated Total Caribou ÷ Area.

^h Applied a Sightability Correction Factor of 1.88 (Lawhead et al. 1994) to correct for low sightability due to patchy snow.

caribou/km² in the eastern and western portions of the BTN at the time of the calving survey. Caribou density then increased by the time of the postcalving survey on 25–27 June (0.81 caribou/km²). Density declined again by the 31 July–1 August survey (<0.01 caribou/km²) during the oestrid fly season and then increased to 0.55 caribou/km² on the late summer survey (29 August), before increasing further to 0.86 caribou/km² for the fall migration survey (September 25). Only 2 calves were seen in the BTN area during the calving survey and only 2 calves were identified during the postcalving survey.

BTS Survey Area

Seven aerial surveys of the BTS survey area were attempted between 16 April and 24 September 2018. All surveys of the BTS survey area were completed as scheduled. The estimated density ranged from a high of 0.93 caribou/km² in September to a low of <0.01 caribou/km² on 31 July (Table 2; Figures 6–7). A total of 278 caribou (0.48 caribou/km²) were observed on the late winter survey on 16–17 April (Table 2; Figures 6–7). The density of caribou declined to 0.13 and 0.19 caribou/km² on the spring migration and calving surveys, respectively. Caribou density then increased on the postcalving survey on 25 June (0.80 caribou/km²). No caribou were observed on the 31 July survey. Densities increased during the late summer survey (0.53 caribou/km²) and again to a high of 0.93 caribou/km² for the fall migration survey on 24 September. No calves were seen in the BTS survey area during the calving or postcalving survey.

Results from both survey areas are within the normal seasonal ranges of caribou densities observed in the previous NPRA survey area since 2001, with the exception of late summer where 2018 densities in the BTN and BTS survey areas were higher than previously observed in the NPRA survey area (Figure 7; Prichard et al. 2018a). It is important to note that these densities were calculated over different survey areas in different years. During most seasons in the previous NPRA survey area, an increasing gradient in caribou density from east to west was apparent. Since the BTN survey area includes the western portion of the previous NPRA survey area, and regions

further to the west of the previous NPRA survey area, higher densities are expected. Results from the seasonal density mapping of caribou recorded on aerial surveys of the NPRA/BTN & BTS survey area during 2002–2018 also showed large differences among seasons (Figure 8). The highest mean density was observed during the oestrid fly season, but that density was strongly affected by several large groups that were observed in only one year (2005).

Miscellaneous Mammal Observations

In 2018, the only other large mammal sightings in the BTN or BTS survey areas were of brown bears (grizzly bears)(Figure 9; Table 3). In total, we observed 15 (12 adults, 3 young) bears in BTN and 2 adults in BTS during caribou aerial surveys. Most bears were observed in central or western BTN and BTS. All bears in BTN were observed either in late June or mid to late August. In BTS, one bear was observed on 31 July and the other was observed on 24 September. Additionally, while the survey crew was commuting to the survey area on 1 August, we observed 3 muskox in one group near Deadhorse. In other surveys for caribou in nearby survey areas, 3 adult brown bears were observed near GMT, 4 adult brown bears were observed on the Colville River delta, one group of at least 20 muskox with an unknown number of calves was observed along the Colville River SE of Alpine, and 2 moose were observed along the Colville River ~65 km (40 mi) south of Nuiqsut (Figure 9; Table 3).

RADIO TELEMETRY

Radio collars provided detailed location and movement data throughout the year for a relatively small number of individual caribou. The telemetry data also provided valuable insight into herd affiliation, which is not available from transect surveys. Mapping of the telemetry data from VHF, satellite (PTT), and GPS collars clearly shows that the study area is located in the eastern extent of the TH range (Figure 10). The majority of collar locations for the TH and CAH occurred west and east of the Colville River, respectively. The composite satellite and GPS telemetry data demonstrate that, although collared TH caribou use the study area to some extent in all seasons, their use peaks during the summer insect season

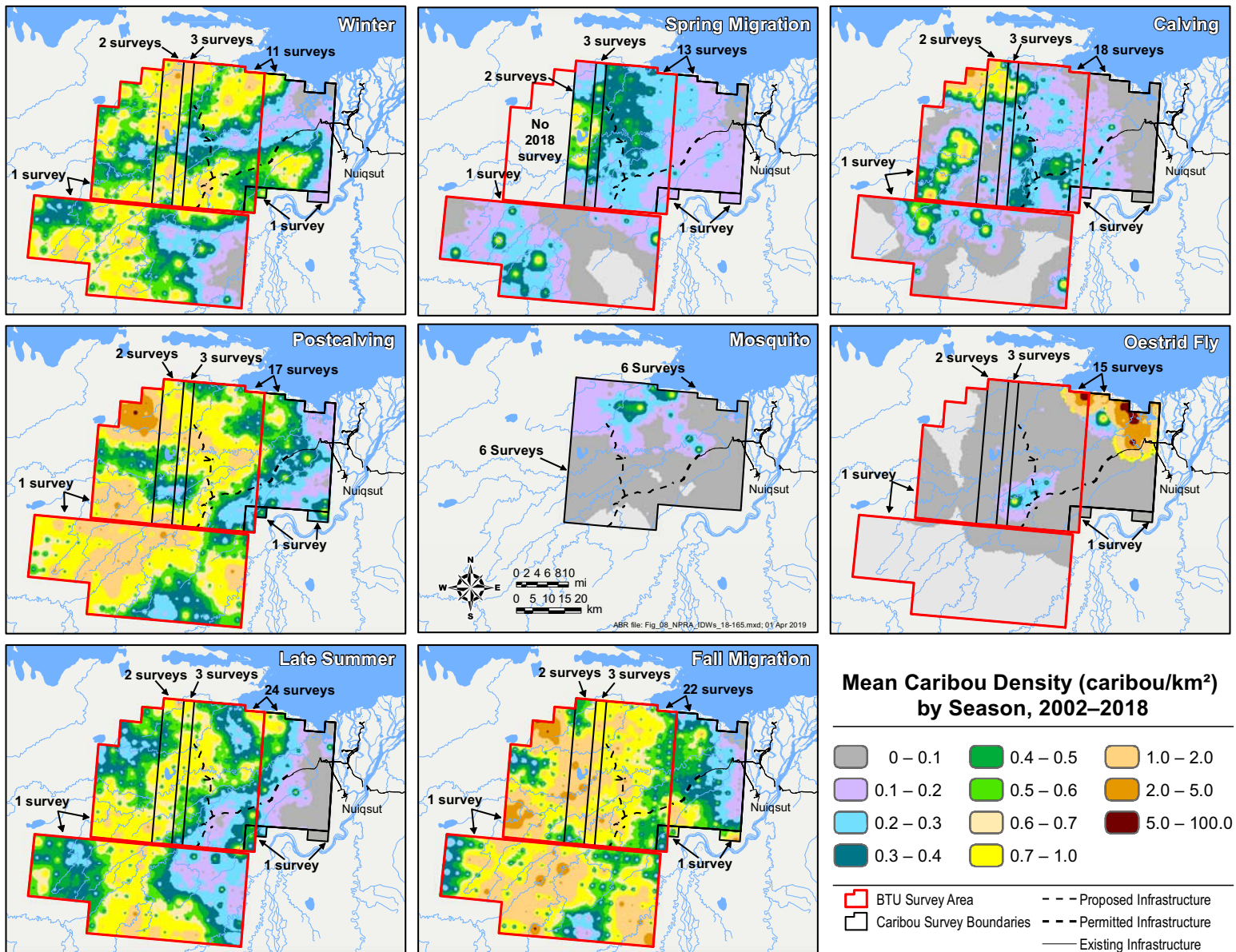


Figure 8. Mean seasonal densities of caribou in the NPRA caribou survey areas based on IDW interpolation of aerial survey results, 2002–2018.

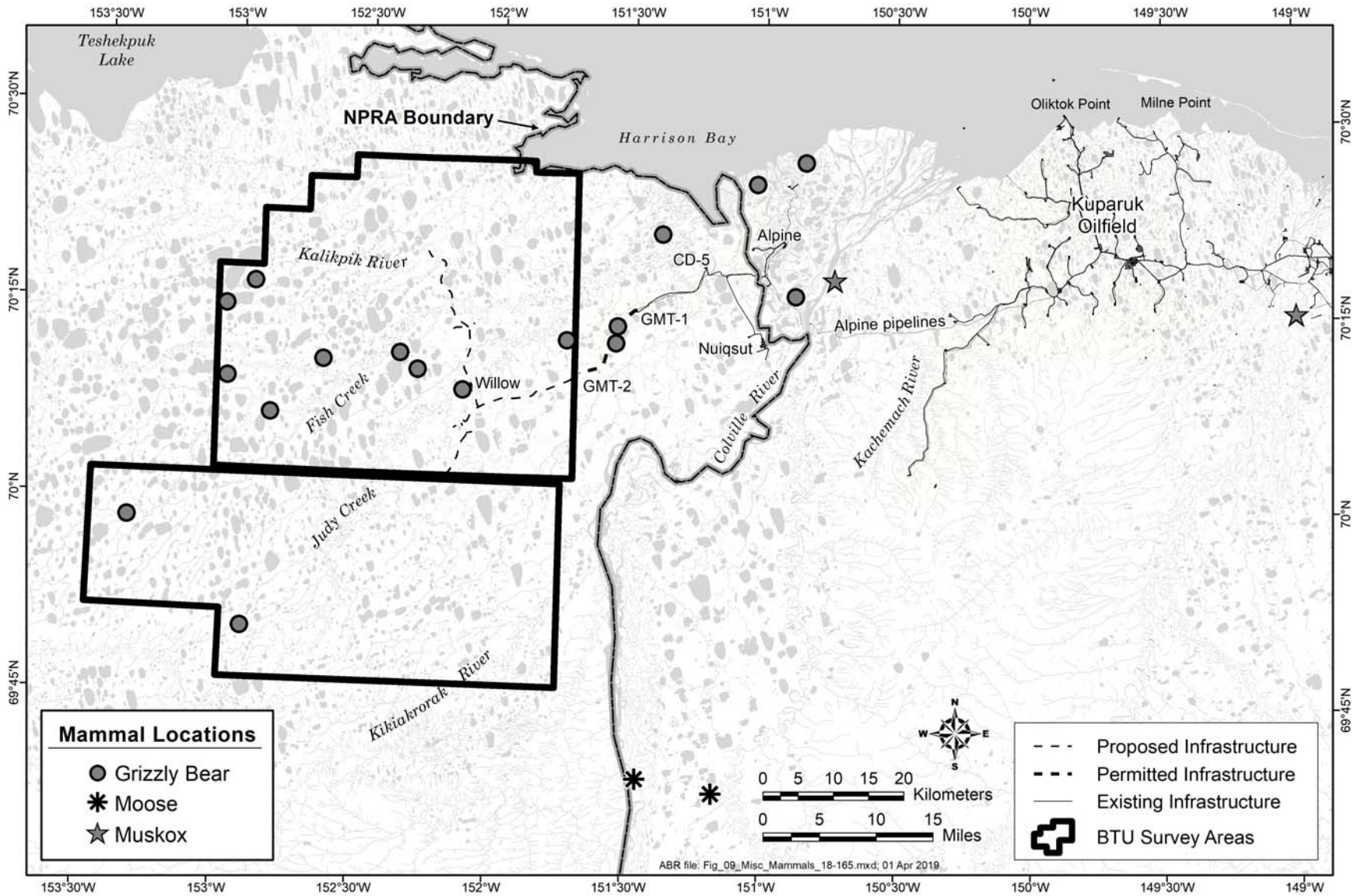


Figure 9. Distribution of other large mammals observed during aerial and ground surveys in the northeastern NPRA, June–September 2018.

Table 3. Location and number of other large mammals observed during aerial and ground wildlife surveys for CPAI, April–September 2018.

| General Location | Species | Date | Adults | Young | Total | Specific Location |
|-----------------------|------------|--------------|--------|-------|-------|-------------------|
| Bear Tooth North | Brown Bear | June 22 | 1 | 3 | 4 | Central |
| | | June 23 | 1 | 0 | 1 | East-central |
| | | June 25 | 2 | 0 | 2 | West-central |
| | | June 27 | 2 | 0 | 2 | Central |
| | | August 17 | 1 | 0 | 1 | SE |
| | | August 28 | 1 | 0 | 1 | SW |
| | | August 28 | 2 | 0 | 2 | Western |
| | | August 28 | 1 | 0 | 1 | SW |
| | | August 28 | 1 | 0 | 1 | West-central |
| Bear Tooth South | Brown Bear | July 31 | 1 | 0 | 1 | SW |
| | | September 24 | 1 | 0 | 1 | NW |
| Greater Moose's Tooth | Brown Bear | June 27 | 1 | 0 | 1 | SW of GMT-1 |
| | | July 1 | 1 | 0 | 1 | SW of GMT-1 |
| | | August 16 | 1 | 0 | 1 | Northern |
| Colville River Delta | Brown Bear | June 13 | 2 | 0 | 2 | CD 4 |
| | | June 15 | 1 | 0 | 1 | West of CD3 |
| | | June 17 | 1 | 0 | 1 | North of CD3 |
| | Muskox | 24 June | 20 | >1 | >20 | SE of Alpine |
| Colville South | Moose | July 31 | 1 | 0 | 1 | Southern |
| | | August 29 | 1 | 0 | 1 | Southern |
| Deadhorse Area | Muskox | August 1 | 3 | 0 | 3 | Near Deadhorse |

(primarily oestrid fly season) and fall migration, followed closely by winter and late summer (Figures 11–12). The least use of the area by collared TH caribou occurred during the spring migration, calving, and postcalving seasons.

Kernel Density Analysis

Seasonal concentration areas were analyzed using fixed-kernel density estimation, based on locations from satellite and GPS collars deployed on 249 TH females and 83 TH males during 1990–2018 and on 140 CAH females and 8 CAH males during 2001–2018. These numbers differ from the number of collar deployments listed earlier (Table 1) because some individuals switched herds after collaring. Kernels were used to produce 50%, 75%, and 95% utilization distribution contours (isopleths), which depict gradations in caribou density for female CAH

caribou and for both sexes of TH caribou (Figures 13–15); the sample size of CAH males was too small for this analysis.

Female CAH caribou generally wintered between the Dalton Highway/TAPS corridor and Arctic Village, migrated north in the spring to calve in two areas on either side of the Sagavanirktok River, spent the mosquito season near the coast (mostly east of Deadhorse), and dispersed across the coastal plain on both sides of the Sagavanirktok River and Dalton Highway/TAPS corridor during the oestrid fly and late summer seasons (Figure 13).

TH caribou generally wintered on the Arctic Coastal Plain between Nuiqsut and Wainwright or in the central Brooks Range near Anaktuvuk Pass, migrated to their calving grounds near Teshekpuk Lake, and spent the rest of the summer on the coastal plain, primarily between Nuiqsut and

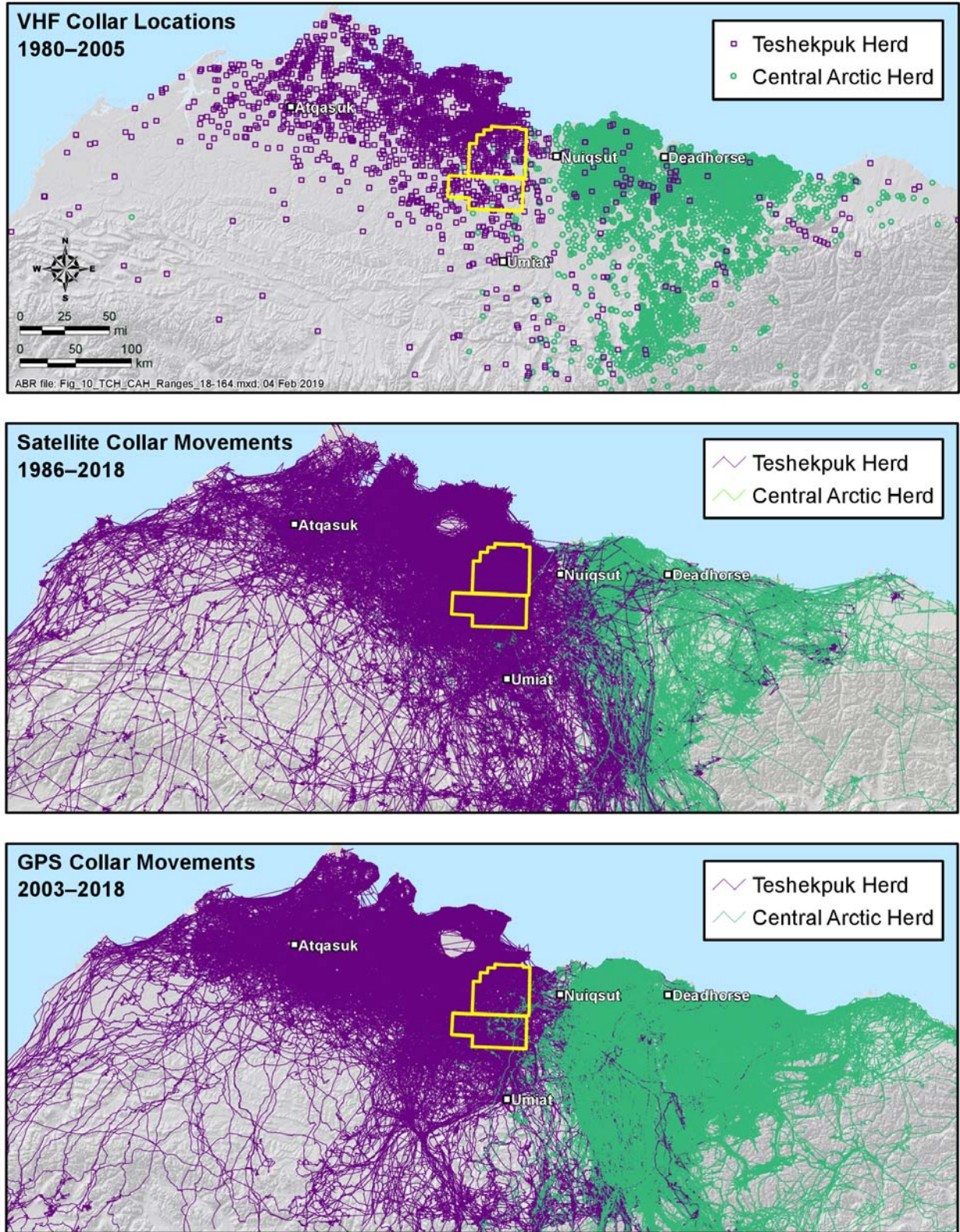


Figure 10. Ranges of TH and CAH caribou in northern Alaska in relation to the study areas, based on VHF, satellite, and GPS radio-telemetry, 1980–2018.

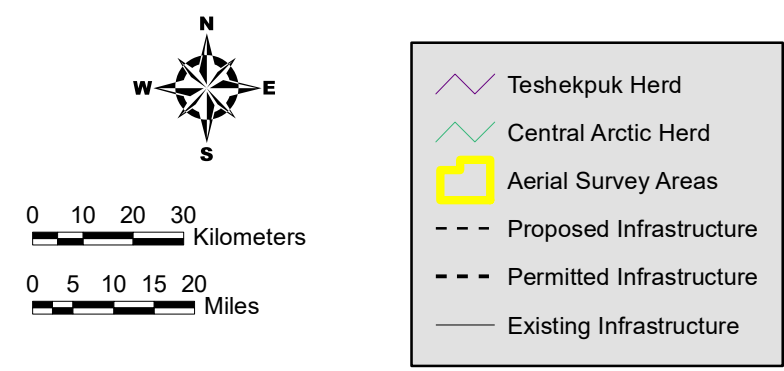
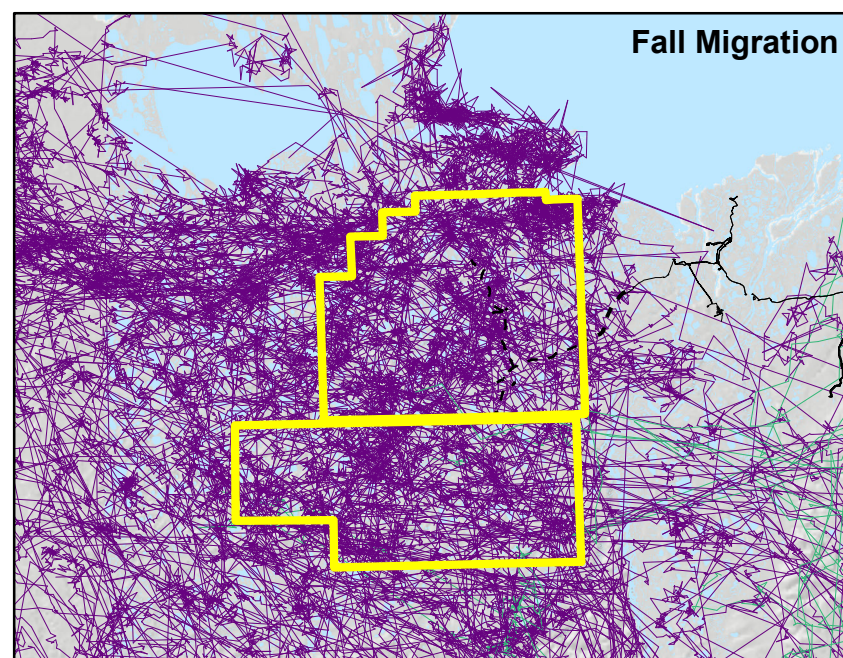
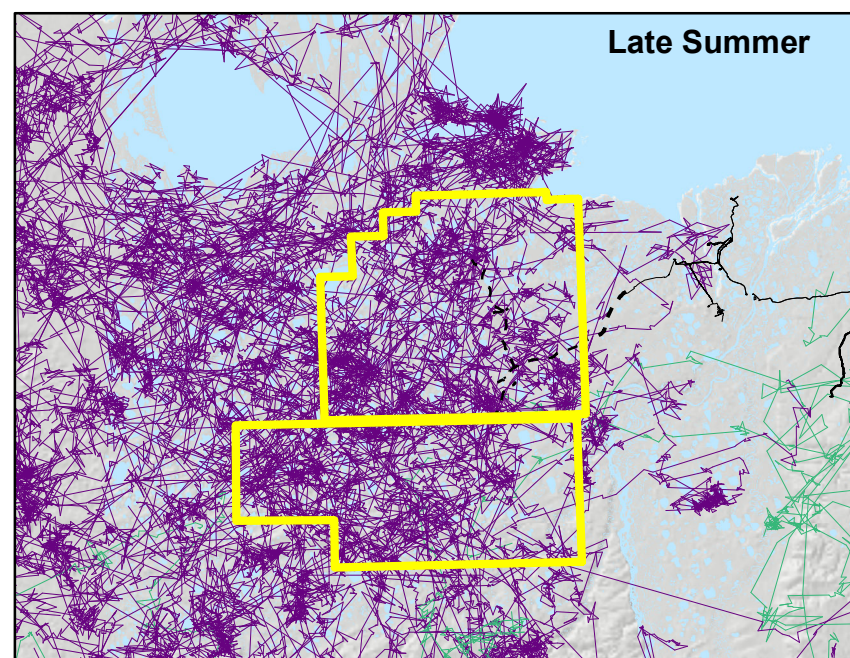
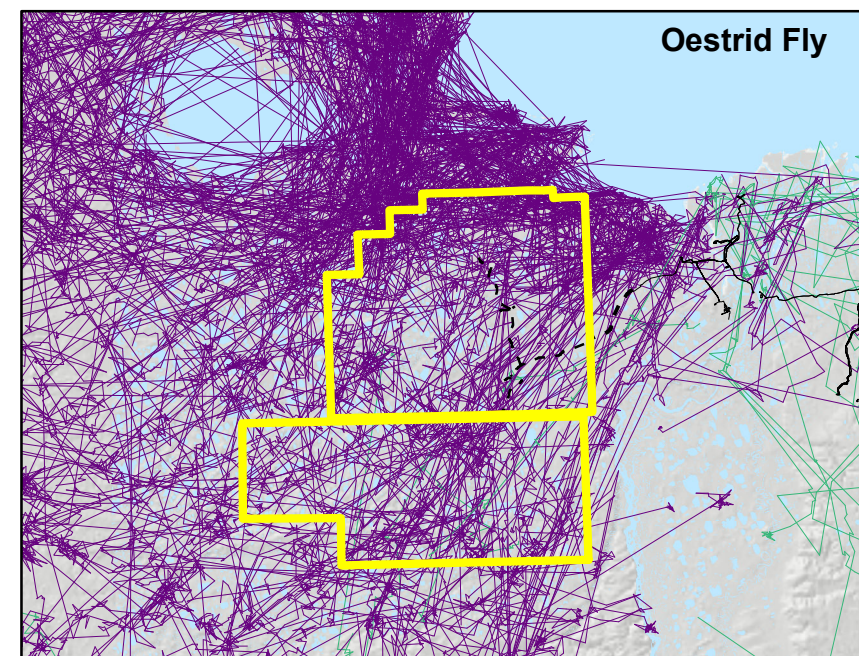
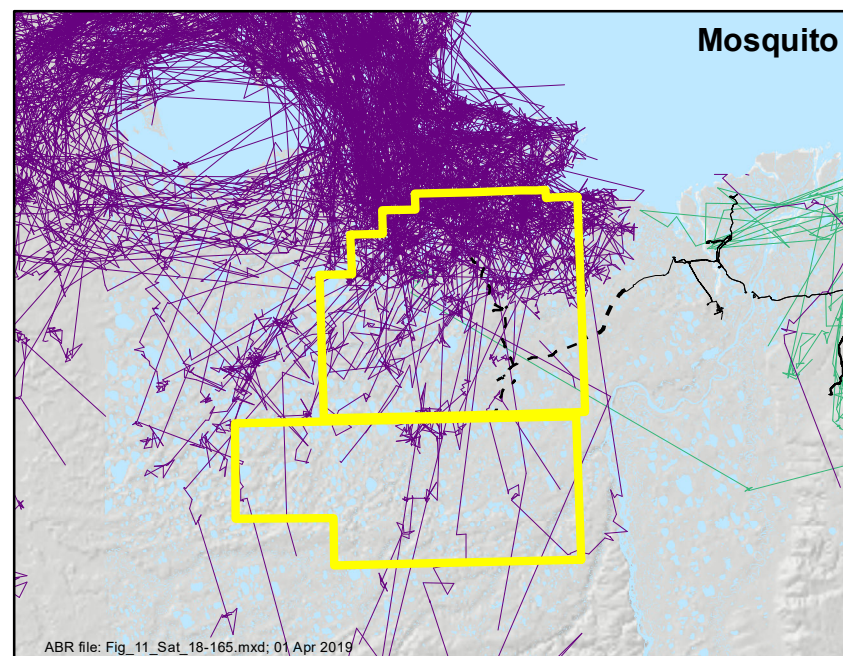
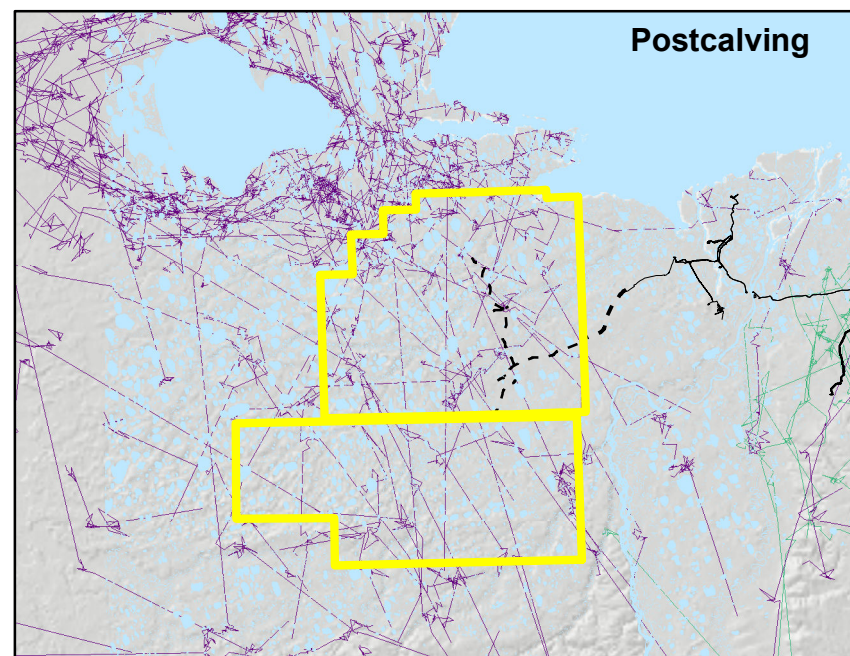
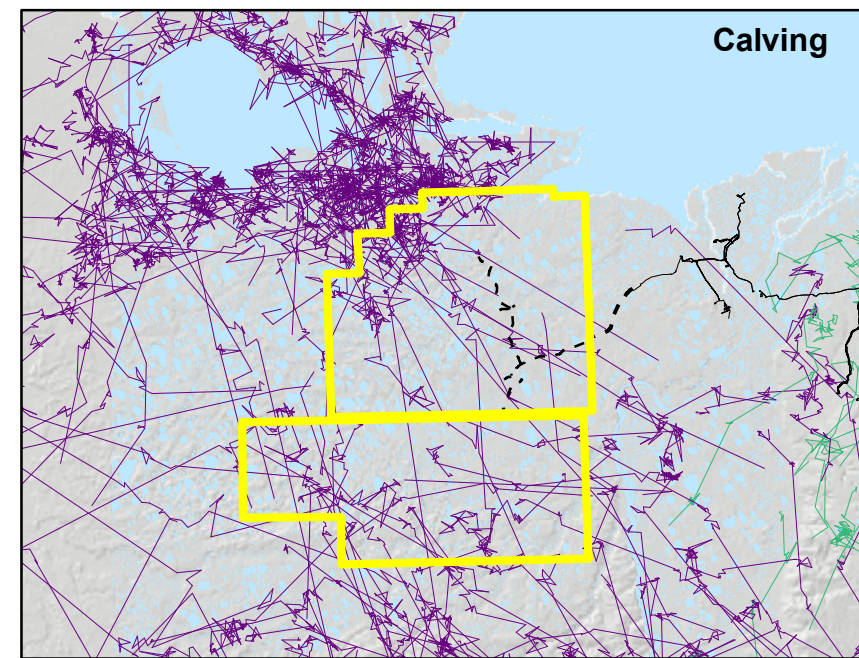
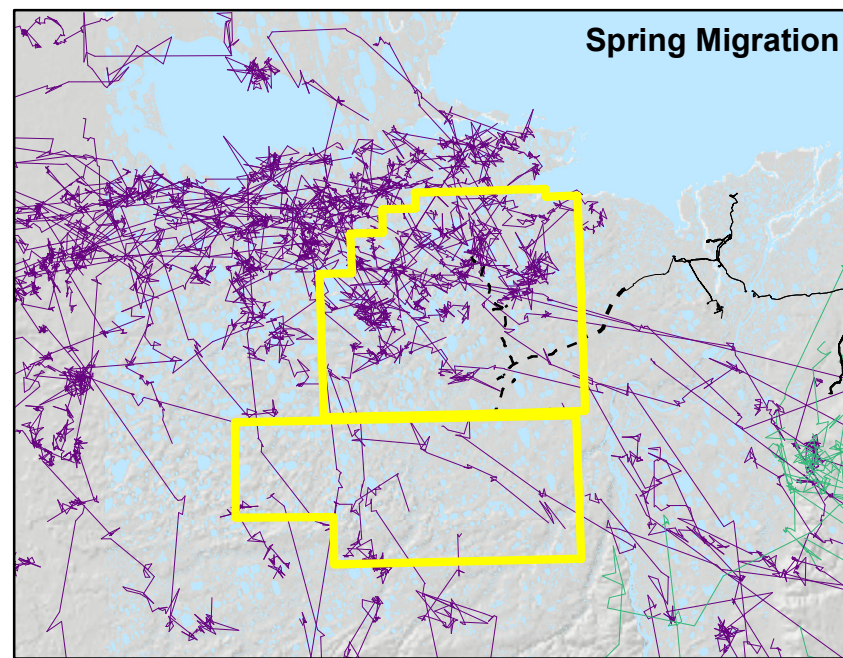
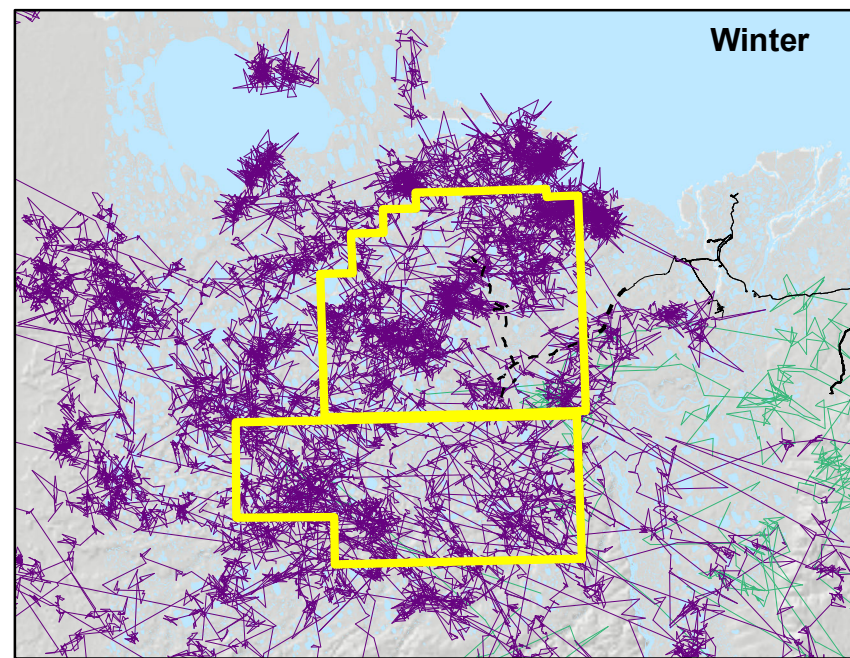


Figure 11.
Movements of satellite-collared caribou
from the TH (1990–2018) and CAH
(1986–1990 and 2001–2015) in the Bear Tooth
North and South survey areas during each of
eight seasons.

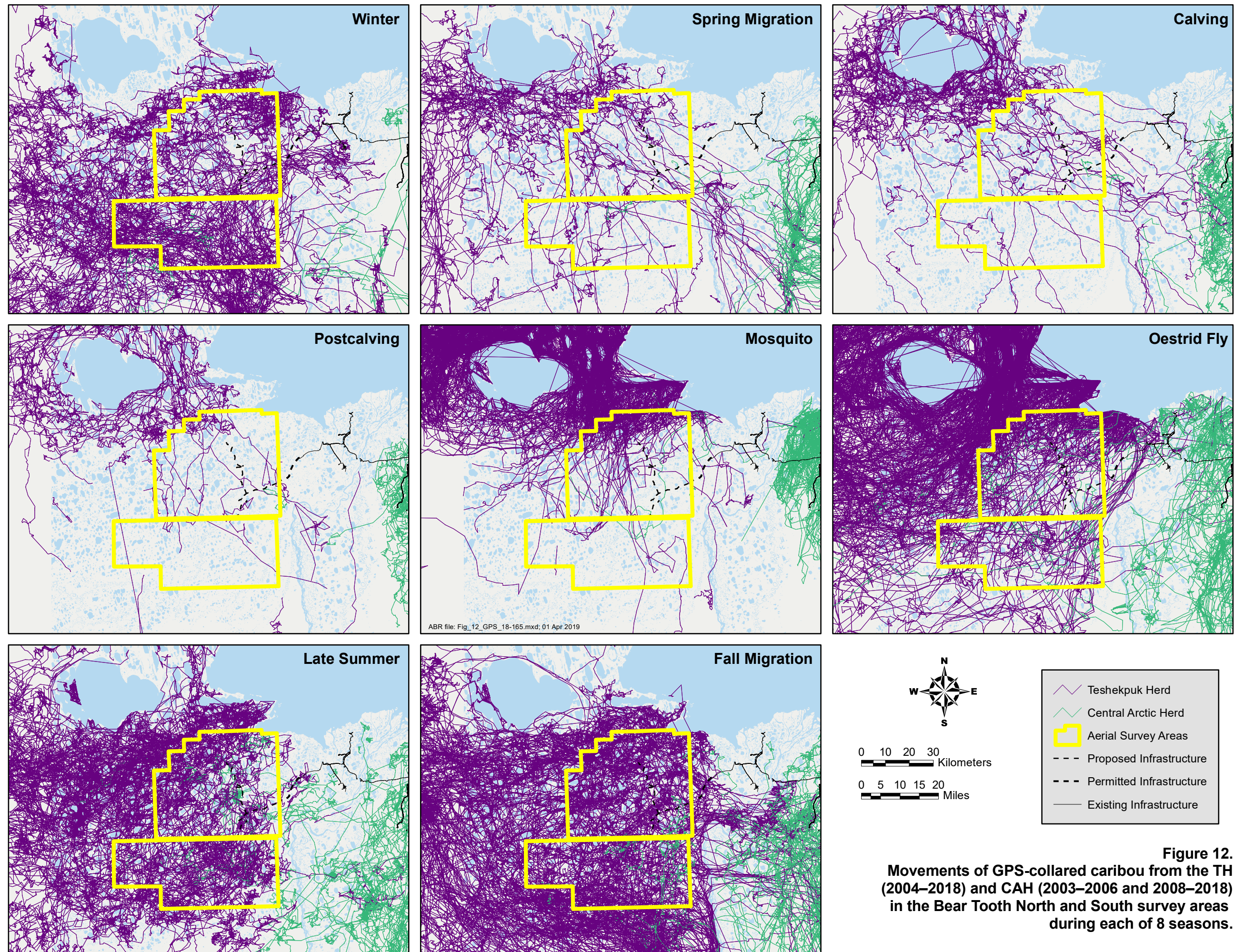


Figure 12.
Movements of GPS-collared caribou from the TH (2004–2018) and CAH (2003–2006 and 2008–2018) in the Bear Tooth North and South survey areas during each of 8 seasons.

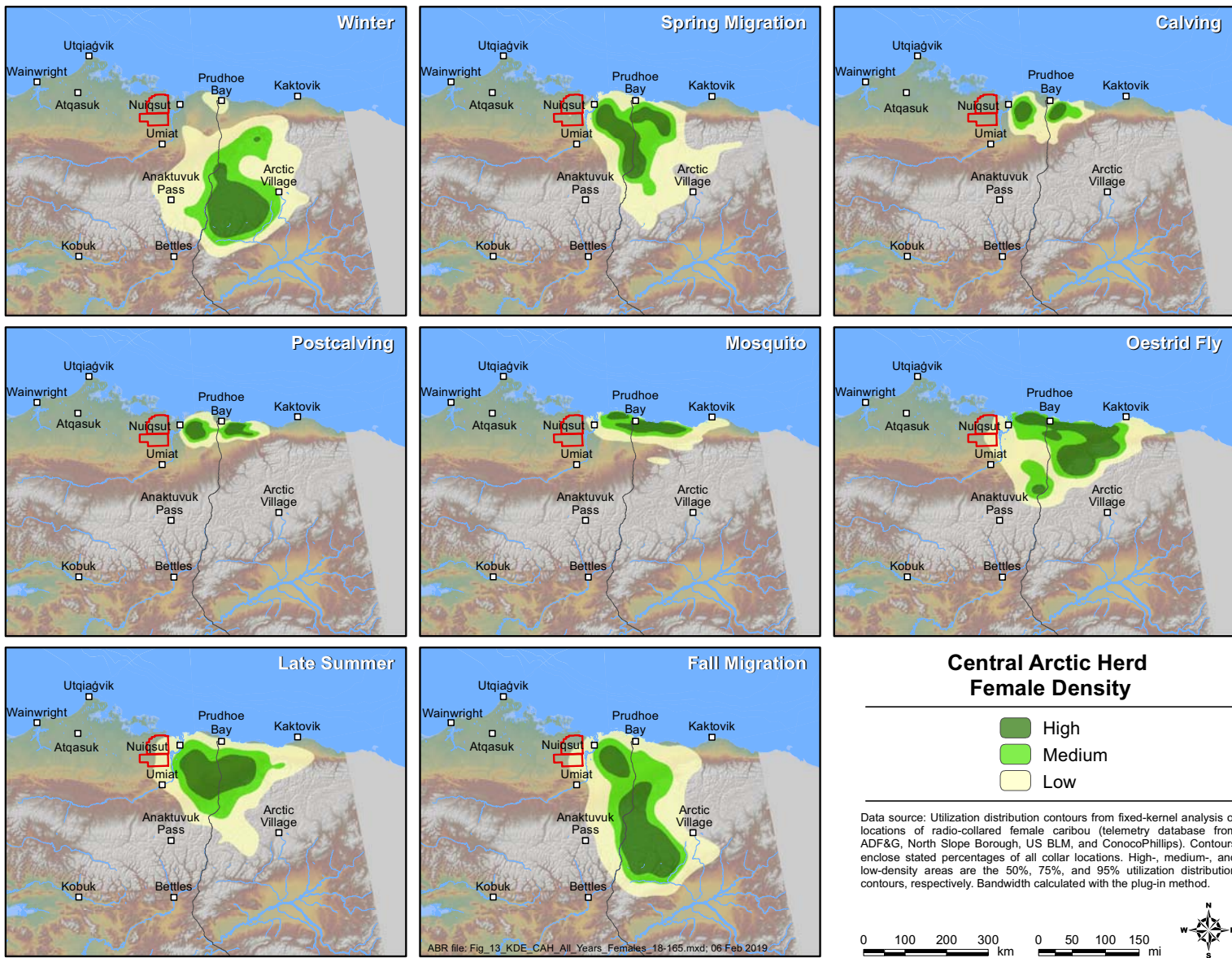


Figure 13. Seasonal distribution of CAH females based on fixed-kernel density estimation of telemetry locations, 2001–2018.

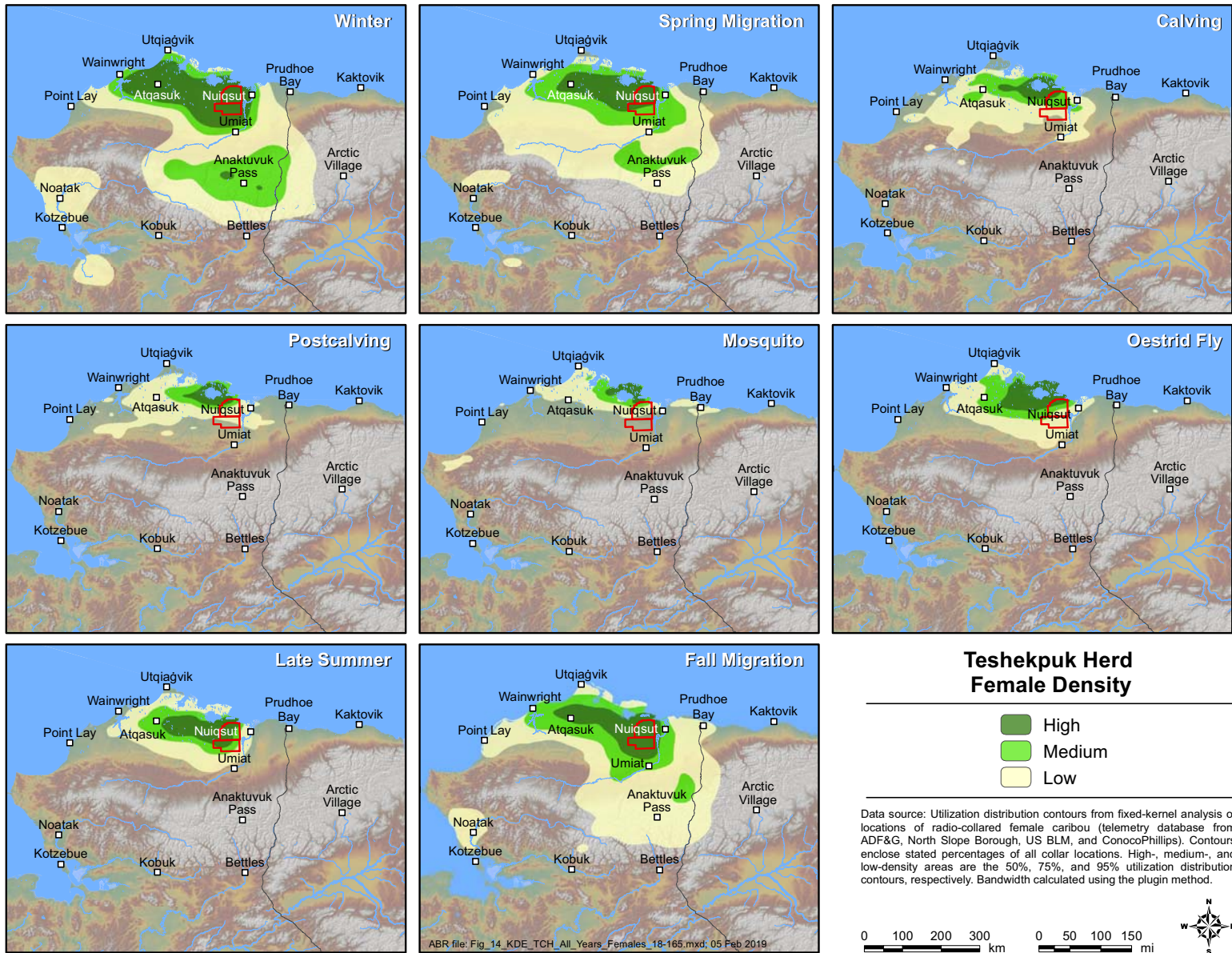


Figure 14. Seasonal distribution of TH females based on fixed-kernel density estimation of telemetry locations, 1990–2018.

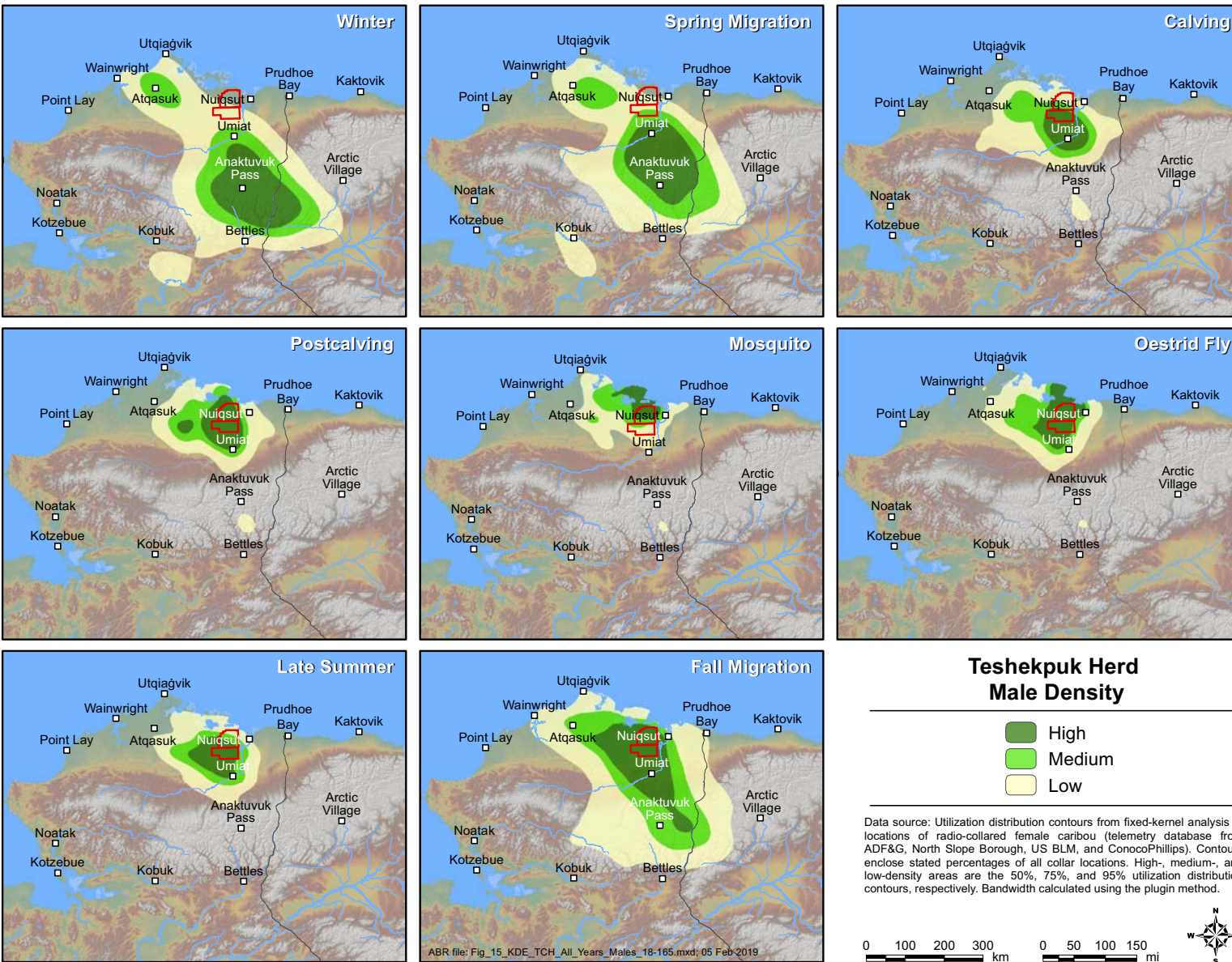


Figure 15. Seasonal distribution of TH males based on fixed-kernel density estimation of telemetry locations, 1997–2018.

Atqasuk (Figures 14–15). Compared with females, males tended to overwinter in the central Brooks Range instead of on the coastal plain more frequently, migrated to the summer range later in the year during the calving and postcalving seasons, and were not distributed as far west during summer (Figures 15). The distribution of parturient TH females during calving (Figure 16) was similar to the distribution of all TH females during calving (Figure 14), but was more concentrated around Teshekpuk Lake.

Examination of the percentage of kernel densities by month showed that collared TH females used the BTN survey area at consistently low levels (4.1–13.8% of total utilization) throughout the year, with the highest level of use

occurring in September (Figure 17). Use of the BTN survey area by TH males increased sharply from May to a peak in July (16.7% of the utilization distribution) during the oestrid fly season. Use by males dipped in August (5.5%) but then rose again in September (11.7%) during the onset of the fall migration before dropping below 1% by November as males migrated into the foothills and mountains of the Brooks Range or toward Atqasuk during the winter (Figure 15). In contrast, there was almost no use (0.0%–0.6%) of the BTN survey area by collared CAH females throughout the year (Figures 13 and 17).

TH females used the BTS survey area at consistently low levels (2.3%–5.6% of total utilization) with the exception that females tend to

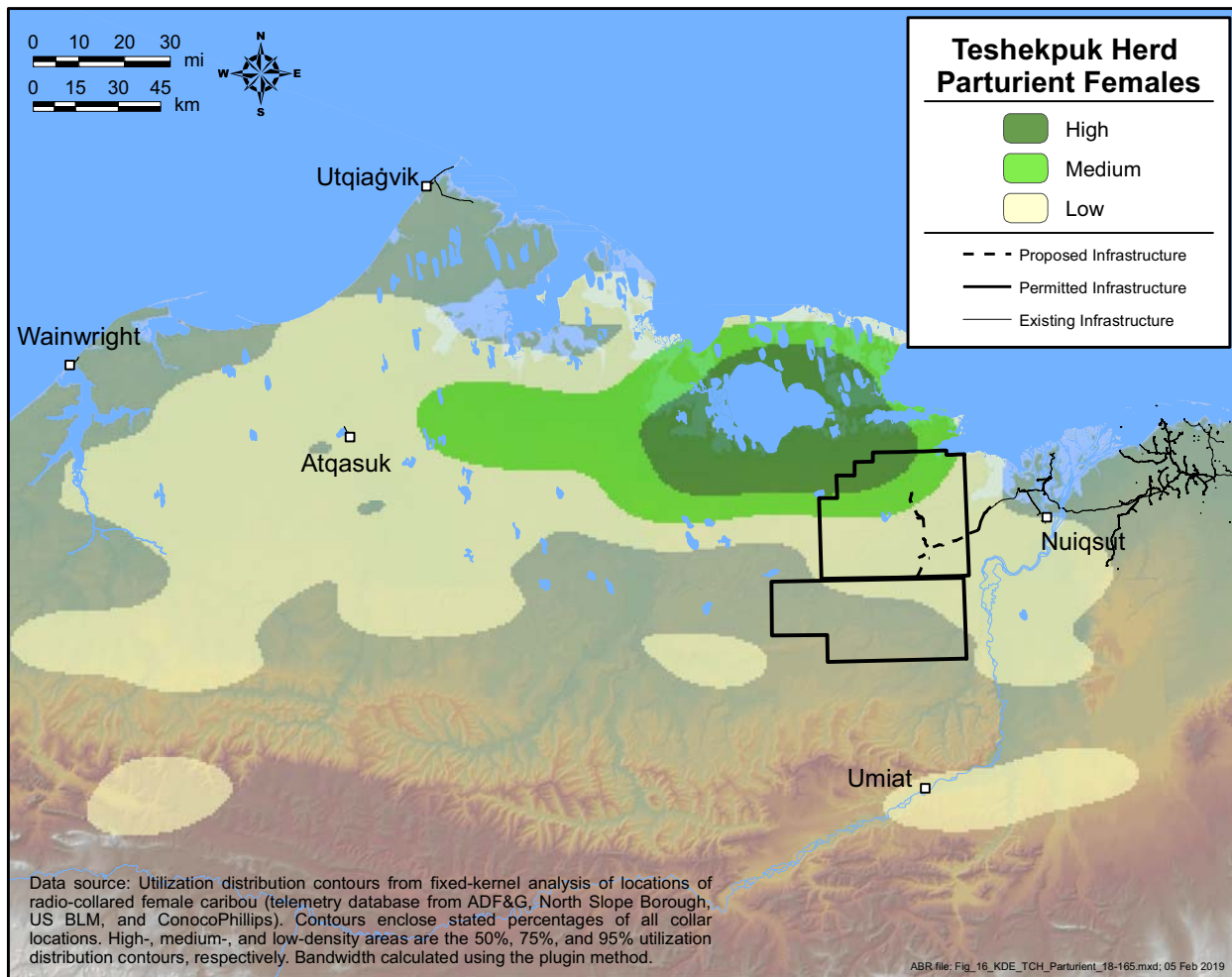


Figure 16. Distribution of parturient females of the Teshekpuk Herd during calving based on fixed-kernel density estimation of telemetry locations, 1990–2018.

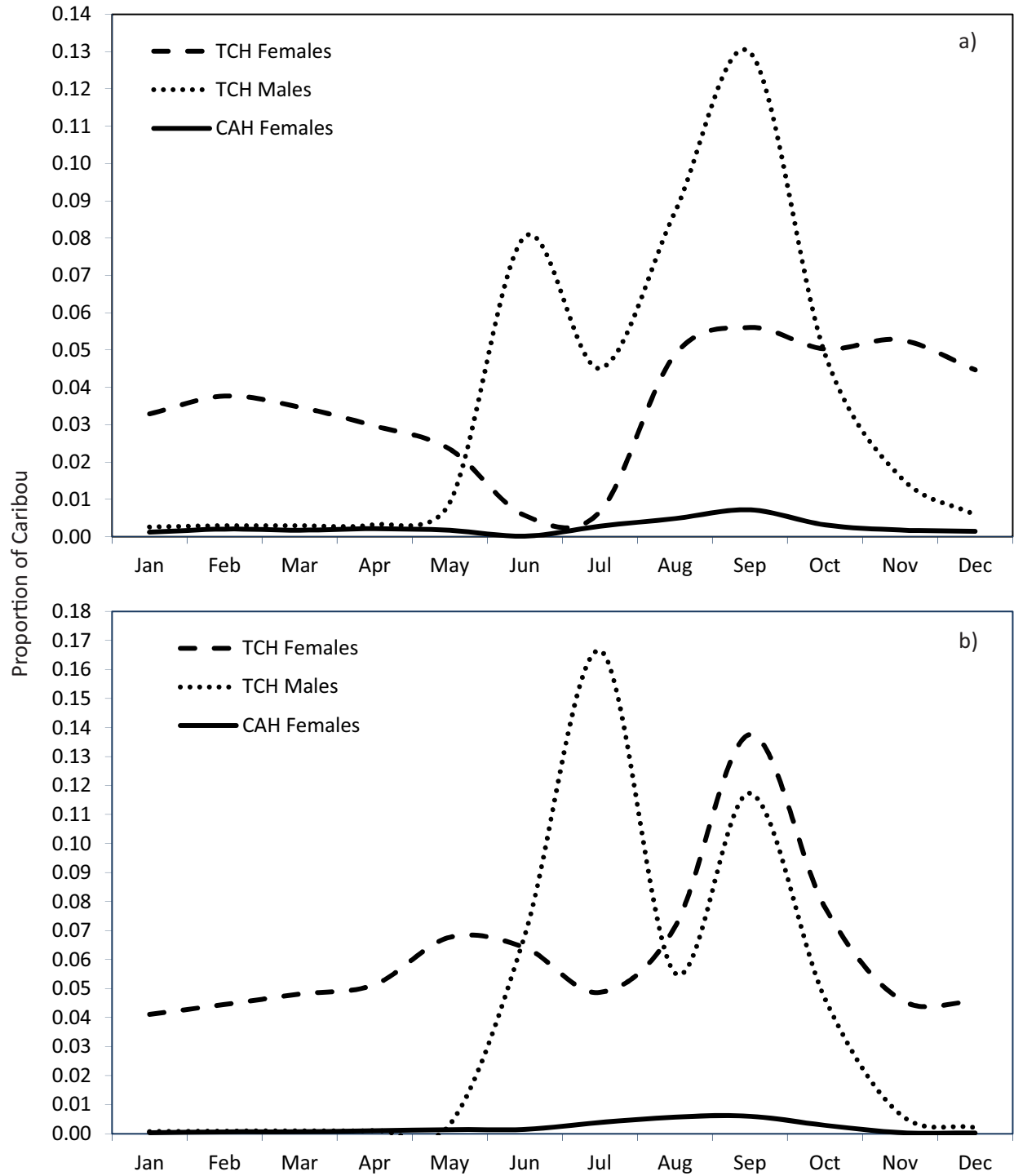


Figure 17. Proportion of CAH and TH caribou within the BTN (top) and BTS (bottom) survey areas, based on fixed-kernel density estimation, 1990–2018.

use the survey area very little (0.6%–0.7%) during June and July when caribou are farther to the north for calving and insect relief (Figures 14 and 17). Use of the survey area by males followed a similar pattern to use of the BTN survey area with little use from November through May (0.3%–1.6%) when males are in their winter ranges, and moderate use (4.5%–13.0%) from June through October. When compared to the BTN survey area, use of BTS was greater in June as males are still migrating north from their winter range, lower in July when caribou are closer to the coast for mosquito relief and higher in August and September when caribou disperse inland as insect harassment abates. There was almost no use (0.0%–0.7%) of the BTN survey area by collared CAH females throughout the year (Figures 13 and 17).

dBBMM

Mapping of movements derived from the dBBMMs by TH caribou in the study area shows that TH females use the BTU survey areas during all seasons, although their use of the area and movement rates vary widely among seasons (Figure 18). During winter, caribou are distributed widely but show low rates of movement. During the spring migration and calving seasons, TH females move across the study area from southeast to northwest as they migrate toward the core calving area bordering Teshekpuk Lake. During the postcalving and mosquito seasons, caribou largely remain west and north of the study area, often traversing the narrow corridors between Teshekpuk Lake and the Beaufort Sea (Yokel et al. 2009). During the oestrid fly season, TH females move rapidly, but tend to disperse inland away from Teshekpuk Lake, with occasional large movements through the survey areas. During late summer, caribou are usually found dispersed inland with the highest densities in the western portions of the survey areas. TH caribou disperse widely during fall migration, including throughout much of the survey areas.

Movements Near Proposed Willow Infrastructure

Movements by collared TH and CAH caribou near proposed Willow infrastructure have occurred more frequently than movements near existing and proposed infrastructure in the GMT and CRD study areas to the east (Figure 19). Percentages of

utilization distributions within 4 km of roads and pads ranged from 0.0%–3.1% with notable differences by sex (Figure 20). Males were most likely to be within 4 km of proposed roads and pads from July through October with almost no occurrence after the fall migration, whereas females maintained a similar presence for most of the winter months, a decrease in occurrence in July and August, and an increase in occurrence in October and November.

Analysis of GPS collars from 2002 through 2018 indicates that there were 477 crossings of the proposed Willow road alignment from 2000–2018. Up to 46.2% of collared caribou cross the proposed Willow road alignment in a given season (Table 4). The highest proportion of collared caribou crossings was during the fall migration season (4.5–46.2%) followed by the spring migration season (0.0–22.7%) and oestrid fly season (0.0–33.3%). The lowest proportion of TH crossings was during the postcalving and mosquito seasons (0.0–4.8%).

AERIAL PHOTOGRAPHY

Flights to test the feasibility of using cameras mounted on survey aircraft to identify caribou were planned for five surveys in 2018. TerraSond provided a report detailing the results of those efforts, which has been included as an appendix to this report (Appendix C). Briefly, TerraSond tested color imagery (RGB) and near-infrared (NIR) cameras while flying at various flight altitudes with cameras directed both vertically and at an oblique angle. Cameras were tested during the spring migration, calving, postcalving, oestrid fly, and fall migration surveys. During the first three surveys, the pilot controlled the cameras (RGB only) from a tablet and photos were recorded during aerial surveys and while in transit to and from Deadhorse. On the final two surveys, camera arrays were more complex (NIR, NIR+RGB) requiring TerraSond technicians to be present during the flights. It was therefore not feasible to collect photos while conducting aerial surveys and dedicated flights after aerial surveys were conducted with the sole purpose of collecting imagery instead. One to two TerraSond technicians accompanied by one ABR biologist collected data during these two test flights.

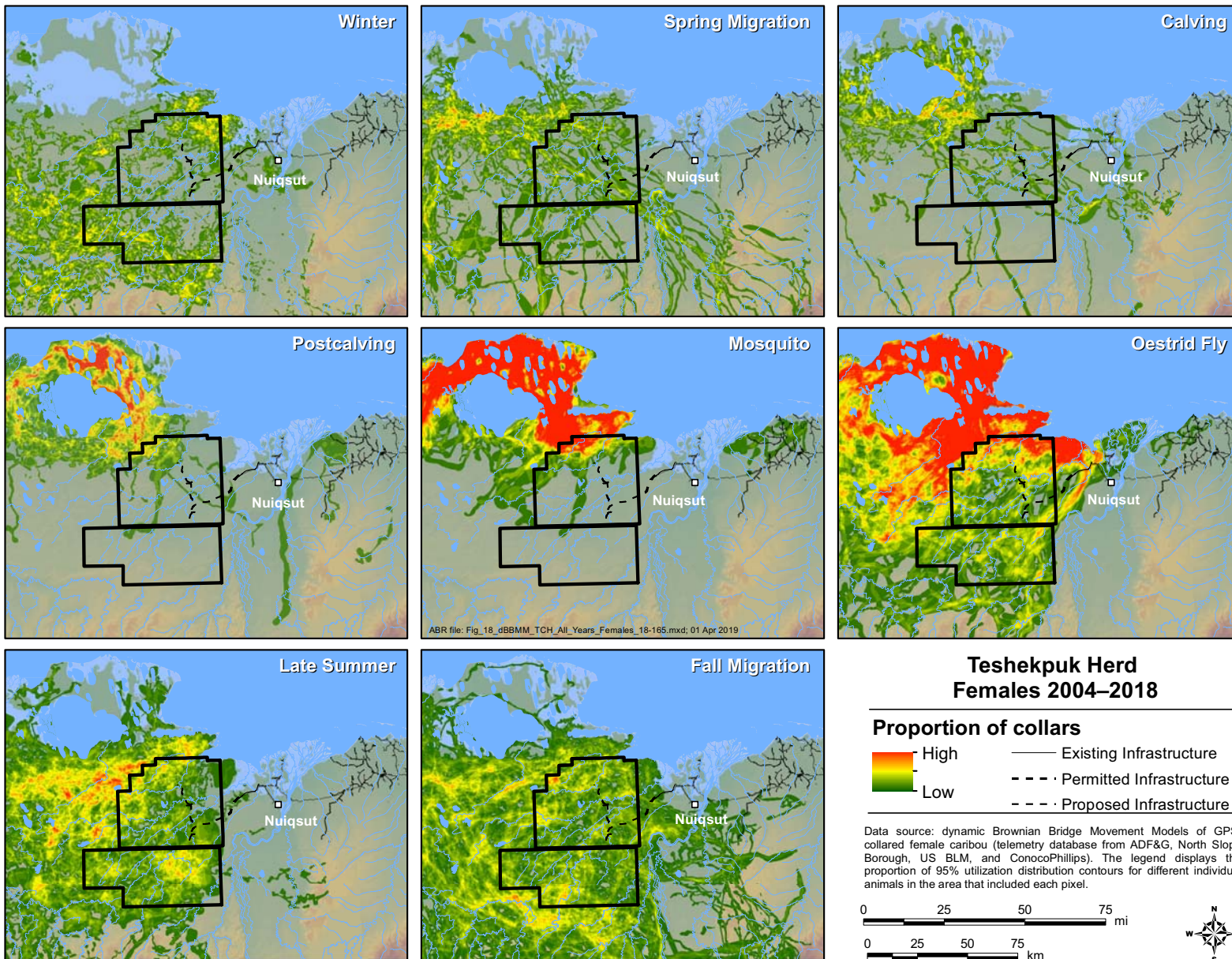


Figure 18. Movements of GPS-collared TH caribou based on 95% isopleths of dynamic Brownian Bridge movement models.

Table 4. Proportion of collared Teshekpuk Herd caribou that crossed the proposed Willow alignment at least once in each season, 2000–2018. Numbers in parenthesis indicate the number of collared caribou used in the analysis.

| Year | Spring Migration | Calving | Postcalving | Mosquito | Oestrud Fly | Late Summer | Fall Migration | Winter |
|-----------|------------------|------------|-------------|------------|-------------|-------------|----------------|------------|
| 2000–2004 | | | | | | 0.00 (10) | 0.30 (10) | 0.20 (10) |
| 2005–2009 | 0.00 (49) | 0.12 (49) | 0.00 (49) | 0.00 (31) | 0.33 (39) | 0.09 (76) | 0.11 (75) | 0.01 (67) |
| 2010–2014 | 0.04 (89) | 0.04 (84) | 0.03 (71) | 0.01 (85) | 0.08 (86) | 0.02 (122) | 0.10 (115) | 0.03 (96) |
| 2015 | 0.10 (21) | 0.06 (18) | 0.00 (14) | 0.00 (16) | 0.07 (15) | 0.08 (25) | 0.46 (26) | 0.04 (23) |
| 2016 | 0.23 (22) | 0.05 (22) | 0.00 (18) | 0.00 (19) | 0.05 (21) | 0.00 (43) | 0.15 (48) | 0.00 (42) |
| 2017 | 0.03 (39) | 0.03 (36) | 0.00 (26) | 0.00 (38) | 0.00 (39) | 0.00 (72) | 0.04 (67) | 0.02 (63) |
| 2018 | 0.04 (54) | 0.04 (52) | 0.05 (21) | 0.03 (62) | 0.00 (58) | 0.07 (83) | 0.14 (78) | |
| All Years | 0.05 (274) | 0.05 (261) | 0.02 (199) | 0.01 (251) | 0.09 (258) | 0.04 (431) | 0.13 (419) | 0.03 (301) |

As described in the Terrasond report (Appendix C), results from the first three flights indicated that RGB cameras were capable of collecting high resolution imagery with adequate resolution to define caribou from >500 ft agl, especially in seasons where there is high contrast between caribou pelage and the background terrain (winter through postcalving seasons). However, it was determined that a NIR camera would likely be necessary for computer identification, as NIR imagery helps differentiating background vegetation from darker caribou pelage when contrast between the two is low (midsummer through the first snowfall). Although few caribou were in the area during the oestrud fly season survey, results from the NIR camera showed good potential, and a NIR+RGB camera array was used during the fall migration survey. Results of this last effort were mixed. It appeared that the combination of the two camera types would likely be useful in collecting imagery suitable for automated caribou counts, however, photos would likely need to be taken from a vertical position which would limit the swath width of imagery that can be collected at certain elevations. Additionally, flight speeds may need to be low (~70 mph) to collect sharp imagery with the NIR camera. This flight speed is only slightly above the stall speed of a Cessna 206 aircraft and therefore could only be safely achieved when flying into a headwind. Technological alternatives will be explored in the coming months to determine if there are ways to circumvent these limitations.

REMOTE SENSING

Because MODIS imagery covers large areas at a relatively coarse resolution (250- to 500-m pixels), it was possible to evaluate snow cover and vegetation indices over a much larger region extending beyond the study area with no additional effort or cost. The region evaluated extends from the western edge of Teshekpuk Lake east to the Canada border and from the Beaufort Sea inland to the northern foothills of the Brooks Range. The ability to examine this large region allowed us to place the study area into a larger geographic context in terms of the chronology of snow melt and vegetation green-up, both of which are environmental variables that have been reported to be important factors affecting caribou distribution in northern Alaska.

Snow Cover

Based on observations from survey crews and records from weather stations in the area (Figure 6; Appendix B), the timing of snow melt was later than average for most of the region in 2018. However, due to persistent cloud cover during early June, there was little satellite imagery available to determine the exact timing or regional pattern of snow melt (Figure 21).

The median dates of snow melt for each pixel computed using 2000–2018 data (where the date of melt was known within one week) indicate that nearly all of the snow on the coastal plain typically melted over a period of three weeks between 25 May and 11 June (Figure 22; Appendix D). Snow

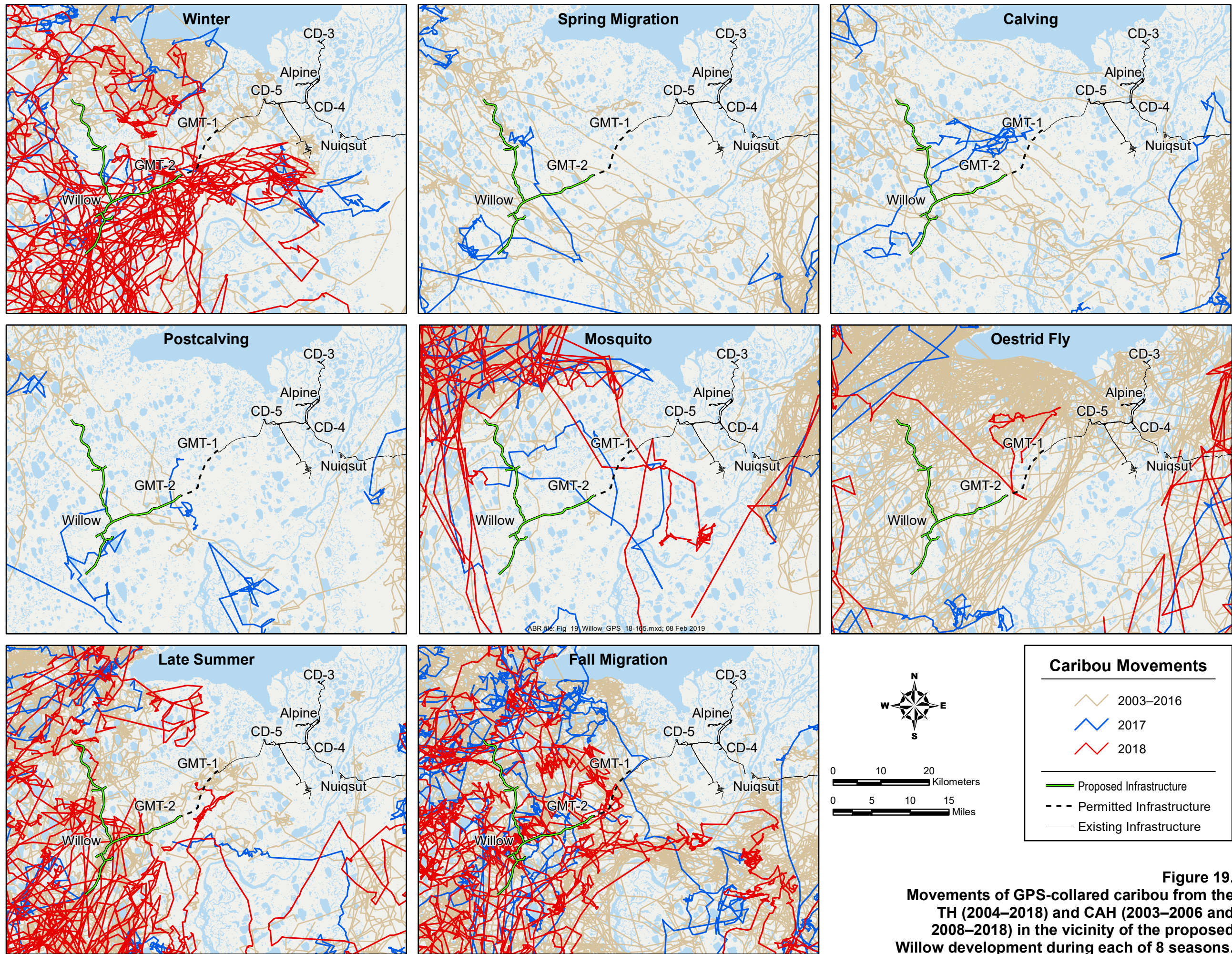


Figure 19.
Movements of GPS-collared caribou from the TH (2004–2018) and CAH (2003–2006 and 2008–2018) in the vicinity of the proposed Willow development during each of 8 seasons.

Page intentionally left blank.

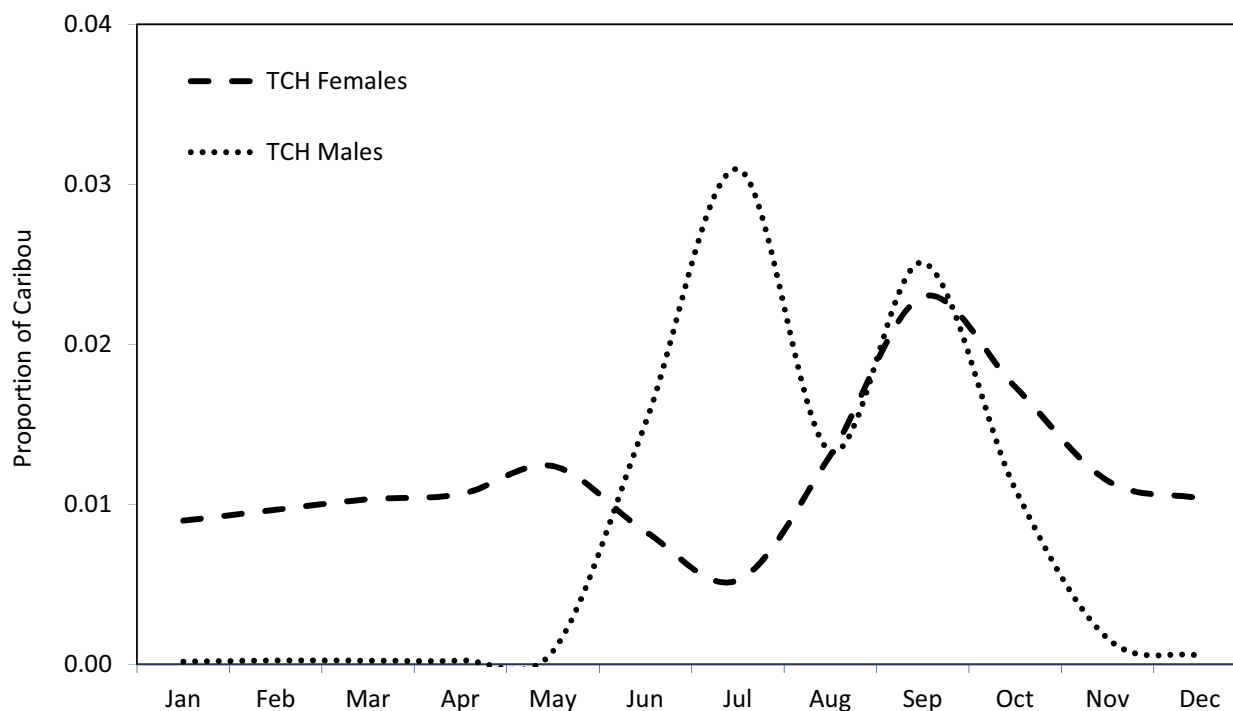


Figure 20. Proportion of TH caribou within 4 km of the proposed Willow development alignments, based on fixed-kernel density estimation, 1990–2018.

melt progressed northward from the foothills of the Brooks Range to the outer coastal plain, occurring earlier in the “dust shadows” of river bars and human infrastructure, and later in the uplands and numerous small drainage gullies southwest of the Kuparuk oilfield. The southern coastal plain, wind-scoured areas, and dust shadows typically melted during the last week of May (Figure 22). The central coastal plain and most of the Colville River delta usually melted in the first week of June, leaving snow on the northernmost coastal plain, in uplands, and in terrain features that trap snow, such as stream gullies. During the second week in June, most of the remaining snow melted, although some deep snow-drift remnants, lake ice, and aufeis persisted into early July (Figure 22). In the BTU survey areas, snow melt occurs earliest near stream channels and a south-to-north gradient was apparent, with snow typically melting several days later near the coast.

Previous comparisons of the performance of the MODIS subpixel-scale snow-cover algorithm with aggregated Landsat imagery suggest that the overall performance of the subpixel algorithm is

acceptable, but that accuracy degrades near the end of the period of snow melt (Lawhead et al. 2006).

VEGETATIVE BIOMASS

Compared with median NDVI since 2000 (Figures 23–24), the estimated vegetative biomass during calving (NDVI_Calving) and during peak lactation (NDVI_621) in 2018 was below average through much of the study area (Figures 23–24; Appendices E–F). Those values are consistent with the persistent snow cover observed during aerial surveys in early June. But peak NDVI was higher than average in 2018 (Figures 23–24; Appendix G), indicating that vegetation grew rapidly after late June. This is consistent with the above average temperatures recorded in much of July (Figure 4). NDVI_621 and NDVI_Peak in 2018 both showed the typical pattern of higher values inland and lower values along small rivers and creeks with exposed barren ground (Figure 24).

Although persistent cloud cover limited that area of analysis, NDVI_Rate in 2018 was low in inland areas closer to the Brooks Range with earlier snowmelt, but high along the coastal plain

Page intentionally left blank.

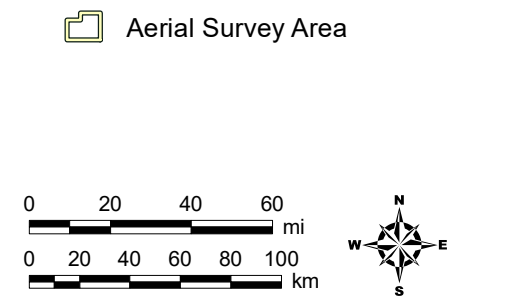
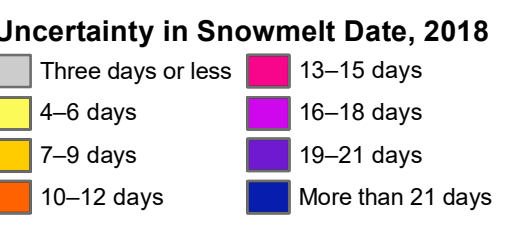
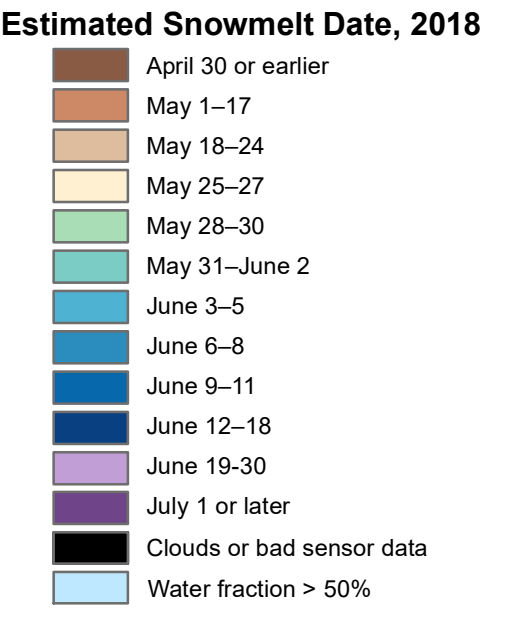
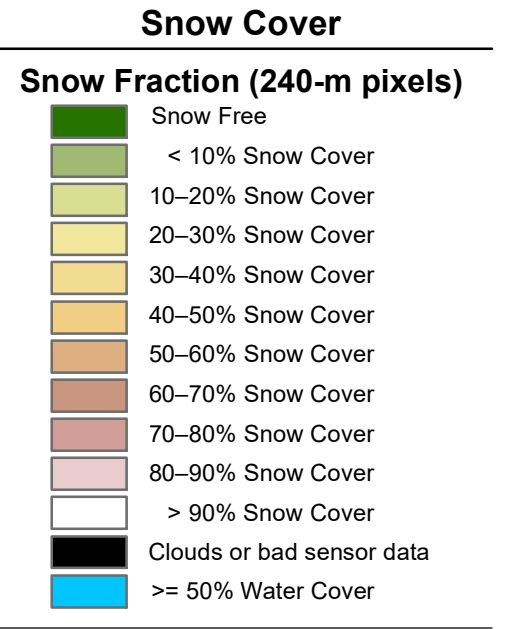
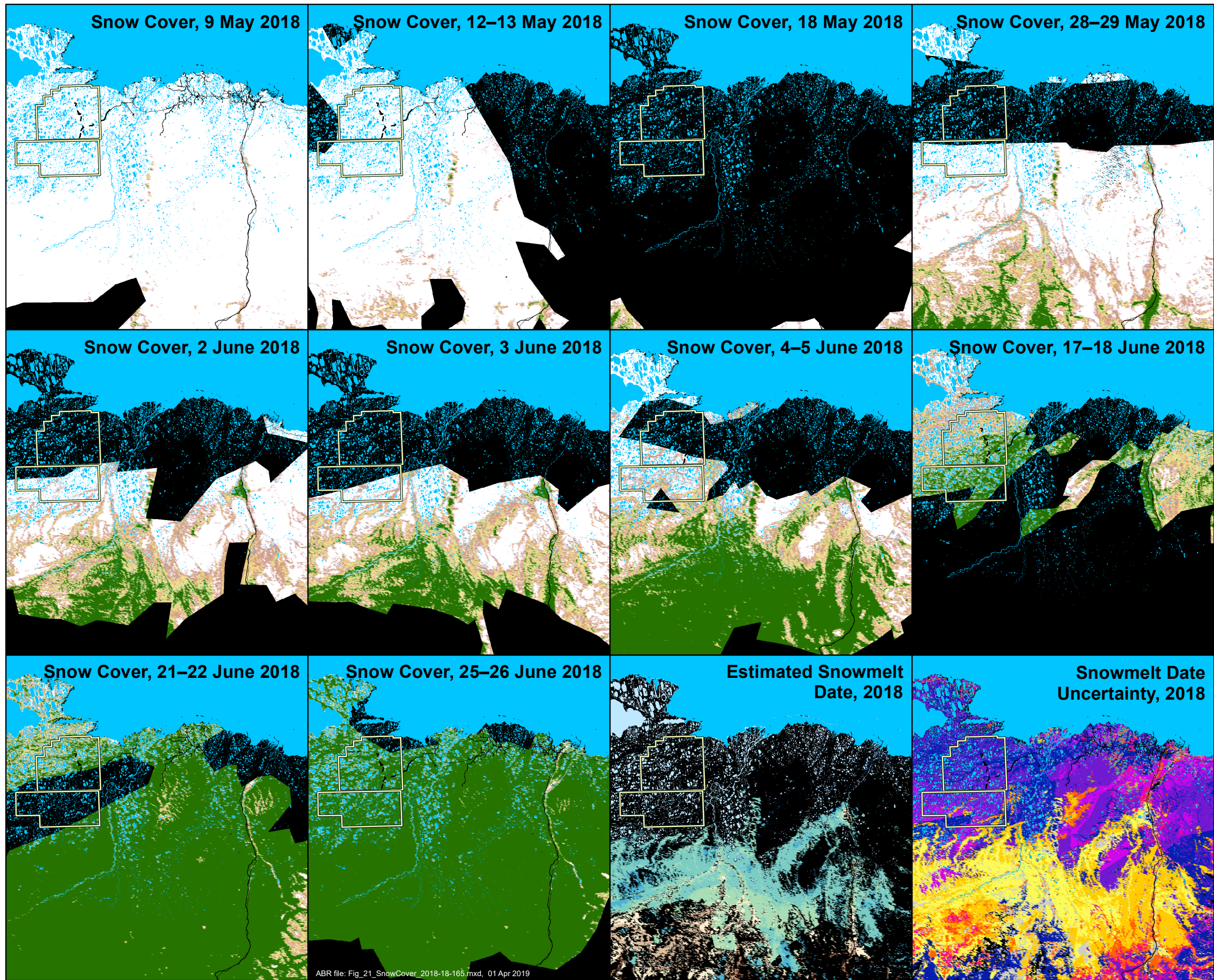
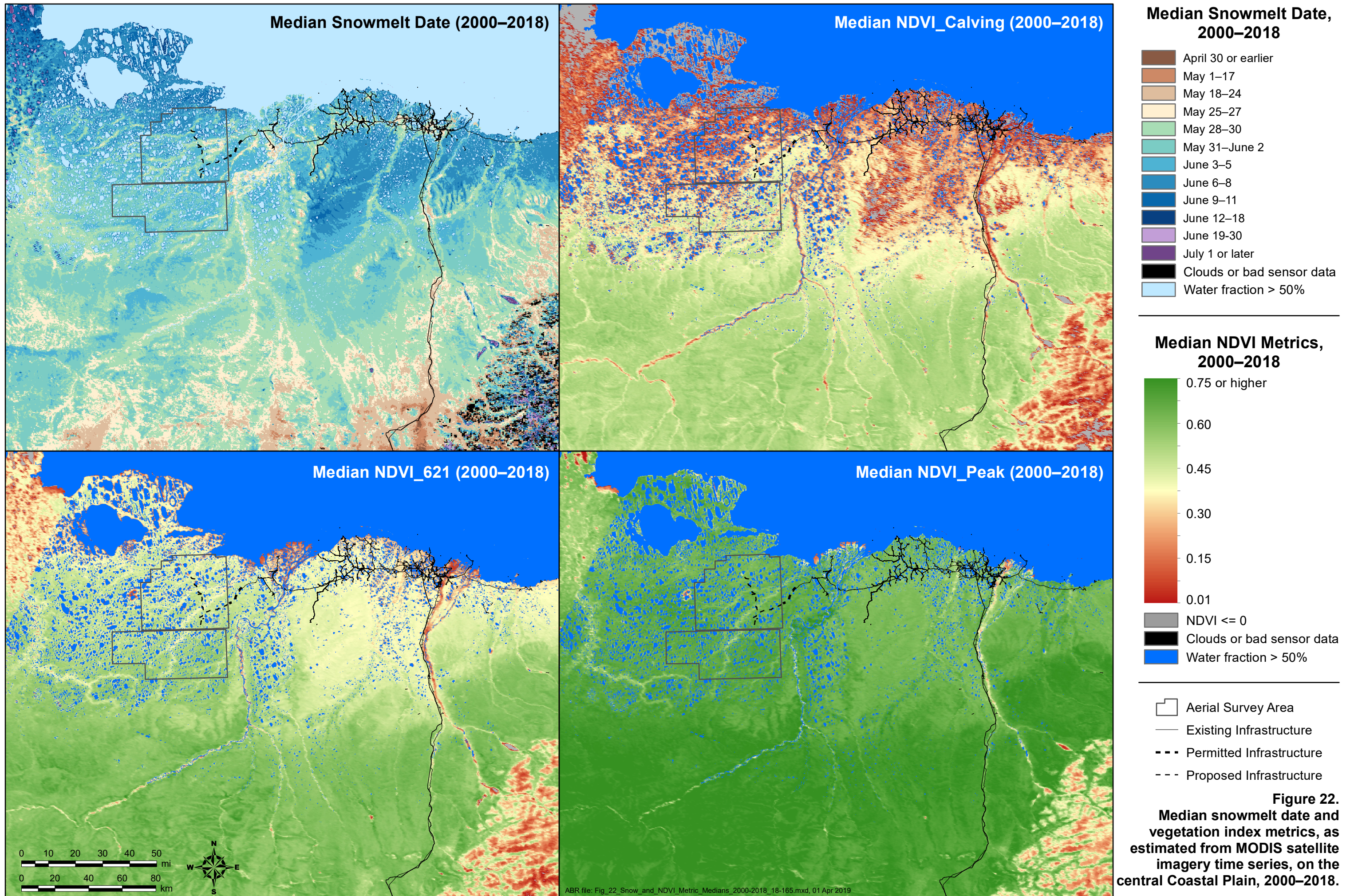
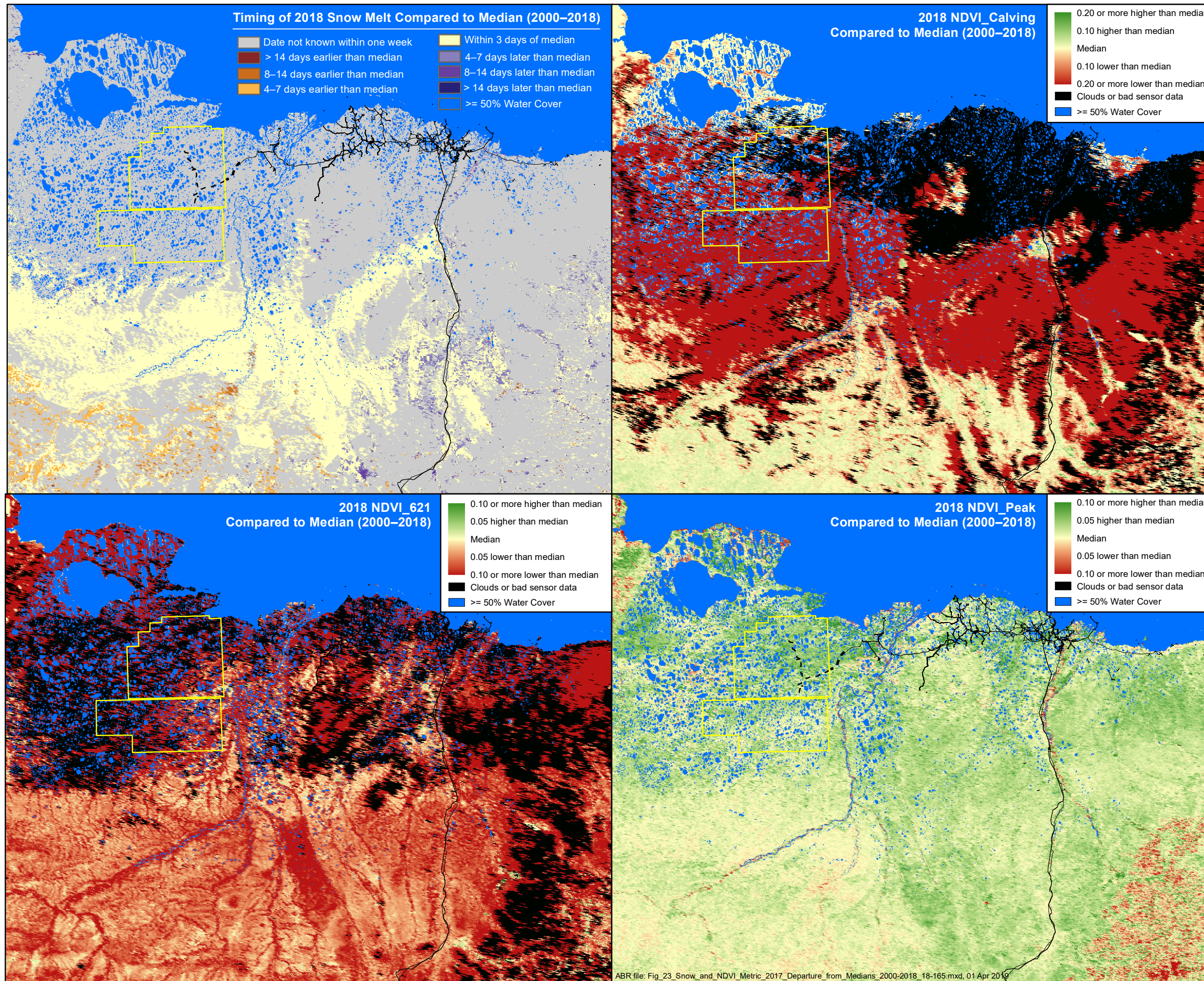
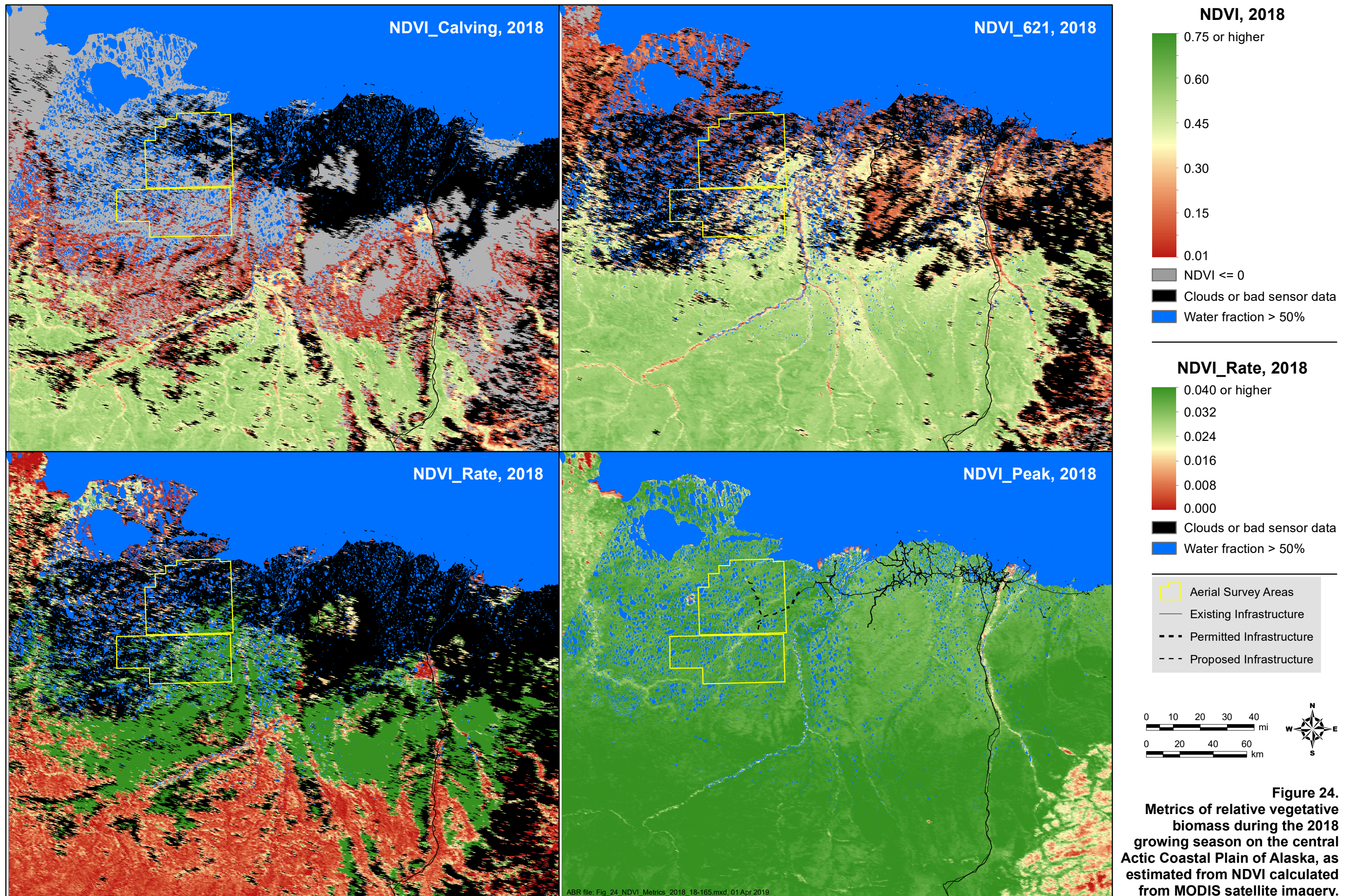


Figure 21. Extent of snow cover between early May and mid-June on the central Arctic Coastal Plain of Alaska in 2018, as estimated from MODIS satellite imagery.







where snowmelt occurred later (Figure 24). This is consistent with a rapid increase in NDVI values soon after snowmelt, as standing dead biomass is exposed and rapid new growth of vegetation occurs.

RESOURCE SELECTION ANALYSIS

The RSF analysis of seasonal caribou density is restricted to the GMT and BTU survey areas. Seasonal sample sizes for the location data used in the RSF analysis ranged from 242 to 2,414 for the years 2002–2018 (Table 5). Most of the top-ranking seasonal models for the survey area contained habitat type, a west-to-east distributional gradient, distance to coast, and landscape ruggedness (Table 6). Vegetative biomass (maximum NDVI or daily NDVI), biomass, nitrogen, and median date of snow melt were included in some of the top seasonal models. Results of the k-fold cross-validation test indicated that the best models for the combined datasets for NPRA had reasonably good model fits (Pearson's $r = 0.87\text{--}0.99$; Table 7). The variables with the highest probability of being in the best RSF model (Table 8) varied by season but caribou resource selection in the area generally followed a gradient of increasing selection from east to west in all seasons and from south to north (distance to coast) in most seasons (Figure 25; Table 9). These results are consistent with the location of the survey area near the eastern edge of the TH annual range.

The RSF model output produced several types of results. These results include the probability of each model being the best model in the set of candidate models (i.e., Akaike weight), which was used to rank the various models (Table 6) and to estimate the probability that each variable is included in the best model (i.e., the sum of Akaike weights for all models containing that variable; Table 8). We used all variables with a 50% or greater probability of being in the best model to produce seasonal RSF maps (Figure 25). In addition, by examining the unconditional parameter estimates we determined which individual parameters were significant (i.e., the 95% confidence interval did not contain zero), while also accounting for model uncertainty (Table 9). These individual parameter estimate results were useful for examining the effect of each habitat type.

For the winter season, all variables except maximum NDVI were included in the best model (Tables 6 and 8), with the snowmelt date being considered a surrogate for snow depth. Areas closer to the coast and farther west and areas with higher values of landscape ruggedness were selected by caribou (Figure 25). Although snowmelt date was included in the best model, the model-weighted variable was not significant. Five habitat types (*Carex aquatilis*, Flooded Tundra, Moss/Lichen, Riverine, and Wet Tundra) were avoided by caribou, relative to the reference category (Sedge/Grass Meadow; Table 9).

Table 5. Number of aerial surveys, radio collars, and locations for each sample type used in RSF analysis for the NPRA survey area, 2002–2018.

| Season | Aerial Surveys | | Telemetry Data | | Total Locations |
|------------------|----------------|-----------|----------------|-----------|-----------------|
| | Surveys | Locations | Collars | Locations | |
| Winter | 13 | 880 | 21 | 686 | 1,566 |
| Spring Migration | 12 | 392 | 24 | 273 | 665 |
| Calving | 20 | 1,060 | 27 | 109 | 1,169 |
| Postcalving | 19 | 1,392 | 19 | 55 | 1,447 |
| Mosquito | 5 | 82 | 36 | 160 | 242 |
| Oestrid Fly | 13 | 259 | 57 | 325 | 584 |
| Late Summer | 26 | 1,222 | 48 | 1,027 | 2,249 |
| Fall Migration | 20 | 1,207 | 64 | 1,207 | 2,414 |
| Total | 128 | 6,494 | 296 | 3,842 | 10,336 |

Table 6. Three top-performing seasonal RSF models, AICc scores, and the probability (Akaike weight) that each model was the best model in the candidate set for the NPRA survey area, 2002–2018 (combined aerial survey and telemetry data).

| Season | RSF Model | AICc | Akaike Weight |
|------------------|---|-----------|---------------|
| Winter | Habitat + EtoW + DistCoast + logRuggedness + Snow | 13,048.48 | 0.576188 |
| | Habitat + maxNDVI + EtoW + DistCoast + logRuggedness + Snow | 13,050.28 | 0.233387 |
| | Habitat + EtoW + DistCoast + logRuggedness | 13,051.42 | 0.132372 |
| Spring Migration | Habitat + maxNDVI + EtoW + DistCoast + logRuggedness | 5,541.74 | 0.319818 |
| | Habitat + maxNDVI + EtoW + DistCoast + logRuggedness + Snow | 5,542.96 | 0.174002 |
| | EtoW + DistCoast + logRuggedness | 5,543.53 | 0.130256 |
| Calving | Habitat + dNDVI + Nitrogen + EtoW + logRuggedness + Snow | 9,730.46 | 0.063564 |
| | Habitat + dNDVI + EtoW + logRuggedness + Snow | 9,730.95 | 0.049914 |
| | Habitat + dNDVI + maxNDVI + Nitrogen + EtoW + DistCoast + logRuggedness + | 9,731.12 | 0.045703 |
| Postcalving | Habitat + dNDVI + Biomass + EtoW + DistCoast + logRuggedness | 12,111.20 | 0.247756 |
| | Habitat + dNDVI + Biomass + Nitrogen + EtoW + DistCoast + logRuggedness | 12,112.62 | 0.121862 |
| | Habitat + dNDVI + EtoW + DistCoast + logRuggedness | 12,112.78 | 0.112792 |
| Mosquito | EtoW + DistCoast + logRuggedness | 1,760.88 | 0.129886 |
| | dNDVI + EtoW + DistCoast + logRuggedness | 1,761.64 | 0.088855 |
| | Biomass + EtoW + DistCoast + logRuggedness | 1,761.74 | 0.084195 |
| Oestrid Fly | Habitat + dNDVI + EtoW + DistCoast + logRuggedness | 4,842.70 | 0.164223 |
| | Habitat + dNDVI + Biomass + EtoW + DistCoast + logRuggedness | 4,843.40 | 0.115823 |
| | Habitat + dNDVI + Nitrogen + EtoW + DistCoast + logRuggedness | 4,843.56 | 0.107226 |
| Late Summer | Habitat + dNDVI + Biomass + EtoW + DistCoast + logRuggedness | 18,995.67 | 0.404707 |
| | Habitat + dNDVI + maxNDVI + Biomass + EtoW + DistCoast + logRuggedness | 18,997.64 | 0.150864 |
| | Habitat + dNDVI + Biomass + Nitrogen + EtoW + DistCoast + logRuggedness | 18,997.67 | 0.149032 |
| Fall Migration | Habitat + EtoW + DistCoast + logRuggedness | 20,073.75 | 0.698580 |
| | Habitat + maxNDVI + EtoW + DistCoast + logRuggedness | 20,075.49 | 0.292806 |
| | Habitat + EtoW + DistCoast | 20,083.23 | 0.006127 |

Table 7. Mean Pearson's rank correlation coefficient (r) of seasonal RSF model fit using k-fold cross-validation for the NPRA survey area, 2002–2018 (combined aerial survey and telemetry data).

| Season | Correlation Coefficient |
|------------------|-------------------------|
| Winter | 0.98 |
| Spring Migration | 0.93 |
| Calving | 0.87 |
| Postcalving | 0.99 |
| Mosquito | 0.98 |
| Oestrid Fly | 0.94 |
| Late Summer | 0.95 |
| Fall Migration | 0.98 |

All of the variables except snowmelt date were included in the best model for spring migration (Tables 6 and 8), although a model with snowmelt date was the second best model (Table 9). The model results were driven primarily by a west-to-east density gradient, with caribou selecting areas farther west reflecting the western distribution of high-density calving by the TH (Figure 16). Areas with higher landscape ruggedness were selected. Although the habitat variable was included in the best model, none of the individual habitat classes were significantly different from the reference class (Sedge/Grass Meadow; Table 9). The selection for higher landscape ruggedness may reflect selection for areas having less snow and spring flooding, or higher proportions of preferred forage species (Nellemann and Thomsen 1994, Nellemann and Cameron 1996).

During the calving season, the variables habitat, daily NDVI, nitrogen, west-to-east, landscape ruggedness, and snowmelt date were included in the best model (Tables 6 and 8), although there was considerable model uncertainty evidenced by the low Akaike weights of all models (Table 6). Caribou were more likely to be located in the western portion of the study area and in areas with high NDVI levels, but lower landscape ruggedness (Table 9; Figure 25), reflecting the western distribution of high-density calving by the TH.

During the postcalving season, the variables habitat, daily NDVI, biomass, west-to-east, distance to coast, and landscape ruggedness were included in the best model (Tables 6 and 8), although there was also some support for including nitrogen in the best model (Table 6). Caribou selected areas farther west, closer to the coast, with higher daily NDVI, and with higher landscape ruggedness (Table 9; Figure 25). Selection of areas in the northwestern portion of the survey area likely reflects caribou movement toward the primary area of mosquito-relief habitat north of Teshekpuk Lake. Selection for higher landscape ruggedness may reflect higher densities of preferred forage species (Nellemann and Thomsen 1994, Nellemann and Cameron 1996).

During the mosquito season, west-to-east gradient, distance to coast, and landscape ruggedness were included in the best model, although there was a fair amount of model uncertainty evidenced by low Akaike weights for the top 3 models (Tables 6 and 8). Models with biomass and daily NDVI also had some support, but habitat only had a 28% chance of being in the best model (Tables 6 and 8). Caribou primarily selected areas farther west, closer to the coast, and with higher ruggedness (Table 9; Figure 25). These results suggest that mosquito harassment is the primary driver of caribou distribution during this season, and the need to access mosquito-relief habitat near the coast is more important than factors such as habitat quality.

During the oestrid fly season, the variables habitat, daily NDVI, west-to-east, distance to coast, and landscape ruggedness were included in the best model, although there was a fair amount of model uncertainty evidenced by low Akaike weights for the top 3 models (Tables 6 and 8). Caribou selected areas farther west, closer to the coast, and with greater ruggedness (Table 9; Figure 25). Relative to Sedge/Grass Meadow habitat, caribou also selected for all other habitats and most strongly for Dwarf Shrub, Riverine and Moss/Lichen.

During late summer, habitat type, daily NDVI, biomass, west-to-east gradient, distance to coast, and landscape ruggedness were included in the best model (Tables 6 and 8). Caribou selected areas farther west, closer to the coast, with higher ruggedness, and with lower biomass. Relative to

Table 8. Independent variables and their probability of being in the best RSF model (i.e., the sum of all Akaike weights for all models that included the variable) for the NPRA survey area during eight seasons, 2002–2018 (combined aerial survey and telemetry data). Variables with a probability ≥ 0.5 were used in RSF maps (Figure 30).

| Variable | Winter | Spring Migration | Calving | Postcalving | Mosquito | Oestrid Fly | Late Summer | Fall Migration |
|-------------------|--------|------------------|---------|-------------|----------|-------------|-------------|----------------|
| West-to-East | 1.00 | 1.00 | 1.00 | 1.00 | 1.00 | 1.00 | 1.00 | 1.00 |
| Distance to Coast | 1.00 | 1.00 | 0.50 | 1.00 | 1.00 | 1.00 | 0.96 | 1.00 |
| Max NDVI | 0.29 | 0.64 | 0.55 | 0.33 | 0.30 | 0.40 | 0.28 | 0.30 |
| Daily NDVI | – | – | 1.00 | 0.99 | 0.36 | 0.61 | 0.80 | – |
| Nitrogen | – | – | 0.55 | 0.37 | 0.29 | 0.35 | 0.28 | – |
| Biomass | – | – | 0.36 | 0.67 | 0.33 | 0.36 | 0.98 | – |
| Snowmelt Date | 0.81 | 0.32 | 0.74 | – | – | – | – | – |
| Ruggedness | 1.00 | 1.00 | 0.96 | 1.00 | 0.96 | 1.00 | 1.00 | 0.99 |
| Habitat | 1.00 | 0.67 | 0.70 | 0.84 | 0.28 | 1.00 | 1.00 | 1.00 |

Table 9. Model-weighted parameter estimates for RSF models for the NPRA survey area during eight seasons, 2002–2018 (combined aerial survey and telemetry data). Coefficients in bold type indicate that the 95 confidence interval did not contain zero.

| Variable | Winter | Spring Migration | Calving | Postcalving | Mosquito | Oestrid Fly | Late Summer | Fall Migration |
|-------------------------------------|--------------|------------------|--------------|--------------|--------------|--------------|--------------|----------------|
| West-to-East | -0.36 | -0.52 | -0.40 | -0.49 | -1.06 | -0.42 | -0.29 | -0.46 |
| Distance to Coast | -0.32 | -0.41 | -0.04 | -0.42 | -1.71 | -0.53 | -0.08 | -0.31 |
| Max NDVI ^a | 0.00 | -0.06 | 0.03 | -0.01 | 0.01 | -0.02 | 0.00 | 0.00 |
| Daily NDVI ^a | – | – | 0.43 | 0.27 | 0.04 | -0.17 | 0.11 | – |
| Biomass ^a | – | – | -0.03 | 0.09 | 0.03 | 0.02 | -0.13 | – |
| Nitrogen ^a | – | – | -0.07 | 0.02 | 0.02 | 0.02 | 0.00 | – |
| Snowmelt Date | 0.05 | -0.01 | 0.05 | – | – | – | – | – |
| Ruggedness | 0.14 | 0.22 | -0.10 | 0.21 | 0.19 | 0.22 | 0.08 | -0.08 |
| <i>Carex aquatilis</i> ^b | -0.54 | -0.25 | -0.14 | -0.25 | 0.00 | 0.59 | -0.44 | -1.19 |
| Dwarf Shrub ^b | 0.25 | -0.12 | -0.26 | 0.10 | 0.11 | 1.06 | 0.17 | 0.13 |
| Flooded Tundra ^b | -0.55 | -0.04 | -0.26 | -0.11 | -0.22 | 0.56 | -0.24 | -0.50 |
| Moss/Lichen ^b | -1.23 | -0.37 | -0.52 | 0.16 | -0.14 | 1.54 | 0.54 | 0.64 |
| Riverine | -1.20 | -0.59 | -0.14 | 0.33 | -0.02 | 1.25 | 0.45 | -0.09 |
| Tussock Tundra | -0.03 | -0.10 | -0.08 | 0.02 | 0.01 | 0.44 | 0.02 | -0.17 |
| Wet Tundra | -0.65 | 0.09 | -0.16 | 0.07 | -0.12 | 0.60 | 0.02 | -0.34 |

^a Max NDVI values were used all year, while the daily NDVI, Biomass, and Nitrogen values which are derived daily during the growing season were used for the Calving, Postcalving, Mosquito, Oestrid Fly, and Late Summer seasons.

^b Habitat classes were compared to the reference class “Sedge/Grass Meadow.”

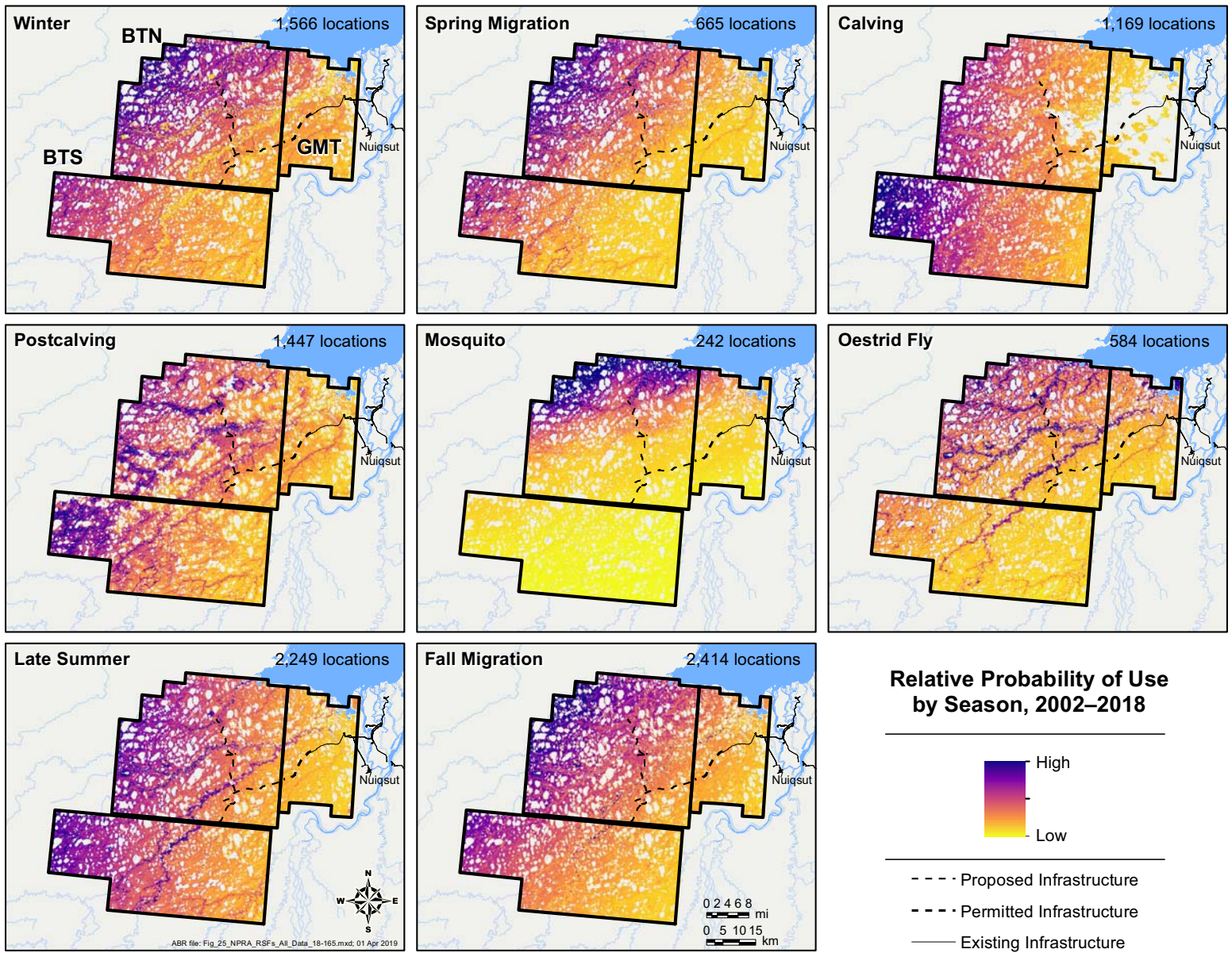


Figure 25. Predicted relative probability of use of the NPRA study area by caribou during each of eight seasons, 2002–2018, based on RSF analysis.

Sedge/Grass Meadow habitat, caribou also selected Moss/Lichen and Riverine habitat types and avoided *Carex aquatilis* and Flooded Tundra habitat types (Table 9; Figure 25).

During fall migration, habitat type, west-to-east, distance to coast, and landscape ruggedness were included in the best RSF model (Tables 6 and 8). Caribou selected areas farther west, closer to the coast, and with low landscape ruggedness. Relative to Sedge/Grass Meadow habitat, caribou also avoided *Carex aquatilis*, Flooded Tundra, Tussock Tundra, and Wet Tundra habitats and selected Moss/Lichen habitat (Table 9; Figure 25).

DISCUSSION

WEATHER, SNOW, AND INSECT CONDITIONS

Weather conditions exert strong effects on caribou populations throughout the year in arctic Alaska. Deep winter snow and icing events increase the difficulty of travel, decrease forage availability, and increase susceptibility to predation (Fancy and White 1985, Griffith et al. 2002). Severe cold and wind events can cause direct mortality of caribou (Dau 2005). Late snow melt can delay spring migration, cause lower calf survival, and decrease future reproductive success (Finstad and Prichard 2000, Griffith et al. 2002, Carroll et al. 2005). In contrast, hot summer weather can depress weight gain and subsequent reproductive success by increasing insect harassment at an energetically stressful time of year, especially for lactating females (Fancy 1986, Cameron et al. 1993, Russell et al. 1993, Weladji et al. 2003).

Variability in weather conditions results in large fluctuations in caribou density during the insect season as caribou aggregate and move rapidly through the study area in response to fluctuating insect activity. On the central Arctic Coastal Plain (including the study area), caribou typically move upwind and toward the coast in response to mosquito harassment and then disperse inland when mosquito activity abates in response to cooler temperatures and increased winds (Murphy and Lawhead 2000, Yokel et al. 2009, Wilson et al. 2012). Hence, temperature and wind

data can be used to predict the occurrence of harassment by mosquitoes (at least five *Aedes* species) and oestrid flies (warble fly *Hypoderma tarandi* and nose bot fly *Cephenemyia trompe*) (White et al. 1975, Fancy 1983, Dau 1986, Russell et al. 1993, Mörschel 1999, Yokel et al. 2009).

Daily air temperatures in 2018 were generally below average in May and June (Appendix B) and accompanied by strong winds in late June resulting in later mosquito emergence than in recent past years. Temperatures in July were above average (Appendix B), likely resulting in high levels of mosquito harassment when winds subsided (Figure 3). Oestrid flies typically emerge by mid-July and, based on the summer weather conditions in 2018, severe oestrid fly harassment likely occurred on multiple days in late July but subsided for most of August due to low temperatures and high winds for most of that month (Figure 5). The absence of mosquitoes during much of June would have been expected to improve caribou body condition after calving, but the warm temperatures during July likely resulted in increased movement rates, decreased foraging, and poorer body condition. Cool conditions in late summer and delayed onset of seasonal snow cover (typical of recent years on the North Slope; Cox et al. 2017) may have allowed improvement of caribou body condition before winter.

CARIBOU DISTRIBUTION AND MOVEMENTS

Analysis of GPS, satellite, and VHF telemetry data sets spanning nearly three decades clearly demonstrates that the study area is in the eastern portion of the annual range of the TH, and west of the annual range of the CAH. Use of the BTN and BTS survey areas by CAH caribou is usually very low, although several notable incursions have been recorded sporadically over the years. A few collared CAH females have switched to the TH or calved west of the Colville River in isolated years (notably 2001), but it is a rare occurrence (Arthur and Del Vecchio 2009; Lenart 2009, 2015; Prichard et al., *in prep.*).

The TH consistently uses the area west of the Colville River to some extent during all seasons of the year. Most TH females calve around Teshekpuk Lake, northwest of the BTN and BTS survey areas

(Kelleyhouse 2001, Carroll et al. 2005, Person et al. 2007, Wilson et al. 2012, Parrett 2015a). Males arrive to the coastal plain usually in June. When mosquito harassment begins in late June or early July, caribou move toward the coast in both study areas where lower temperatures and higher wind speeds prevail (Murphy and Lawhead 2000, Parrett 2007, Yokel et al. 2009, Wilson et al. 2012). The TH typically moves to the area between Teshekpuk Lake and the Beaufort Sea. After oestrid fly harassment begins in mid-July, the large groups that formed in response to mosquito harassment begin to break up and caribou disperse inland, seeking elevated or barren habitats such as sand dunes, mudflats, and river bars, with some using shaded locations in the oilfields under elevated pipelines and buildings (Lawhead 1988, Murphy and Lawhead 2000, Person et al. 2007, Wilson et al. 2012). Females overwinter primarily on the coastal plain whereas males tend to migrate south into the foothills and mountains of the Brooks Range after the rut.

Since we began transect surveys in portions of the northeastern NPRA in 2001, the highest caribou densities have tended to have been observed during the oestrid fly (which overlaps with the typical period of mosquito activity) and fall migration seasons, although there is much variation among seasonal densities (Figure 7). In 2018, caribou density was low during the spring migration and calving seasons, and then increased to moderately high densities during the postcalving survey. Transect surveys during mosquito season are inefficient for locating caribou aggregations because of the rapid speed of caribou movements during that period (Prichard et al. 2014). Caribou density decreased to close to zero during the oestrid fly season, but then increased during the late summer season. The highest densities of caribou in both survey areas were observed during the fall migration survey before densities decreased to average levels in the winter. Poor flying conditions caused by persistent inclement weather have limited our ability to conduct surveys consistently during fall migration. Only nine surveys could be conducted in our previous NPRA survey area in September and October during the years 2009–2018. High densities also have been recorded sporadically in the NPRA survey area in late winter (2.4 caribou/km² in April 2003) and the

postcalving season (1.5 caribou/km² in late June 2001) (Burgess et al. 2002, Johnson et al. 2004, Lawhead et al. 2010).

The area near proposed Willow infrastructure is used more often than the area near existing and proposed ASDP and GMT infrastructure. Few crossings of the new or proposed road alignments GMT-1 or GMT-2 by collared caribou have occurred since 2004 (Prichard et al. 2018, *in prep.*) However, as much as 13% of collared caribou crossed the proposed Willow alignment at least once during a fall migration ($n = 419$; Table 4).

The harvest of caribou by Nuiqsut hunters tends to peak during the months of July and August, with lower percentages of caribou usually being taken in June and September–October and the smallest level of harvest occurring in other months (Pedersen 1995, Brower and Opie 1997, Fuller and George 1997, Braem et al. 2011, SRB&A 2017). Historically, the greatest proportion of the Nuiqsut caribou harvest has been taken by boat-based hunters during the open-water period (SRB&A 2017). The timing of hunting activity in relation to seasonal use of the study area by caribou suggests that caribou harvested on the Colville River delta by hunters in July and August could be from either herd, depending on the year. In contrast, caribou harvested upstream of the delta on the Colville River during the open-water period and west and south of Nuiqsut during October and the winter months are likely to be TH animals. Using harvest data (Braem et al. 2011) and telemetry data from 2003–2007, Parrett (2013) estimated that TH caribou comprised 86% of the total annual harvest by Nuiqsut hunters during those years. The construction of the Nuiqsut Spur Road and CD-5 access road resulted in increased use of those roads for subsistence harvest of caribou (SRB&A 2017) and the new GMT-1 road and the planned GMT-2 road and proposed Willow roads are likely to increase subsistence hunter access to seasonal ranges used consistently year-round by TH caribou.

RESOURCE SELECTION

The two data sets (aerial transect surveys and radio telemetry) that we combined for the RSF analysis provided complementary information for investigating broad patterns of resource selection. Telemetry data have higher spatial accuracy than

do aerial survey data and are collected continuously throughout the year, albeit for a fairly small sample of individual caribou. Because of high variability in the amount of time spent in the study area by collared animals, we did not attempt to adjust for individual differences, other than limiting the frequency of locations in the analytical data set to one every 48 h. In contrast, aerial transect survey data provide information on all caribou groups detected in the area (subject to sightability constraints) at the time of each survey, but the locations have lower spatial accuracy and surveys are only conducted periodically throughout the year. That lower accuracy necessitated the consolidation of the most common mapped habitats into 210-m by 210-m quadrats, rather than the habitat types in individual 30-m pixels that could have been used for the telemetry data alone. This need to consolidate adjacent habitat pixels may have reduced the accuracy of habitat selection analysis for uncommon habitats in the survey area. The two different data types also had different timing, especially during the winter season; only one aerial survey was conducted in that season (mid to late April) in any given year, whereas telemetry locations were collected throughout the entire season. Despite these potential limitations, the combination of the two survey methods produced larger samples than were available for either data set alone and the resulting RSF models are broadly interpretable within the context of general patterns of caribou movements on the central Arctic Coastal Plain.

Use of the BTU and GMT survey areas by caribou varies widely among seasons. These differences are related to snow cover, vegetative biomass, distribution of habitat types, distance to the coast and west-to-east gradients, and landscape ruggedness. In general, broad geographic patterns in distribution (west to east, distance to coast) were the strongest predictors of caribou distribution, but other factors such as vegetative biomass and habitat types were important in some seasons, after taking into account the broad geographic patterns exhibited during key life cycle stages and reflected in the seasonal distribution patterns (Figures 14–15).

These geographic patterns in TH distribution are most pronounced during calving and the mosquito season. Because the NPRA survey area is

on the eastern edge of the TH range, a natural west-to-east gradient of decreasing density occurs throughout the year. Caribou density typically is lowest in the east and southeastern sections of the survey areas in which the proposed GMT-2 road alignment would be located, and higher to the north and west. During calving, the highest densities of TH females typically calve near Teshekpuk Lake (Figure 16; Person et al. 2007, Wilson et al. 2012, Parrett 2015a), so caribou density decreases with increasing distance to the east, away from the lake. Hence, more caribou are likely to occur in the western portion of the BTN survey area than in the eastern portion in that season. It is important to recognize that this pattern of distribution existed before construction of any BTU pipelines, roads, or any other infrastructure. During the postcalving season, caribou are more widely distributed to the south and east into the BTN and BTS survey areas as they spread out from the calving grounds prior to insect emergence. TH Caribou migrating north from their wintering grounds in the Brooks Range, which are primarily males, also usually arrive to the region during the postcalving season.

Because caribou aggregate into large groups when mosquitoes are present and move quickly when harassed by insects, density during the mosquito season and early part of the oestrid fly season fluctuates widely. Caribou density in the area of the proposed infrastructure in the BTN survey area generally is low during the mosquito and oestrid fly seasons. Aerial-transect surveys in other regions of the oilfields during the mosquito and oestrid fly seasons have been sparse due to the difficulty of adequately sampling the highly variable occurrence of caribou at that time of year with that survey method, and therefore surveys are no longer conducted during mosquito harassment. Caribou density from late summer through winter was fairly consistent with higher densities of caribou to the north and west.

During most seasons, caribou selected for higher landscape ruggedness, which tends to occur in riparian areas in the study area. Different studies have reported conflicting conclusions regarding the importance of ruggedness, which may be related in part to the ways in which it has been calculated. Nellemann and Thomsen (1994) and Nellemann and Cameron (1996) reported that CAH caribou

selected areas of greater terrain ruggedness (as calculated by hand from topographic maps) in the Milne Point calving concentration area, but Wolfe (2000) and Lawhead et al. (2004), using a digital method of calculating terrain ruggedness, found no consistent relationship with terrain ruggedness in a larger calving area used by CAH females during calving. Those calculations of terrain ruggedness differed from the landscape ruggedness method we used in this study (developed by Sappington et al. 2007), which provides a finer-scale analysis based on digital elevation models and is much less correlated with slope than are the previous methods.

The primary finding of the habitat selection analysis was avoidance of *Carex aquatilis*, Wet Tundra, and Flooded Tundra during fall and winter, patterns that had been documented in previous years using different analyses (Lawhead et al. 2015), as well as selection of Riverine habitat along Fish and Judy creeks during the oestrid fly season and late summer and avoidance of Riverine habitat during winter and spring (Table 9). The riparian habitats along Fish and Judy creeks provide a complex interspersion of barren ground, dunes, and sparse vegetation (Figure 3) that provide good fly-relief habitat near foraging areas, but collect deep snow in the winter. In winter, all habitats except Dwarf Shrub were avoided by comparison with the reference habitat, Sedge/Grass Meadow.

Comparison of caribou habitat use across studies is complicated by the fact that different investigators have used different habitat classifications. Kelleyhouse (2001) and Parrett (2007) reported that TH caribou selected wet graminoid vegetation during calving and Wolfe (2000) reported that CAH caribou selected wet graminoid or moist graminoid classes; those studies used the vegetation classification by Muller et al. (1998, 1999). Using a habitat classification similar to the one developed by Jorgenson et al. (2003), Lawhead et al. (2004) found that CAH caribou in the Meltwater study area in the southwestern Kuparuk oilfield and the adjacent area of concentrated calving selected Moist Sedge–Shrub Tundra, the most abundant type in their study area, during calving. Wilson et al. (2012) used TH telemetry data and the same habitat classification as us (BLM and Ducks

Unlimited 2002) to investigate summer habitat selection at two different spatial scales, concluding that TH caribou consistently selected Sedge/Grass Meadow and avoided flooded vegetation.

During calving, caribou in the RSF analysis area tended to use areas of higher vegetative biomass (daily NDVI) but the confidence interval for date of snowmelt and habitat both included zero indicating no large effect. Habitat selection during the calving season may vary annually, depending on the timing of snow melt and plant phenology. In 2018, the distribution of collared TH females, as well as our aerial survey results, suggest that the TH calving distribution was farther west than usual.

We used NDVI to estimate vegetative biomass in this study because other researchers have reported significant relationships between caribou distribution and biomass variables (NDVI at time of calving [NDVI_Calving], NDVI on 21 June [NDVI_621], and NDVI rate of change [NDVI_Rate]) during the calving period. The first flush of new vegetative growth that occurs in spring among melting patches of snow is valuable to foraging caribou (Kuropat 1984, Klein 1990, Johnstone et al. 2002), but the spectral signal of snow, ice, and standing water complicates NDVI-based inferences in patchy snow and recently melted areas. Snow, water, and lake ice all depress NDVI values. Therefore, estimates of NDVI variables (NDVI_Calving, NDVI_Rate, NDVI_621) change rapidly as snow melts and exposes standing dead biomass, which has positive NDVI values (Sellers 1985 [cited in Hope et al. 1993], Stow et al. 2004), and the initial flush of new growth begins to appear.

Griffith et al. (2002) reported that the annual calving grounds used by the PH during 1985–2001 generally were characterized by a higher daily rate of change in biomass than was available over the entire calving grounds. In addition, the area of concentrated calving contained higher biomass (NDVI_Calving and NDVI_621) values than was available in the annual calving grounds. They concluded that caribou used calving areas with high forage quality (inferred from an estimated high daily rate of change) and that, within those areas, caribou selected areas of high biomass. The relationship between annual NDVI_621 and June calf survival for the PH was strongly positive, as

was the relationship between NDVI_Calving and the percentage of marked females calving on the coastal plain of ANWR (Griffith et al. 2002). We found that there was selection for areas that typically have high NDVI values during calving in our RSF analysis area for all years combined.

Because of the high correlation between NDVI values and habitat, it is difficult to distinguish whether caribou select specific habitats and areas with greater NDVI or simply avoid wet areas and barrens during the calving season. Vegetation sampling in the NPRA survey area in 2005 indicated that moist tussock tundra had higher biomass than did moist sedge–shrub tundra (similar to Tussock Tundra and Sedge/Grass Meadow types in our classification), but that difference disappeared when evergreen shrubs, which are unpalatable caribou forage, were excluded (Lawhead et al. 2006). Tussock Tundra supports higher biomass of plant species that are preferred by caribou, such as tussock cottongrass (*Eriophorum vaginatum*), forbs, and lichens, however. Caribou appear to use wetter habitats (*C. aquatilis*, Wet Tundra, and Flooded Tundra) less during calving and those areas tend to have lower NDVI values in both late June and midsummer.

Johnson et al. (2018) used daily NDVI values as well as habitat type, distance to coast, and days from peak NDVI to develop models to predict biomass, nitrogen, and digestible energy for a given location on a given day. These models should, if successful, provide metrics that are more directly related to caribou forage needs than NDVI alone. In our RSF models, inclusion of these variables was not consistent in seasons where it was included as a possible variable (calving through late summer). Biomass was included in at least one of the three top-performing RSF models during all seasons except calving. Nitrogen was included in at least one of the three top-performing RSF models during all seasons except the mosquito season. However, nitrogen was not a significant variable in any season and the only season in which biomass was significant was late summer and the model indicated that areas with higher estimated forage biomass values were avoided (Table 9). These results suggest that these derived values are not good predictors of caribou distribution in this area and at this scale of selection.

It is possible that these models do not predict biomass and nitrogen well in this area. Johnson et al. (2018) used a land cover map (Boggs et al. 2016) that was based on a land cover map created by Ducks Unlimited for the North Slope Science Initiative (NSSI 2013) that has discontinuities in classification methodology and imagery in our RSF analysis area. These discontinuities could translate into inaccurate forage metrics in our analysis area. Alternatively, caribou may not be selecting for forage nitrogen or forage biomass at this scale of selection and caribou distribution may be better predicted by high NDVI values which tend to be correlated with locations that have both large amounts of vegetation and less surface water in the pixel. Caribou movements are influenced by many factors other than forage and only a portion of GPS locations represent caribou that are actively feeding.

Previous studies have not produced consistent results concerning the calving distribution of northern Alaska caribou herds in relation to snow cover. Kelleyhouse (2001) concluded that TH females selected areas of low snow cover during calving and Carroll et al. (2005) reported that TH caribou calved farther north in years of early snow melt. Wolfe (2000) did not find any consistent selection for snow-cover classes during calving by the CAH, whereas Eastland et al. (1989) and Griffith et al. (2002) reported that calving PH caribou preferentially used areas with 25–75% snow cover. The presence of patchy snow in calving areas is associated with the emergence of highly nutritious new growth of forage species, such as tussock cottongrass (Kuropat 1984, Griffith et al. 2002, Johnstone et al. 2002), and it also may increase dispersion of caribou and create a complex visual pattern that reduces predation (Bergerud and Page 1987, Eastland et al. 1989). Interpretation of analytical results is complicated by the fact that caribou do not require snow-free areas in which to calve and are able to find nutritious forage even in patchy snow cover. Interpretation also is complicated by high annual variability in the extent of snow cover and the timing of snowmelt among years, as well as by variability in detection of snowmelt dates on satellite imagery because of cloud cover.

The current emphasis of this study is to monitor caribou distribution and movements in

relation to the proposed infrastructure in the BTN and BTS survey areas and to compile predevelopment baseline data on caribou density and movements. Detailed analyses of the existing patterns of seasonal distribution, density, and movements are providing important insights about the ways in which caribou currently use the study area and why. Although both the TH and CAH recently underwent sharp declines in population due to decreased survival of both adults and calves, particularly after the prolonged winter of 2012–2013, both herds increased in size in the latest counts from July 2017. In recent years, the TH calving distribution has expanded both to the west and the southeast, whereas the winter distribution has varied widely among years (Parrett 2013). The CAH has shown indications of increased mortality, as well as changes in seasonal distribution, with more caribou remaining farther north during fall and early winter and more intermixing with adjacent herds (ADFG 2017).

For this report, we incorporated multiple types of data and several different analyses to better understand the seasonal distributions, movements, and herd associations of caribou in the area. Aerial surveys provided detailed information on caribou density and distribution at a specific time during the year and by conducting aerial surveys during different seasons over the course of 18 years in northeastern NPRA, we have compiled an extensive dataset that allows us to understand the seasonal patterns as well as the variability in caribou distribution over this specific area. The use of telemetry data provided high-resolution locations for a subset of caribou throughout the year. This large and growing database allows us to understand caribou movements through the area for the two different herds which use the area but it also allows us to put local caribou movements in the study area into the broader context of the annual herd ranges and seasonal herd distributions. Lastly, we incorporated aerial survey results and telemetry data with remote sensing information on land cover, vegetative biomass, forage nitrogen, and snow cover to better understand the factors determining caribou seasonal distribution. This understanding of the underlying factors that are important to caribou will be useful when

evaluating potential future changes in caribou distribution that may be attributable to development or a changing climate.

LITERATURE CITED

- ADFG (Alaska Department of Fish and Game). 2017. Central Arctic caribou herd news. Winter 2016–17 edition. Alaska Department of Fish and Game, Division of Wildlife Conservation, Fairbanks. 6 pp.
- Arthur, S. M., and P. A. Del Vecchio. 2009. Effects of oil field development on calf production and survival in the Central Arctic Herd. Final research technical report, June 2001–March 2006. Federal Aid in Wildlife Restoration Project 3.46, Alaska Department of Fish and Game, Juneau. 40 pp.
- Bergerud, A. T., and R. E. Page. 1987. Displacement and dispersion of parturient caribou as antipredator tactics. *Canadian Journal of Zoology* 65: 1597–1606.
- BLM (Bureau of Land Management) and Ducks Unlimited. 2002. National Petroleum Reserve–Alaska earth-cover classification. U.S. Department of the Interior, BLM Alaska Technical Report 40, Anchorage. 81 pp.
- Boggs, K., L. Flagstad, T. Boucher, T. Kuo, D. Fehringer, S. Guyer and M. Aisu. 2016. Vegetation Map and Classification: Northern, Western, and Interior Alaska. Second edition. Prepared by Alaska Center for Conservation Science, University of Alaska Anchorage, Anchorage, Alaska. 110 pp.
- Boyce, M. S., and L. L. McDonald. 1999. Relating populations to habitats using resource selection functions. *Trends in Ecology and Evolution* 14: 268–272.
- Boyce, M. S., P. R. Vernier, S. E. Nielsen, and F. K. A. Schmiegelow. 2002. Evaluating resource selection functions. *Ecological Modelling* 157: 281–300.
- Braem, N. M., S. Pedersen, J. Simon, D. Koster, T. Kaleak, P. Leavitt, J. Patkotak, and P. Neakok. 2011. Monitoring of annual caribou harvests in the National Petroleum Reserve in Alaska:

- Atqasuk, Barrow, and Nuiqsut, 2003–2007. Technical Paper No. 361, Alaska Department of Fish and Game, Division of Subsistence, Fairbanks. 201 pp.
- Brower, H. K., and R. T. Opie. 1997. North Slope Borough subsistence harvest documentation project: data for Nuiqsut, Alaska, for the period July 1, 1994 to June 30, 1995. North Slope Borough Department of Wildlife Management, Barrow.
- Brown, J., R. K. Haugen, and S. Parrish. 1975. Selected climatic and soil thermal characteristics of the Prudhoe Bay region. Pages 3–11 in J. Brown, editor. Ecological investigations of the tundra biome in the Prudhoe Bay region, Alaska. Biological Papers of the University of Alaska, Special Report No. 2, Fairbanks.
- Burgess, R. M., C. B. Johnson, P. E. Seiser, A. A. Stickney, A. M. Wildman, and B. E. Lawhead. 2002. Wildlife studies in the Northeast Planning Area of the National Petroleum Reserve–Alaska, 2001. Report for Phillips Alaska, Inc., Anchorage, by ABR, Inc., Fairbanks. 71 pp.
- Burnham, K. P., and D. R. Anderson. 2002. Model Selection and Multimodel Inference: A Practical Information–Theoretic Approach. 2nd edition. Springer–Verlag, New York. 488 pp.
- Calcagno, V., and C. de Mazancourt. 2010. *glmulti*: an R package for easy automated model selection with (Generalized) Linear Models. *Journal of Statistical Software* 34: 1–29.
- Cameron, R. D., W. T. Smith, and S. G. Fancy. 1989. Distribution and productivity of the Central Arctic Caribou Herd in relationship to petroleum development. Research progress report, Federal Aid in Wildlife Restoration Project 3.35, Alaska Department of Fish and Game, Juneau. 52 pp.
- Cameron, R. D., D. J. Reed, J. R. Dau, and W. T. Smith. 1992. Redistribution of calving caribou in response to oil-field development on the Arctic Slope of Alaska. *Arctic* 45: 338–342.
- Cameron, R. D., W. T. Smith, S. G. Fancy, K. L. Gerhart, and R. G. White. 1993. Calving success of female caribou in relation to body weight. *Canadian Journal of Zoology* 71: 480–486.
- Cameron, R. D., E. Lenart, D. J. Reed, K. R. Whitten, and W. T. Smith. 1995. Abundance and movements of caribou in the oilfield complex near Prudhoe Bay, Alaska. *Rangifer* 15: 3–7.
- Carroll, G. M., A. K. Prichard, R. S. Suydam, L. S. Parrett, and D. A. Yokel. 2004. Unexpected movements of the Teshekpuk caribou herd. Paper presented at the 10th North American Caribou Workshop, 4–6 May 2004, Girdwood, AK. [abstract only]
- Carroll, G. M., L. S. Parrett, J. C. George, and D. A. Yokel. 2005. Calving distribution of the Teshekpuk caribou herd, 1994–2003. *Rangifer, Special Issue* 16: 27–35.
- CLS. 2016. Argos user’s manual. CLS, Toulouse, France. Available online: <http://www.argos-system.org/manual/> (accessed 16 February 2018).
- Cox, C. J., R. S. Stone, D. C. Douglas, D. M. Stanitski, G. J. Divoky, G. S. Dutton, C. Sweeney, J. C. George, and D. U. Longenecker. 2017. Drivers and environmental responses to the changing annual snow cycle of northern Alaska. *Bulletin of the American Meteorological Society* 98: 2559–2577.
- Dau, J. R. 1986. Distribution and behavior of barren-ground caribou in relation to weather and parasitic insects. M.S. thesis, University of Alaska, Fairbanks. 149 pp.
- Dau, J. 2005. Two caribou mortality events in northwestern Alaska: possible causes and management implications. *Rangifer, Special Issue* 16: 37–50.
- Dau, J. R., and R. D. Cameron. 1986. Effects of a road system on caribou distribution during calving. *Rangifer, Special Issue* 1: 95–101.

- Dick, B. L., S. L. Findholt, and B. K. Johnson. 2013. A self-adjusting expandable GPS collar for male elk. *Journal of Wildlife Management* 37: 887–892.
- Duong, T. 2017. *ks: Kernel Smoothing*. R package version 1.10.7. Available online: <https://CRAN.R-project.org/package=ks> (accessed 16 February 2018).
- Eastland, W. G., R. T. Bowyer, and S. G. Fancy. 1989. Caribou calving sites relative to snow cover. *Journal of Mammalogy* 70: 824–828.
- Fancy, S. G. 1983. Movements and activity budgets of caribou near oil drilling sites in the Sagavanirktok River floodplain, Alaska. *Arctic* 36: 193–197.
- Fancy, S. G. 1986. Daily energy budgets of caribou: a simulation approach. Ph.D. dissertation, University of Alaska, Fairbanks. 226 pp.
- Fancy, S. G., and R. G. White. 1985. Energy expenditure by caribou while cratering in snow. *Journal of Wildlife Management* 49: 987–993.
- Fancy, S. G., K. R. Whitten, N. E. Walsh, and R. D. Cameron. 1992. Population dynamics and demographics of caribou in developed and undeveloped areas of the Arctic Coastal Plain. Pages 1–21 in T. R. McCabe, D. B. Griffith, N. E. Walsh, and D. D. Young, editors. *Terrestrial research: 1002 Area, Arctic National Wildlife Refuge*. Interim report, 1988–1990. U.S. Fish and Wildlife Service, Anchorage.
- Finstad, G. L., and A. K. Prichard. 2000. Climatic influence on forage quality, growth, and reproduction of reindeer on the Seward Peninsula, II: Reindeer growth and reproduction. *Rangifer*, Special Issue 12: 144.
- Fuller, A. S., and J. C. George. 1997. Evaluation of subsistence harvest data from the North Slope Borough 1993 census for eight North Slope villages for calendar year 1992. North Slope Borough Department of Wildlife Management, Barrow.
- Gasaway, W. C., S. D. DuBois, D. J. Reed, and S. J. Harbo. 1986. Estimating moose population parameters from aerial surveys. *Biological Papers of the University of Alaska*, No. 22, Fairbanks. 108 pp.
- Gorelick, N., M. Hancher, M. Dixon, S. Ilyushchenko, D. Thau, and R. Moore. 2017. Google Earth Engine: planetary-scale geospatial analysis for everyone. *Remote Sensing of Environment* 202: 18–27.
- Griffith, D. B., D. C. Douglas, N. E. Walsh, D. D. Young, T. R. McCabe, D. E. Russell, R. G. White, R. D. Cameron, and K. R. Whitten. 2002. Section 3: The Porcupine caribou herd. Pages 8–37 in D. C. Douglas, P. E. Reynolds, and E. B. Rhode, editors. *Arctic Refuge coastal plain terrestrial wildlife research summaries*. U.S. Geological Survey, Biological Resources Division, Biological Science Report USGS/BRD/BSR-2002-0001.
- Hope, A. S., J. S. Kimball, and D. A. Stow. 1993. The relationship between tussock tundra spectral properties and biomass and vegetation composition. *International Journal of Remote Sensing* 14: 1861–1874.
- Horne, J. S., E. O. Garton, S. M. Krone, and J. S. Lewis. 2007. Analyzing animal movements using Brownian bridges. *Ecology* 88: 2354–2363.
- Jensen, P. G., and L. E. Noel. 2002. Caribou distribution in the northeast National Petroleum Reserve–Alaska, summer 2001. Chapter 3 in M. A. Cronin, editor. *Arctic Coastal Plain caribou distribution, summer 2001*. Report for BP Exploration (Alaska) Inc., Anchorage, by LGL Alaska Research Associates, Inc., Anchorage.
- Johnson, C. B., R. M. Burgess, A. M. Wildman, A. A. Stickney, P. E. Seiser, B. E. Lawhead, T. J. Mabee, J. R. Rose, and J. E. Shook. 2004. *Wildlife studies for the Alpine Satellite Development Project, 2003*. Annual report for ConocoPhillips Alaska, Inc., and Anadarko Petroleum Corp., Anchorage, by ABR, Inc., Fairbanks. 155 pp.

- Johnson, C. B., J. P. Parrett, T. Obritschkewitsch, J. R. Rose, K. B. Rozell, and P. E. Seiser. 2015. Avian studies for the Alpine Satellite Development Project, 2014. Twelfth annual report for ConocoPhillips Alaska, Inc., and Anadarko Petroleum Corp., Anchorage, by ABR, Inc., Fairbanks. 124 pp.
- Johnson, H. E., D. D. Gustine, T. S. Golden, L. G. Adams, L. S. Parrett, E. A. Lenart, and P. S. Barboza. 2018. NDVI exhibits mixed success in predicting spatiotemporal variation in caribou summer forage quality and quantity. *Ecosphere*. 9: 10.
- Johnstone, J., D. E. Russell, and D. B. Griffith. 2002. Variations in plant forage quality in the range of the Porcupine caribou herd. *Rangifer* 22: 83–91.
- Jorgenson, M. T., J. E. Roth, E. R. Pullman, R. M. Burgess, M. Reynolds, A. A. Stickney, M. D. Smith, and T. Zimmer. 1997. An ecological land survey for the Colville River delta, Alaska, 1996. Report for ARCO Alaska, Inc., Anchorage, by ABR, Inc., Fairbanks. 160 pp.
- Jorgenson, M. T., J. E. Roth, M. Emers, S. Schlentner, D. K. Swanson, E. R. Pullman, J. Mitchell, and A. A. Stickney. 2003. An ecological land survey for the Northeast Planning Area of the National Petroleum Reserve–Alaska, 2002. Report for ConocoPhillips Alaska, Inc., Anchorage, by ABR, Inc., Fairbanks. 84 pp.
- Jorgenson, M. T., J. E. Roth, M. Emers, W. Davis, E. R. Pullman, and G. V. Frost. 2004. An ecological land survey for the Northeast Planning Area of the National Petroleum Reserve–Alaska, 2003. Addendum to 2002 report for ConocoPhillips Alaska, Inc., Anchorage, and Anadarko Petroleum Corporation, Anchorage, by ABR, Inc., Fairbanks. 40 pp.
- Kelleyhouse, R. A. 2001. Calving-ground selection and fidelity: Teshekpuk Lake and Western Arctic herds. M.S. thesis, University of Alaska, Fairbanks. 124 pp.
- Klein, D. R. 1990. Variation in quality of caribou and reindeer forage plants associated with season, plant part, and phenology. *Rangifer*, Special Issue 3: 123–130.
- Klimstra, R. 2018. Summary of Teshekpuk caribou herd photocensus conducted July 14, 2017. State of Alaska memorandum, Department of Fish and Game, Division of Wildlife Conservation (Northwest), Fairbanks. 6 pp.
- Kranstauber, B., K. Safi, and F. Bartumeus. 2014. Bivariate Gaussian bridges: directional factorization of diffusion in Brownian bridge models. *Movement Ecology* 2: 5. doi.org/10.1186/2051-3933-2-5.
- Kranstauber, B., M. Smolla, and A.K. Scharf. 2017. *Move*: visualizing and analyzing animal track data. R package version 3.0.1. Available online: <https://CRAN.R-project.org/package=move> (accessed 16 February 2018).
- Kuropat, P. J. 1984. Foraging behavior of caribou on a calving ground in northwestern Alaska. M.S. thesis, University of Alaska, Fairbanks. 95 pp.
- Lair, H. 1987. Estimating the location of the focal center in red squirrel home ranges. *Ecology* 68: 1092–1101.
- Lawhead, B. E. 1988. Distribution and movements of Central Arctic Herd caribou during the calving and insect seasons. Pages 8–13 in R. Cameron and J. Davis, editors. Proceedings of the 3rd North American Caribou Workshop. Wildlife Technical Bulletin No. 8, Alaska Department of Fish and Game, Juneau.
- Lawhead, B. E., C. B. Johnson, and L. C. Byrne. 1994. Caribou surveys in the Kuparuk oilfield during the 1993 calving and insect seasons. Report for ARCO Alaska Inc., Kuparuk River Unit, by Alaska Biological Research, Inc., 43 pp.
- Lawhead, B. E., A. K. Prichard, M. J. Macander, and M. Emers. 2004. Caribou mitigation monitoring study for the Meltwater Project, 2003. Third annual report for ConocoPhillips Alaska, Inc., Anchorage, by ABR, Inc., Fairbanks. 104 pp.

- Lawhead, B. E., A. K. Prichard, and M. J. Macander. 2006. Caribou monitoring study for the Alpine Satellite Development Program, 2005. First annual report for ConocoPhillips Alaska, Inc., Anchorage, by ABR, Inc., Fairbanks. 102 pp.
- Lawhead, B. E., A. K. Prichard, and M. J. Macander. 2007. Caribou monitoring study for the Alpine Satellite Development Program, 2006. Second annual report for ConocoPhillips Alaska, Inc., Anchorage, by ABR, Inc., Fairbanks. 75 pp.
- Lawhead, B. E., A. K. Prichard, and M. J. Macander. 2008. Caribou monitoring study for the Alpine Satellite Development Program, 2007. Third annual report for ConocoPhillips Alaska, Inc., Anchorage, by ABR, Inc., Fairbanks. 89 pp.
- Lawhead, B. E., A. K. Prichard, and M. J. Macander. 2009. Caribou monitoring study for the Alpine Satellite Development Program, 2008. Fourth annual report for ConocoPhillips Alaska, Inc., Anchorage, by ABR, Inc., Fairbanks. 91 pp.
- Lawhead, B. E., A. K. Prichard, and M. J. Macander. 2010. Caribou monitoring study for the Alpine Satellite Development Program, 2009. Fifth annual report for ConocoPhillips Alaska, Inc., Anchorage, by ABR, Inc., Fairbanks. 101 pp.
- Lawhead, B. E., A. K. Prichard, and M. J. Macander. 2011. Caribou monitoring study for the Alpine Satellite Development Program, 2010. Sixth annual report for ConocoPhillips Alaska, Inc., Anchorage, by ABR, Inc., Fairbanks. 101 pp.
- Lawhead, B. E., A. K. Prichard, and M. J. Macander. 2012. Caribou monitoring study for the Alpine Satellite Development Program, 2011. Seventh annual report for ConocoPhillips Alaska, Inc., Anchorage, by ABR, Inc., Fairbanks. 90 pp.
- Lawhead, B. E., A. K. Prichard, M. J. Macander, and J. H. Welch. 2013. Caribou monitoring study for the Alpine Satellite Development Program, 2012. Eighth annual report for ConocoPhillips Alaska, Inc., Anchorage, by ABR, Inc., Fairbanks. 88 pp.
- Lawhead, B. E., A. K. Prichard, M. J. Macander, and J. H. Welch. 2014. Caribou monitoring study for the Alpine Satellite Development Program, 2013. Ninth annual report for ConocoPhillips Alaska, Inc., Anchorage, by ABR, Inc., Fairbanks. 94 pp.
- Lawhead, B. E., A. K. Prichard, M. J. Macander, and J. H. Welch. 2015. Caribou monitoring study for the Alpine Satellite Development Program, 2014. Tenth annual report for ConocoPhillips Alaska, Inc., Anchorage, by ABR, Inc., Fairbanks. 100 pp.
- Lenart, E. A. 2009. GMU 26B and 26C, Central Arctic Herd. Pages 299–325 *in* P. Harper, editor. Caribou management report of survey and inventory activities, 1 July 2006–30 June 2008. Federal Aid in Wildlife Restoration Project 3.0, Alaska Department of Fish and Game, Juneau.
- Lenart, E. A. 2015. Units 26B and 26C, Central Arctic. Chapter 18 *in* P. Harper and L. A. McCarthy, editors. Caribou management report of survey and inventory activities, 1 July 2012–30 June 2014. Alaska Department of Fish and Game, Species Management Report ADF&G/DWC/SMR-2015-4, Juneau.
- Lenart, E. A. 2017. 2016 Central Arctic caribou photocensus results. State of Alaska memorandum, Department of Fish and Game, Division of Wildlife Conservation, Fairbanks. 5 pp.
- Lenart, E. A. 2018. 2017 Central Arctic caribou digital camera system photocensus results. State of Alaska memorandum, Department of Fish and Game, Division of Wildlife Conservation, Fairbanks. 7 pp.
- Macander, M. J., C. S. Swingley, K. Joly, and M. K. Reynolds. 2015. Landsat-based snow persistence map for northwest Alaska. *Remote Sensing of Environment* 163: 23–31.

- Manly, B. F. J., L. L. McDonald, D. L. Thomas, T. L. McDonald, and W. P. Erickson. 2002. Resource selection by animals: statistical design and analysis for field studies. Second edition. Kluwer Academic Publishers, Dordrecht, The Netherlands. 209 pp.
- McNay, R. S., J. A. Morgan, and F. L. Bunnell. 1994. Characterizing independence of observations in movements of Columbian black-tailed deer. *Journal of Wildlife Management* 58: 422–429.
- Mörschel, F. M. 1999. Use of climatic data to model the presence of oestrid flies in caribou herds. *Journal of Wildlife Management* 63: 588–593.
- Muller, S. V., D. A. Walker, F. E. Nelson, N. A. Auerbach, J. G. Bockheim, S. Guyer, and D. Sherba. 1998. Accuracy assessment of a land-cover map of the Kuparuk River basin, Alaska: considerations for remote regions. *Photogrammetric Engineering and Remote Sensing* 64: 619–628.
- Muller, S. V., A. E. Racoviteanu, and D. A. Walker. 1999. Landsat-MSS-derived land-cover map of northern Alaska: extrapolation methods and a comparison with photo-interpreted and AVHRR-derived maps. *International Journal of Remote Sensing* 20: 2921–2946.
- Murphy, S. M., and B. E. Lawhead. 2000. Caribou. Chapter 4, pages 59–84 in J. Truett and S. R. Johnson, editors. *The Natural History of an Arctic Oil Field: Development and the Biota*. Academic Press, San Diego, CA.
- Nellemann, C., and R. D. Cameron. 1996. Effects of petroleum development on terrain preferences of calving caribou. *Arctic* 49: 23–28.
- Nellemann, C., and M. G. Thomsen. 1994. Terrain ruggedness and caribou forage availability during snowmelt on the Arctic Coastal Plain, Alaska. *Arctic* 47: 361–367.
- Nicholson, K. L., S. M. Arthur, J. S. Horne, E. O. Garton, and P. A. Del Vecchio. 2016. Modeling caribou movements: seasonal ranges and migration routes of the Central Arctic Herd. *PLoS One* 11(4): e0150333. doi:10.1371/journal.pone.0150333.
- Noel, L. E. 1999. Calving caribou distribution in the Teshekpuk Lake area, June 1998. Data report for BP Exploration (Alaska) Inc., Anchorage, by LGL Alaska Research Associates, Inc., Anchorage. 31 pp.
- Noel, L. E. 2000. Calving caribou distribution in the Teshekpuk Lake area, June 1999. Report for BP Exploration (Alaska) Inc., Anchorage, by LGL Alaska Research Associates, Inc., Anchorage. 29 pp.
- Noel, L. E., and J. C. George. 2003. Caribou distribution during calving in the northeast National Petroleum Reserve–Alaska, June 1998 to 2000. *Rangifer*, Special Issue 14: 283–292.
- NSSI. 2013. North Slope Science Initiative land-cover mapping summary report. Report for NSSI by Ducks Unlimited, Inc., Rancho Cordova, CA. 51 pp. + maps.
- Parrett, L. S. 2007. Summer ecology of the Teshekpuk caribou herd. M.S. thesis, University of Alaska, Fairbanks. 149 pp.
- Parrett, L. S. 2009. Unit 26A, Teshekpuk caribou herd. Pages 271–298 in P. Harper, editor. Caribou management report of survey and inventory activities, 1 July 2006–30 June 2008. Federal Aid in Wildlife Restoration Project 3.0, Alaska Department of Fish and Game, Juneau.
- Parrett, L. S. 2013. Unit 26A, Teshekpuk Caribou Herd. Pages 314–355 in P. Harper, editor. Caribou management report of survey and inventory activities, 1 July 2010–30 June 2012. Alaska Department of Fish and Game, Species Management Report ADF&G/DWC/SMR-2013-3, Juneau.

- Parrett, L. S. 2015a. Unit 26A, Teshekpuk caribou herd. Chapter 17 in P. Harper and L. A. McCarthy, editors. Caribou management report of survey and inventory activities, 1 July 2012–30 June 2014. Alaska Department of Fish and Game, Species Management Report ADF&G/DWC/SMR-2015-4, Juneau.
- Parrett, L. S. 2015b. Summary of Teshekpuk Caribou Herd photocensus conducted July 6, 2015. State of Alaska memorandum, Department of Fish and Game, Division of Wildlife Conservation (Northwest), Fairbanks. 6 pp.
- Pebesma, E. J. 2004. Multivariate geostatistics in S: the *gstat* package. *Computers & Geosciences* 30: 683–691.
- Pedersen, S. 1995. Nuiqsut. Chapter 22 in J. A. Fall and C. J. Utermohle, editors. An investigation of the sociocultural consequences of Outer Continental Shelf development in Alaska, Vol. V: Alaska Peninsula and Arctic. Technical Report No. 160, OCS Study MMS 95-014, Minerals Management Service, Anchorage.
- Pennycuik, C. J., and D. Western. 1972. An investigation of some sources of bias in aerial transect sampling of large mammal populations. *East African Wildlife Journal* 10: 175–191.
- Person, B. T., A. K. Prichard, G. M. Carroll, D. A. Yokel, R. S. Suydam, and J. C. George. 2007. Distribution and movements of the Teshekpuk caribou herd, 1990–2005: prior to oil and gas development. *Arctic* 60: 238–250.
- Philo, L. M., G. M. Carroll, and D. A. Yokel. 1993. Movements of caribou in the Teshekpuk Lake Herd as determined by satellite tracking, 1990–1993. North Slope Borough Department of Wildlife Management, Barrow; Alaska Department of Fish and Game, Barrow; and U.S. Department of Interior, Bureau of Land Management, Fairbanks. 60 pp.
- Prichard, A. K., D. A. Yokel, C. L. Rea, B. T. Person, and L. S. Parrett. 2014. The effect of frequency of telemetry locations on movement-rate calculations in arctic caribou. *Wildlife Society Bulletin* 38: 78–88.
- Prichard, A. K., M. J. Macander, J. H. Welch, and B. E. Lawhead. 2017. Caribou monitoring study for the Alpine Satellite Development Program, 2015 and 2016. Twelfth annual report for ConocoPhillips Alaska, Inc., Anchorage, by ABR, Inc., Fairbanks. 62 pp.
- Prichard, A. K., M. J. Macander, J. H. Welch, and B. E. Lawhead. 2018a. Caribou monitoring study for the Alpine Satellite Development Program, 2017. Thirteenth annual report for ConocoPhillips Alaska, Inc., Anchorage, by ABR, Inc., Fairbanks. 63 pp.
- Prichard, A. K., J. H. Welch, and B. E. Lawhead. 2018b. Mammal surveys in the Greater Kuparuk Area, northern Alaska, 2017. Report for ConocoPhillips Alaska, Inc., Anchorage, by ABR, Inc., Fairbanks. 52 pp.
- Prichard, A. K., M. J. Macander, J. H. Welch, and B. E. Lawhead. *In preparation*. Caribou monitoring study for the Bear Tooth Unit, 2017. Annual report for ConocoPhillips Alaska, Inc., Anchorage, by ABR, Inc., Fairbanks.
- R Core Team. 2017. The R Project for statistical computing. R Foundation for Statistical Computing, Vienna, Austria. Available online: <http://www.R-project.org/> (accessed 16 February 2018).
- Riggs, G. A., and D. K. Hall. 2015. MODIS snow products Collection 6 user guide. National Snow and Ice Data Center. Available online: <https://nsidc.org/sites/nsidc.org/files/files/MODIS-snow-user-guide-C6.pdf> (accessed 16 February 2018).
- Rouse, J. W., R. H. Haas, J. A. Schell, and D. W. Deering. 1973. Monitoring vegetation systems in the Great Plains with ERTS. Third Earth Resources Technology Satellite Symposium, Greenbelt, MD, NASA (SP-351) 1: 309–317.
- Russell, D. E., A. M. Martell, and W. A. C. Nixon. 1993. Range ecology of the Porcupine caribou herd in Canada. *Rangifer*, Special Issue 8. 167 pp.

- Salomonson, V. V., and I. Appel. 2004. Estimating fractional snow cover from MODIS using the normalized difference snow index. *Remote Sensing of Environment* 89: 351–360.
- Sappington, J., K. M. Longshore, and D. B. Thompson. 2007. Quantifying landscape ruggedness for animal habitat analysis: a case study using bighorn sheep in the Mojave Desert. *Journal of Wildlife Management* 71: 1419–1426.
- Schaaf, C. and Z. Wang. 2015. MCD43A4 MODIS/Terra+Aqua BRDF/Albedo Nadir BRDF Adjusted Ref Daily L3 Global - 500m V006. Distributed by NASA EOSDIS Land Processes DAAC, <https://doi.org/10.5067/MODIS/MCD43A4.006>
- Sellers, P. J. 1985. Canopy reflectance, photosynthesis, and transpiration. *International Journal of Remote Sensing* 21: 143–183. [original not seen; cited in Hope et al. 1993]
- SRB&A. 2017. Nuiqsut caribou subsistence monitoring project: results of Year 8 hunter interviews and household harvest surveys. Report for ConocoPhillips Alaska, Inc., Anchorage, by Stephen R. Braund & Associates, Anchorage. 47 pp. + appendices.
- Stow, D. A., A. Hope, D. McGuire, D. Verbyla, J. Gamon, F. Huemmrich, S. Houston, C. Racine, M. Sturm, K. Tape, L. Hinzman, K. Yoshikawa, C. Tweedie, B. Noyle, C. Silapaswan, D. Douglas, B. Griffith, G. Jia, H. Epstein, D. Walker, S. Daeschner, A. Pertersen, L. Zhou, and R. Myneni. 2004. Remote sensing of vegetation and land-cover change in arctic tundra ecosystems. *Remote Sensing of Environment* 89: 281–308.
- Walker, H. J. 1983. Guidebook to permafrost and related features of the Colville River delta, Alaska. Guidebook 2. Alaska Division of Geological and Geophysical Surveys, Anchorage. 34 pp.
- Walker, H. J., and H. H. Morgan. 1964. Unusual weather and riverbank erosion in the delta of the Colville River, Alaska. *Arctic* 17: 41–47.
- Weladji, R. B., G. Steinheim, Ø. Holand, S. R. Moe, T. Almøy, and T. Ådnøy. 2003. Use of climatic data to assess the effect of insect harassment on the autumn weight of reindeer (*Rangifer tarandus*) calves. *Journal of Zoology* 260: 79–85.
- White, R. G., B. R. Thomson, T. Skogland, S. J. Person, D. E. Russell, D. F. Holleman, and J. R. Luick. 1975. Ecology of caribou at Prudhoe Bay, Alaska. Pages 151–201 in J. Brown, editor. *Ecological investigations of the tundra biome in the Prudhoe Bay region, Alaska*. Biological Papers of the University of Alaska, Special Report No. 2, Fairbanks.
- Wilson, R. R., A. K. Prichard, L. S. Parrett, B. T. Person, G. M. Carroll, M. A. Smith, C. L. Rea, and D. A. Yokel. 2012. Summer resource selection and identification of important habitat prior to industrial development for the Teshekpuk caribou herd in northern Alaska. *PLoS One* 7(11): e48697. doi:10.1371/journal.pone.0048697.
- Wolfe, S. A. 2000. Habitat selection by calving caribou of the Central Arctic Herd, 1980–95. M.S. thesis, University of Alaska, Fairbanks. 83 pp.
- Yokel, D. A., A. K. Prichard, G. Carroll, L. Parrett, B. Person, and C. Rea. 2009. Teshekpuk caribou herd movement through narrow corridors around Teshekpuk Lake, Alaska. *Alaska Park Science* 8(2): 64–67.
- Zuur, A. F., E. N. Ieno, N. J. Walker, A. A. Saveliev, and G. M. Smith. 2009. *Mixed-effects models and extensions in ecology with R*. Springer, New York, NY. 574 pp.

Appendix A. Cover-class descriptions of the NPRA earth-cover classification (BLM and Ducks Unlimited 2002).

| Cover Class | Description |
|---|---|
| Clear Water | Fresh or saline waters with little or no particulate matter. Clear waters typically are deep (>1 m). This class may contain small amounts of <i>Arctophila fulva</i> or <i>Carex aquatilis</i> , but generally has <15 surface coverage by these species. |
| Turbid Water | Waters that contain particulate matter or shallow (<1 m), clear waterbodies that differ spectrally from Clear Water class. This class typically occurs in shallow lake shelves, deltaic plumes, and rivers and lakes with high sediment loads. Turbid waters may contain small amounts of <i>Arctophila fulva</i> or <i>Carex aquatilis</i> , but generally have <15 surface coverage by these species. |
| <i>Carex aquatilis</i> | Associated with lake or pond shorelines and composed of 50–80 clear or turbid water >10 cm deep. The dominant species is <i>Carex aquatilis</i> . Small percentages of <i>Arctophila fulva</i> , <i>Hippuris vulgaris</i> , <i>Potentilla palustris</i> , and <i>Caltha palustris</i> may be present. |
| <i>Arctophila fulva</i> | Associated with lake or pond shorelines and composed of 50–80 clear or turbid water >10 cm deep. The dominant species is <i>Arctophila fulva</i> . Small percentages of <i>Carex aquatilis</i> , <i>Hippuris vulgaris</i> , <i>Potentilla palustris</i> , and <i>Caltha palustris</i> may be present. |
| Flooded Tundra– Low-centered Polygons | Polygon features that retain water throughout the summer. This class is composed of 25–50 water; <i>Carex aquatilis</i> is the dominant species in permanently flooded areas. The drier ridges of polygons are composed mostly of <i>Eriophorum russeolum</i> , <i>E. vaginatum</i> , <i>Sphagnum</i> spp., <i>Salix</i> spp., <i>Betula nana</i> , <i>Arctostaphylos</i> spp., and <i>Ledum palustre</i> . |
| Flooded Tundra– Non-patterned | Continuously flooded areas composed of 25–50 water. <i>Carex aquatilis</i> is the dominant species. Other species may include <i>Hippuris vulgaris</i> , <i>Potentilla palustris</i> , and <i>Caltha palustris</i> . Non-patterned class is distinguished from low-centered polygons by the lack of polygon features and associated shrub species that grow on dry ridges of low-centered polygons. |
| Wet Tundra | Associated with areas of super-saturated soils and standing water. Wet tundra often floods in early summer and generally drains of excess water during dry periods, but remains saturated throughout the summer. It is composed of 10–25 water; <i>Carex aquatilis</i> is the dominant species. Other species may include <i>Eriophorum angustifolium</i> , other sedges, grasses, and forbs. |
| Sedge/Grass Meadow | Dominated by the sedge family, this class commonly consists of a continuous mat of sedges and grasses with a moss and lichen understory. The dominant species are <i>Carex aquatilis</i> , <i>Eriophorum angustifolium</i> , <i>E. russeolum</i> , <i>Arctagrostis latifolia</i> , and <i>Poa arctica</i> . Associated genera include <i>Cassiope</i> spp., <i>Ledum</i> spp., and <i>Vaccinium</i> spp. |
| Tussock Tundra | Dominated by the tussock-forming sedge <i>Eriophorum vaginatum</i> . Tussock tundra is common throughout the arctic foothills north of the Brooks Range and may be found on well-drained sites in all areas of the NPRA. Cottongrass tussocks are the dominant landscape elements and moss is the common understory. Lichen, forbs, and shrubs are also present in varying densities. Associated genera include <i>Salix</i> spp., <i>Betula nana</i> , <i>Ledum palustre</i> , and <i>Carex</i> spp. |
| Moss/Lichen | Associated with low-lying lakeshores and dry sandy ridges dominated by moss and lichen species. As this type grades into a sedge type, graminoids such as <i>Carex aquatilis</i> may increase in cover, forming an intermediate zone. |
| Dwarf Shrub | Associated with ridges and well-drained soils and dominated by shrubs <30 cm in height. Because of the relative dryness of the sites on which this cover type occurs, it is the most species-diverse class. Major species include <i>Salix</i> spp., <i>Betula nana</i> , <i>Ledum palustre</i> , <i>Dryas</i> spp., <i>Vaccinium</i> spp., <i>Arctostaphylos</i> spp., <i>Eriophorum vaginatum</i> , and <i>Carex aquatilis</i> . This class frequently occurs over a substrate of tussocks. |

Appendix A. Continued.

| Cover Class | Description |
|-------------------------|--|
| Low Shrub | Associated with small streams and rivers, but also occurs on hillsides in the southern portion of the NPRA. This class is dominated by shrubs 0.3–1.5 m in height. Major species include <i>Salix</i> spp., <i>Betula nana</i> , <i>Alnus crispa</i> , and <i>Ledum palustre</i> . |
| Dunes/Dry Sand | Associated with streams, rivers, lakes and coastal beaches. Dominated by dry sand with <10 vegetative cover. Plant species may include <i>Poa</i> spp., <i>Salix</i> spp., <i>Astragalus</i> spp., <i>Carex</i> spp., <i>Stellaria</i> spp., <i>Arctostaphylos</i> spp., and <i>Puccinellia phryganodes</i> . |
| Sparsely Vegetated | Occurs primarily along the coast in areas affected by high tides or storm tides, in recently drained lake or pond basins, and in areas where bare mineral soil is being recolonized by vegetation. Dominated by non-vegetated material with 10–30 vegetative cover. The vegetation may include rare plants, but the most common species include <i>Stellaria</i> spp., <i>Poa</i> spp., <i>Salix</i> spp., <i>Astragalus</i> spp., <i>Carex</i> spp., <i>Arctostaphylos</i> spp., and <i>Puccinellia phryganodes</i> . |
| Barren Ground/ Other | Associated with river and stream gravel bars, mountainous areas, and human development. Includes <10 vegetative cover. May incorporate dead vegetation associated with salt burn from ocean water. |

Appendix B. Snow depth (cm) and cumulative thawing degree-days ($^{\circ}\text{C}$ above freezing) at the Kuparuk airstrip, 1983–2018.

| Year | Snow Depth (cm) | | | Cumulative Thawing Degree-days ($^{\circ}\text{C}$) | | | | | | |
|-------------------|-----------------|--------|-----------------|---|-----------|-----------|------------|-----------|------------|-------------|
| | 1 April | 15 May | 31 May | 1–15 May | 16–31 May | 1–15 June | 16–30 June | 1–15 July | 16–31 July | 1–15 August |
| 1983 | 10 | 5 | 0 | 0 | 3.6 | 53.8 | 66.2 | 74.7 | 103.8 | 100.3 |
| 1984 | 18 | 15 | 0 | 0 | 0 | 55.6 | 75.3 | 122.8 | 146.4 | 99.5 |
| 1985 | 10 | 8 | 0 | 0 | 10.3 | 18.6 | 92.8 | 84.7 | 99.4 | 100.0 |
| 1986 | 33 | 20 | 10 | 0 | 0 | 5.0 | 100.8 | 112.2 | 124.7 | 109.4 |
| 1987 | 15 | 8 | 3 | 0 | 0.6 | 6.7 | 61.4 | 112.2 | 127.8 | 93.1 |
| 1988 | 10 | 5 | 5 | 0 | 0 | 16.7 | 78.1 | 108.3 | 143.1 | 137.5 |
| 1989 | 33 | – | 10 ^a | 0 | 5.6 | 20.6 | 109.4 | 214.7 | 168.1 | 215.8 |
| 1990 | 8 | 3 | 0 | 0 | 16.1 | 39.7 | 132.2 | 145.0 | 150.0 | 82.5 |
| 1991 | 23 | 8 | 3 | 0 | 7.8 | 14.4 | 127.6 | 73.3 | 115.0 | 70.6 |
| 1992 | 13 | 8 | 0 | 0.3 | 20.3 | 55.0 | 85.3 | 113.9 | 166.1 | 104.2 |
| 1993 | 13 | 5 | 0 | 0 | 8.6 | 33.6 | 94.4 | 175.8 | 149.7 | 96.1 |
| 1994 | 20 | 18 | 8 | 0 | 4.4 | 49.2 | 51.7 | 149.7 | 175.8 | 222.2 |
| 1995 | 18 | 5 | 0 | 0 | 1.1 | 59.4 | 87.5 | 162.8 | 106.9 | 83.3 |
| 1996 | 23 | 5 | 0 | 8.1 | 41.7 | 86.1 | 121.1 | 138.9 | 168.1 | 95.8 |
| 1997 | 28 | 18 | 8 | 0 | 20.8 | 36.1 | 109.7 | 101.7 | 177.8 | 194.2 |
| 1998 | 25 | 8 | 0 | 3.6 | 45.8 | 74.2 | 135.0 | 158.9 | 184.4 | 174.4 |
| 1999 | 28 | 15 | 10 | 0 | 1.4 | 30.3 | 67.8 | 173.3 | 81.1 | 177.5 |
| 2000 | 30 | 23 | 13 | 0 | 0 | 36.7 | 169.7 | 113.3 | 127.5 | 118.6 |
| 2001 | 23 | 30 | 5 | 0 | 0.8 | 51.9 | 72.2 | 80.0 | 183.9 | 131.7 |
| 2002 | 30 | trace | 0 | 4.2 | 30.3 | 57.8 | 70.3 | 92.2 | 134.4 | 106.1 |
| 2003 | 28 | 13 | trace | 0 | 10.8 | 23.6 | 77.5 | 140.0 | 144.7 | 91.9 |
| 2004 | 36 | 10 | 5 | 0 | 8.9 | 26.4 | 185.6 | 148.1 | 151.4 | 153.3 |
| 2005 | 23 | 13 | 0 | 0 | 2.5 | 14.2 | 78.1 | 67.5 | 79.4 | 176.7 |
| 2006 | 23 | 5 | 0 | 0 | 23.3 | 93.3 | 153.1 | 82.2 | 186.1 | 109.7 |
| 2007 | 25 | 46 | 5 | 0 | 0 | 46.4 | 81.7 | 115.0 | 138.9 | 134.4 |
| 2008 | 20 | 18 | 0 | 0 | 32.8 | 71.7 | 138.9 | 172.2 | 132.5 | 86.1 |
| 2009 | 36 | 13 | 0 | 0 | 16.7 | 71.7 | 44.4 | 142.8 | 126.4 | 133.6 |
| 2010 | 41 | 43 | 13 | 0 | 1.4 | 53.3 | 51.1 | 126.7 | 168.9 | 149.2 |
| 2011 ^a | 25 | 18 | 0 | 0 | 27.8 | 12.5 | 101.2 | 122.4 | 171.6 | 143.2 |
| 2012 ^a | 48 | 53 | 2 | 0 | 1.7 | 26.8 | 137.3 | 140.2 | 195.2 | 143.5 |
| 2013 | 33 | 18 | 2 | 0 | 4.2 | 79.2 | 131.7 | 112.8 | 188.0 | 185.4 |

Appendix B. Continued.

| Year | Snow Depth (cm) | | | Cumulative Thawing Degree-days (°C) | | | | | | |
|------|-----------------|----------------|----------------|-------------------------------------|-----------|-----------|------------|-----------|------------|-------------|
| | 1 April | 15 May | 31 May | 1–15 May | 16–31 May | 1–15 June | 16–30 June | 1–15 July | 16–31 July | 1–15 August |
| 2014 | 33 | 0 ^b | 0 ^b | 11.1 | 4.2 | 28.6 | 82.0 | 127.2 | 102.3 | 67.9 |
| 2015 | 38 | 14 | 3 | 1.4 | 46.4 | 78.9 | 197.2 | 117.9 | 95.7 | 106.9 |
| 2016 | 25 | 0 | 0 | 15.6 | 12.4 | 63.7 | 131.2 | 174.7 | 130.8 | 98.1 |
| 2017 | 36 | 14 | 0 | 0 | 12.1 | 5.2 | 121.3 | 173.4 | 174.5 | 150.5 |
| 2018 | 41 | 20 | 15 | 1.35 | 0 | 6.6 | 47.7 | 137 | 195.9 | 55.25 |
| Mean | 25.6 | 14.4 | 3.3 | 1.3 | 11.8 | 41.8 | 101.9 | 128.0 | 144.9 | 125.0 |

^a Kuparuk weather data were not available for 17 June–9 December 2011, 4–14 August 2012, and 30–31 August 2012, so cumulative TDD for those periods were estimated by averaging Deadhorse and Nuiqsut temperatures (Lawhead and Prichard 2012).

^b Kuparuk airport station reported no snow after 8 May 2014, whereas other weather stations nearby reported snow until 31 May and patchy snow was present in the GKA survey areas into early June. Therefore, if accurate, the airport information was not representative of the study area.

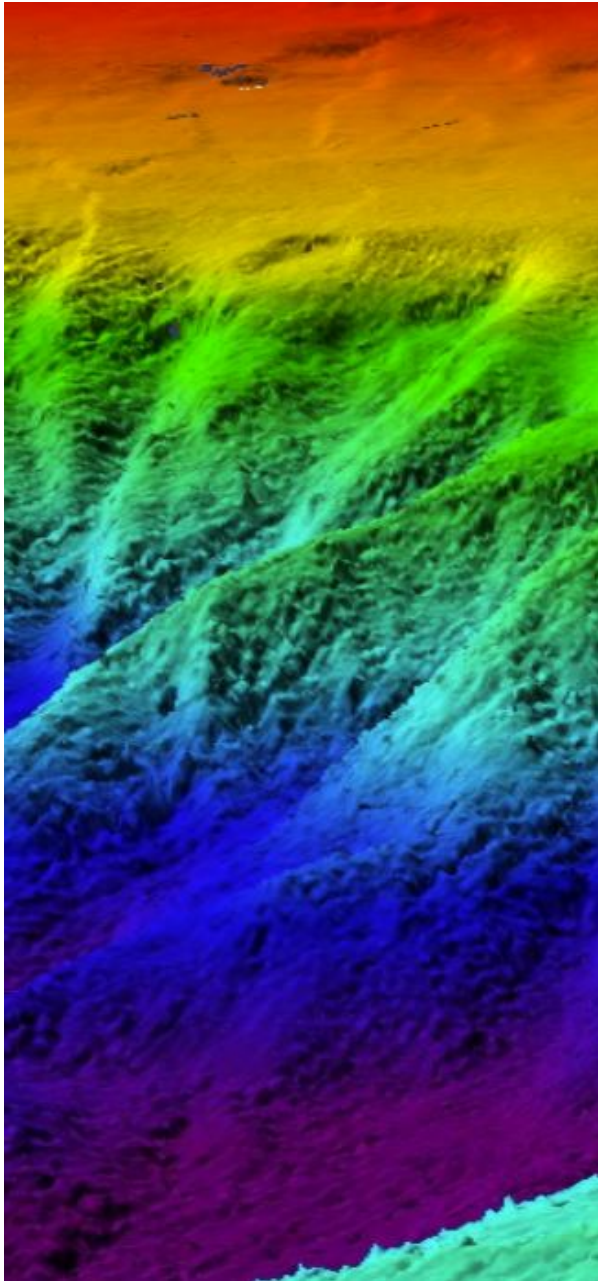
Page intentionally left blank.

Appendix C. 2018 North Slope caribou aerial imagery survey. Survey report submitted by TerraSond, Inc.

Page intentionally left blank.



2018 North Slope Caribou Aerial Imagery Survey



Survey Dates:

Summer and Fall 2018

SURVEY REPORT

Report Date:

January 2, 2019

Submitted to:

ABR Inc



Submitted by:

TerraSond

1617 South Industrial Way, Suite 3
Palmer, AK 99645
907.745-7215

WWW.TERRASOND.COM

QUALITY ASSURANCE

| Date | Rev | Description | Prepared | Checked | Approved |
|----------|-----|--------------|----------|---------|----------|
| 1/2/2019 | 0 | Draft | pt | ew | pt/gj |
| | 1 | Final Report | | | |
| | | | | | |
| | | | | | |

Table of Contents

1 SUMMARY 1

2 OVERVIEW 1

3 IMAGERY OVERVIEW 2

 3.1 Early Summer RGB Imagery..... 2

 3.2 Late Summer Flights..... 3

 3.3 Vertical versus Oblique Imagery in Detection of Caribou 4

4 VARIABLES IN ACQUISITION 6

 4.1 Decreasing Variability 9

5 CONCLUSION.....11

6 NEXT STEP.....11

TABLE OF FIGURES

FIGURE 1 RGB WALDO IMAGE OF CARIBOU TAKEN AT 500 FEET ABOVE THE GROUND IN THE EARLY SUMMER OF 2018. IMAGE SHOWS CARIBOU WITH A VARYING BACKGROUND.4

FIGURE 2 CARIBOU WITH CALVES DELINEATED IN DIFFERENT RELATIVE POSITIONS.8

FIGURE 3 CARIBOU DEPICTED IN LOW RESOLUTION NIR IMAGERY FROM 500 FEET ABOVE THE GROUND USING 3MP CAMERA SYSTEM IN EARLY SUMMER 2018.8

FIGURE 4 NIR OBLIQUE IMAGE (X20 ZOOM) OF CARIBOU TAKEN FROM 1500’ ABOVE THE GROUND AT A SLANT RANGE OF APPROXIMATELY 1-MILE. THE PIXEL RESOLUTION IS APPROXIMATELY 17CM.10

FIGURE 5 RGB IMAGE OF AREA WHERE CARIBOU ARE PRESENT. THE CARIBOU ARE LOST IN THE TUNDRA BACKGROUND.....10

FIGURE 6 GOOGLE IMAGE WITH POINT OF REFERENCE OVERLAY TO DETERMINE THE SLANT RANGE FROM THE CESSNA 207 (POSITION REPORTED USING WAAS GPS DATA) AND THE SUBJECT CARIBOU.....11

FIGURE 7 SECOND IMAGE OF THE SAME CARIBOU GROUP TAKEN FROM A SOUTHERN POSITION AT 1500’ AGL. THE SLANT DISTANCE TO THE CARIBOU WAS ABOUT 4200 FEET WITH A 15CM PIXEL RESOLUTION.13

APPENDICES

A. Additional Figures

1 SUMMARY

During the summer of 2018 TerraSond and ABR, in a collaborative agreement, investigated the feasibility of applying aerial imagery as a tool in the counting of caribou on the North Slope. ABR has provided significant insight into the environmental conditions that make aerial visual counting challenging. TerraSond planned to use this information to apply RGB, NIR, and thermal camera systems as applicable to support the desktop manual count which may later result in automated caribou counts.

During the season, the goal was for TerraSond to install cameras on 70North's Cessna 207 during 5 of the scheduled ABR caribou counting flights. In the early summer flights, TerraSond employed a small array of RGB cameras that produced imagery that clearly indicated that in the early summer RGB imagery could be useful to visually count the caribou in some environments. However, it is believed that the RGB imagery without NIR imagery will not produce results that can assist with automated processing nor will this imagery be useful in the later portions of the year when the caribou color is a very close match to the tundra.

In addition to the RGB camera array, in mid-summer TerraSond employed an array of 3mp NIR cameras that were mounted vertically on the Cessna 207. The purpose was to determine if NIR could be used to differentiate the tundra from the caribou. These cameras produced results that clearly indicated that the NIR imagery had applicability in the counting of caribou and that at least in the mid-summer season the tundra grass has sufficient chlorophyll to produce a contrasting reflectance to the caribou.

Finally, in the late summer early fall, TerraSond mounted the 30mp NIR and an RGB camera in an oblique orientation to determine if the resolution was sufficient and there was significant contrast of the tundra reflectance and caribou when the cameras were not looking directly down on the animals. While there is a level of contrast of the reflectance which could make NIR useful, it was determined that the slant range to the caribou in this orientation and the high variability of the sun angles, glare off the water and snow to make an oblique acquisition unfruitful.

The results of the season's effort indicate that two 30mp NIR cameras and two 30mp RGB cameras mounted in tandem at a speed of 70mph with nearly vertical orientation should on most summer and early fall days generate relatively crisp ~6cm GSD imagery that can be mosaiced and fused to support semi-automated caribou counts for a swath of approximately 1/2 mile.

2 OVERVIEW

The early summer flights TerraSond employed, what we refer to as the "Waldo" camera system that has two 20mp RGB cameras on a fixed angle mount designed to produce minimal overlapping images at 1000 feet above the ground. The cameras were mounted in an orientation that placed one camera in a vertical orientation and the second camera in an oblique orientation. The intent was to determine the usefulness of RGB imagery in the early summer when there was snow on the ground, calves present and the animal's coats light in color compared to the tundra grass. During this early season the pilot operating the "Waldo" with the aircraft at 500 feet above the ground struggled operating the control computer. It was later determined that the computer touch screen was damaged. On the next flight a technician operated the computer and a new touchscreen was installed. While hundreds of images were acquired most of the images did not have animals in the pictures. However, there were a couple

of frames that had clear images with caribou sufficient to answer the questions. These images at approximately 3-4cm GSD were taken at 1/4000th of a second and were relatively crisp and the caribou including the calves could be counted in a slight-oblique orientation using RGB imagery.

During the late summer and early fall, TerraSond installed a 30mp RGB and NIR camera system in an oblique orientation. In the first attempt the crew didn't locate any caribou due to weather conditions. When weather cleared, a second flight was conducted to specifically locate animals. The crew did locate a significant number of caribou with one small group of approximately 20 that remained in the same location while the aircraft flew near them several times. One important observation was that with the airplane operating at 1500 feet, the caribou did not appear to be nearly as aware as when the aircraft had been operated at lower altitudes.

The oblique orientation of the late summer flights produced imagery that was at very high GSD (low pixel resolution). Additionally, the low sun angle and glare off the water created significant problems for the operators to compensate. The result was most of the images were of extremely poor quality. However, there were sufficient images of enough quality to determine that the NIR cameras could (in the right sunlight) produce enough contrast in the oblique orientation to differentiate the caribou from the tundra. However, due to the low resolution, it is believed that the usefulness of this imagery for animal counts is extremely limited.

During these flights the NIR cameras were using a 50mm lens with an 850nm filter with a 40nm wide bypass filter to determine if the wider bypass would support faster shutter speeds allowing the Cessna to operate at faster than 70mph. During these flights the Cessna 207 was operated at approximately 80mph. It is believed that further testing of filters for this purpose is required to develop a clear conclusion. It is unclear if a wider bandpass is needed or what center wavelength is appropriate. However, during the early summer tests with the smaller cameras it was clearly seen that 810nm at 5nm bandpass were effective.

3 IMAGERY OVERVIEW

3.1 Early Summer RGB Imagery

In the month of June TerraSond supported ABR with a Remote Sensing Analyst and 2 camera RGB arrays referred to as the "Waldo" to acquire data of early caribou imagery. During the period of interest, the number of the caribou in the initial area of interest was extremely low, however the ABR crew located an area where a small cluster of animals were present, and the camera was able to acquire a few images with caribou. One specific image Figure 1, was extremely valuable in this survey study. This figure contains 33 caribou and 15 calves with a mixture of backgrounds to include: snow, ice, water, and various shades of tundra grass. Additionally, this image has many cow and calf visual combinations that will help in testing automated algorithms. This single image is the ideal product, in that our technical staff worked with the smallest possible dataset and had a significant variation of conditions. These circles help to delineate the variety of conditions that we were able to capture in this small area. We were fortunate to get the two cows and calves over the small snow-covered area. In Figure 2 the imagery gives examples of calves in various orientations and proximity to the cow, including the cow masking the calf and that calf is near the cow. These will be useful examples for process development.

Additionally, because these images are low angle oblique orientations it does help confirm the potential effectiveness of a two-camera array with cameras mounted at approximately 22-degree off vertical angles.

On the next flight Mr. Teagarden, the remote analyst installed a small multispectral camera system on the aircraft. Flights were flown specifically to find caribou further west. He was successful in locating a small group of caribou and acquired enough images with the 3mp multispectral camera at an altitude of 500 feet to determine if certain filters would be useful. It was determined that the NIR region of the spectrum is useful to differentiate the animals from the tundra grass. However, due to weather and very few caribou, achieving the planned acquisition was not possible.

Figure 3 denotes caribou at approximately 8cm pixel resolution using the 3mp camera image in the NIR spectrum. The tundra has significant tundra chlorophyll reflectance (light gray and white), whereas the caribou have virtually no reflectance (almost black). The application of a higher resolution camera in vertical orientation with a similar filter would, with little doubt, create a very large void of reflectance. Thus, as depicted here, the only requirement would be to differentiate between animals and water (both of which are nearly black). This can be accomplished through RGB imagery and the fact that the reflectance of water in NIR is almost NIL versus the caribou being about 10% reflectance.

3.2 Late Summer Flights

It was determined that the final flight of the season would be using the NIR camera on an oblique orientation. The 30mp camera system was designed for vertical acquisition with a constant distance to the earth's surface and approximately the same light settings during acquisition. However, it was believed important to determine the effectiveness of the camera system in the oblique orientation to collect the same view as the observers in the aircraft. As such, the focus, exposure, shutter speed and gain controls were manual making it very difficult for use with the high variability in oblique configuration. The crew compensated by setting some pre-configurations the day before departing Dead Horse to provide some assistance during the acquisition.

The primary camera for this acquisition was the Lumenera 30mp CCD Near Infrared (NIR) scientific grade camera with a Canon 50mm lens. The second camera was a Lumenera 30mp CCD RGB scientific grade camera with a similar 50mm lens. The NIR camera had 850nm center wavelength bandpass filter with 40nm on either side of the center wavelength. This encompassed from 810nm to 880nm which means the system is accepting significantly more signal and thus noise than the 810nm center wavelength bandpass filter with 5nm on either side of the center wavelength used during the flight that produced the Figure 3 imagery. A change was made to the bandpass filter in order to determine if a wider bandpass filter would still produce a reasonable contrast. The system included a WAAS GPS that recorded the camera's position for each image that was taken.

On September 26, 2018, the flight crew flew in a known area of caribou populations with a camera array including a NIR and RGB imaging system to determine if accurate counts could be obtained using oblique imagery given the very low light angles, potential for ice and snow, and the large areas of water. During the flight, the aircraft was generally flown on routes that placed the camera either looking directly into the sun or with the sun behind the aircraft. The flight crew (the pilot and an observer from ABR) did not have intercom communications with the camera crew which made coordination difficult. The camera was mounted on the right side of the aircraft so that when the aircraft was level the image was just below the horizon and the lower part of the image was about 60 degrees below the horizon which approximates the view that a person can see from the right side of the aircraft. This imaging strategy caused problems for the camera system to develop crisp imagery of the caribou. In addition, and probably even more important was that fact that the highly variable orientation of the body of the caribou and

the relationship of the caribou's body with the earth's surface led to unpredictable textural contrast compared to Figure 3 that was taken as a vertical image. The surface was more predictable in the localized area around each animal. When imagery is taken from above, the caribou's body is more predictable and the distance from the animal's back to the surface of the earth has less than a three-foot deviation. This is desirable with the multispectral imagery giving it a more consistent contrast to the earth's surface.

Additionally, the distance to the ground for most of the area in the camera view was greater than 15cm pixel size which is far too low resolution to clearly differentiate between a caribou and other surface features. Thus, the pixel size at the surface needs to be 6-7cm. This will help prevent motion blur caused by using an airplane and ensure the clear differentiation of caribou versus other surface features. Third, the NIR filters need to be narrower wavelength to reduce the noise causing a far more contrasting signature. From this season's test it was determined that the 810nm was successful, however we should examine other wavelength with similar narrow notch filters perhaps 800nm, 820nm, and 790nm to determine if these may be a better fit.



Figure 1 RGB Waldo Image of Caribou taken at 500 feet above the ground in the early Summer of 2018. Image shows caribou with a varying background.

3.3 Vertical versus Oblique Imagery in Detection of Caribou

Oblique imagery creates some difficulties in performing semi-automated detection of 3D targets. When we look at a 3D caribou against varied background the number of potential variants is virtually limitless. The different angles to view the animal are unlimited and the tundra/snow/ice/water/rock/dirt surfaces generate complexities for the automated recognition. As mentioned earlier, the sun angles and shadows create complexities which can be nearly impossible to compensate for using image processing algorithms. In contrast, the use of vertical imagery produces a very consistent product that has only one angle, the surface. Shadows will be present but because of the consistency of shadows at a given time they will be helpful in the validation that the ground object has a vertical height component.

This report contains two NIR oblique images taken of the same caribou in the same area within 20 minutes of each other. The first NIR image (Figure 4) was acquired while the airplane was at 1500 feet above the ground at a speed of 77 knots. The camera was looking nearly due south into the sun. Both the NIR and the RGB (Figure 5) had extreme difficulty focusing and setting light levels due to the high variability in the light levels and the low sun angles. However, in Figure 4 the NIR imagery does clearly show the small black specs which are caribou at a slant range of 1-mile. The RGB image, even with the soft focus show the difficulty in seeing the caribou against the tundra environment. The second NIR image (Figure 10) is digitally zoomed and clearly shows the presence of caribou with the contrasting reflectance of the chlorophyll versus the hair on the animal.

A Google Earth image (Figure 6) with the yellow pin depicting the GPS location of the airplane at the time both the RGB and NIR images were acquired. The location was verified by the three physical features; the lake in the bottom right of the images, the river on the top of the images, and the lake on top of the images adjacent to the river. The images taken are clearly a match for the mapped area.

Using the Google Earth (Figure 6), the location of the caribou was overlaid, and the ground distance was measured to be 4500 feet. Then using the known aircraft altitude of 1500', the slant range was determined to be approximately 5000' or 1-statute mile. Using this slant range, the approximate pixel size at the surface can be calculated using the following formula: At a pixel size of approximately 16cm, the images have approximately 5 pixels to depict the shape of the caribou. In some cases, with this definition in Figure 4 you can with great effort visually ascertain with some of the black objects the shape of the animal grazing. The only clear indication that these are caribou versus other ground features are the shadows seen next to the caribou and the fact that the flight crew had flown around these animals several times for this acquisition. This resolution would not be acceptable for a population count based on the imagery alone.

3.4 Additional Image from the Same Caribou Group

Thankfully, these caribou remained in the same basic area grazing for nearly 30 minutes as we flew the Cessna 207 near them. This supports the belief that 1500' altitude will reduce the impact to the herd during the aerial acquisitions. In (Figure 7) the image depicts the same caribou group located in the same basic vicinity from a southern orientation with the sun behind the camera. The pixel resolution is virtually the same and the results clearly indicate that the cameras can ascertain the contrast of the caribou from the late Summer to early Fall tundra grass but that a range of nearly a mile in an oblique orientation does not produce an acceptable image for caribou counts. If the camera crew did not know that caribou were present in the images these caribou could have been mistaken for other objects or animals. However, it is believed that with a pixel resolution of approximately 6cm from a vertical orientation that these animals could be clearly delineated.

A Google Image (Figure 8) has been placed in an oblique angle depicting a close approximation of the flight crews view of the area where the caribou group were located. The water features clearly match the imagery and can be used to determine the range to the caribou group as to determine an approximate pixel resolution. In all the range determinations the range indicated was a very conservative estimate. It is possible the actual range could have been as much as 25% more than the slant range indicated.

4 VARIABLES IN ACQUISITION

The 2018 project exposed the significant variability of counting caribou using imagery from a fixed wing airplane. While research projects are designed for such a purpose, this season was extremely difficult due to the number of camera variations that were employed. It was clear that designing a prototype camera without having the ability to flight test prior to using it in the field reduced the effectiveness of our results.

In the application of aerial cameras for the purposes of counting caribou there are eight predominate variables that must be considered:

1. Pixel size on the surface which we will refer to as Ground Sample Distance (GSD). The GSD is an important factor because it is directly related to the size of an object that can be clearly delineated through the imagery. Animals the size of the caribou need several pixels to be able to see the outline of the animal. At 2cm images can clearly see the shape of the animal and one could determine that the animal was perhaps a deer or a caribou. At 6cm one can get a basic shape and see that the animals are likely caribou and by using the relative size you can determine an adult from a calf. Beyond 6cm it is difficult to clearly determine if the image is an animal, particularly using NIR imagery which is simply looking for the lack of chlorophyll reflectance of the grass. As such, it is most desirable to have a GSD of 5-6cm.
2. Camera Orientation: The orientation of the cameras had a significant effect on the imagery products for counting caribou. The most obvious from this season was the effect of the North Slope sun angles. However, beyond this most obvious result was the high variability of the caribou's body orientation in relation to the observer. In an oblique orientation the caribou distance from the camera can be significantly different giving very little relative size and image detail information of the caribou. On a single image, the caribou can be in a portion of the image where the GSD is 20cm and another caribou can be in an area of less than 5cm. Additionally, the oblique imagery can have animals oriented with the entire body perpendicular to the camera or animals facing the lens producing a very small area. In single images you can expect a nearly unlimited amount of variability of animal orientations and relative size in the image making an automated caribou count extremely difficult. Conversely, in the vertical imagery the low sun angle does not change the glare based on the direction of the camera, the animals are always nearly the same relative size because all areas of the images have similar GSD. And because the camera is directly above the animals the only difference in the orientation is the direction the animal is facing. This makes the differentiation of calves and adults significantly easier.
 - a. Vertical - Camera mounted looking down towards the earth.
 - b. Oblique - Camera mounted in an oblique angle that replicates the approximate view of the visual observer outside the airplane windows.
3. Motion Blur - The speed of the camera traveling over the earth's surface in relation to the size of the image GSD. While the camera shutter is open to acquire the image, the airplane must not travel forward more than 50% (industry rule of thumb) of the size of the GSD otherwise the image will have motion blur. Thus, an airplane traveling at 70mph is moving forward at 31.29 meters/second, which equates to 3129 centimeters/second.
4. Camera Shutter Speed - The time that the camera shutter is open allowing light to be collected by the CCD sensor. At 1/1000th of a second a camera mounted on an airplane traveling 70mph or 3129cm/s is traveling 3.129 centimeters while the camera shutter is open.

5. Ambient Light - The ambient light affects the three variables of the camera itself:
 - a. Shutter Speed -As previously discussed there is a direct relationship between the shutter speed at the GSD. The shutter speed is limited by the amount of ambient light in relation to the F-Stop enough light to be acquired to produce a crisp image. There are techniques to help clean the noise produced by a high gain setting. However, in analysis of the data these noise cleaning algorithms can result in erroneous data values.
6. NIR Filter - Most aerial imagery is collecting images in the Red/Blue/Green light spectrum from 400nm to 700nm (nanometers). Above the 700nm there is a region known as the Near Infrared (NIR) from 800nm to 2500nm. This project focused on the 400nm to 900nm region of the light spectrum. A common use of the NIR is in measuring the health of a plant which includes a camera with a NIR filter of around the 800nm wavelength. This reflectance is a result of the chlorophyll that is present and even plants that do not have significant green in the leaves generally have some level of reflectance in the 800nm region. However, different plants have different portions of the NIR where their reflectance is presence. One important consideration for NIR filters is the width of the “bandpass” or the width of the spectrum that the light will be permitted to enter the camera. The narrower the bandpass the more gain that is needed to produce an image. The wider the bandpass the more “environmental noise” that is useless data is collected. It is best to have the narrowest bandpass for reflectance to be collected balanced by the need for light to allow for a shutter speed to prevent motion blur.
7. Altitude and Lens Focal Length - The altitude the airplane flies above the ground and the focal length of the lens are directly related to the GSD or pixel size of the image and the swath coverage, for a camera sensor. One of the objectives for this project was to eventually allow the airplane to fly at an altitude of 1000-1500 feet above the ground and to cover as wide a swath as possible. Preferably 1/2 to 3/4 of a mile. Given the CCD sensor which is 30mp at 1500 feet above the ground with a 40mm lens, it produces a GSD of approximately 6.55cm with swath of 1300 feet, or a quarter of a mile. At 1800 feet, it produces a GSD of 8.73cm and a swath of a third of a mile. The answer for this is to increase the focal length of the lens to 60mm which would decrease the GSD to 5.8cm but would also decrease the swath back to a quarter mile. Thus, when you have a need for a GSD of 6cm and a swath of a half mile the only viable option may be multiple cameras.
8. Camera Array - To acquire a swath of a half mile in a single flight line using vertical or nearly vertical imagery a two-camera array is needed. With a two-camera array mounted approximately 15 degrees of oblique from vertical it is possible to produce nearly a ½ mile swath with 6cm imagery with a slight overlap between the two cameras. While three cameras will produce a slightly wider swath the amount of swath increased is probably not worth the cost of the cameras and increased processing.

Each of these variables play an important factor in producing imagery that can be used in the delineation of caribou from the environmental conditions.



Figure 2 Caribou with calves delineated in different relative positions.

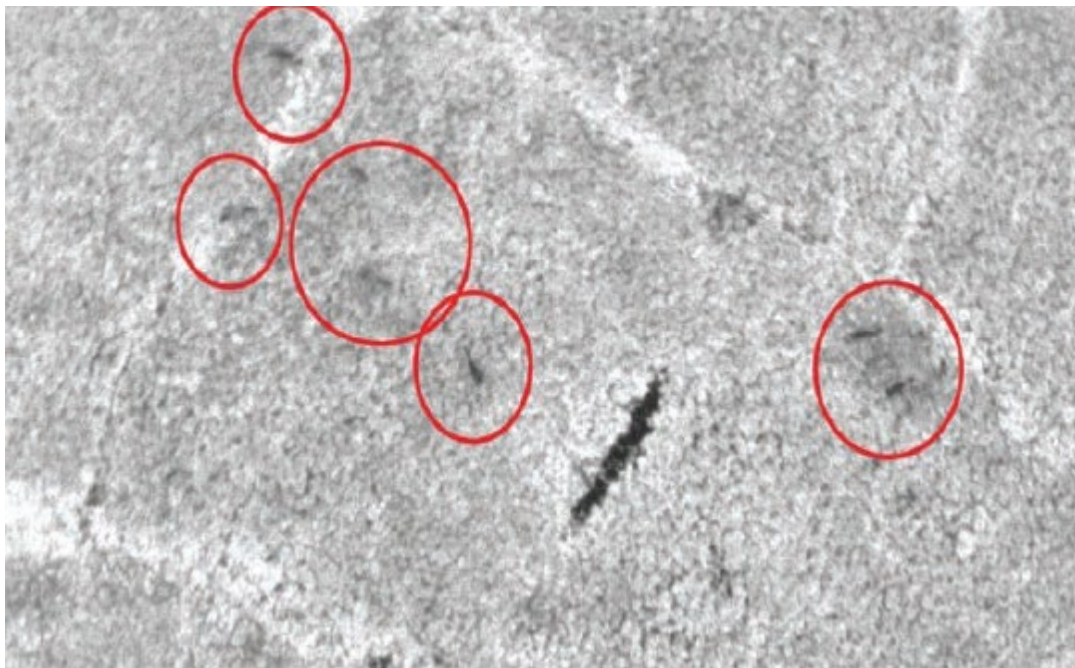


Figure 3 Caribou depicted in low resolution NIR imagery from 500 feet above the ground using 3mp camera system in early Summer 2018.

4.1 Decreasing Variability

After this season it was clear that future work of this type needs to have significantly less variability, as well as flight testing of the camera configurations prior to mounting the camera on an airplane on the North Slope. However, even with the challenges we believe it clear that imagery can be used to generate semi-automatic caribou counts from an altitude above 1300 feet agl acquiring vertical 6cm GSD imagery using two RGB cameras and 2 NIR 30mp cameras with a swath of just under 1/2 mile in conditions that include snow, water, rocky and tundra conditions.

The two variables that we don't have control over is the weather and the speed of the airplane. The weather on the North Slope often has ceilings of 700 foot overcast which is too low for image collection flights at 1500-foot agl. It is believed that a cloud ceiling of 2200 feet would be required. This could interfere with the current scheduled caribou counting flights. Additionally, it is unlikely that future flight testing could be performed in conjunction with the active counting of caribou. The second variable is the speed of the Cessna 207 airplane. Most single fixed-wing airplanes operate safely at 70-80mph. With the low light conditions that are normal for the North Slope, it is difficult for the NIR cameras to be effective at shutter speeds significantly lower than 1/1000th of a second. However, we believe that although there will be some motion blur in the NIR imagery, that when correlated with the RGB should be able to be acquired as a crisp image and the fused product should be very usable.

This season's flights have clearly shown variabilities need to be reduced for a semi-automated caribou count. It would be nice to be able to change one of the variables and achieve a success. We need to have a continuous relationship between the camera lens and the sunlight needs to be as constant as possible by mounting the camera in a vertical orientation. The distance between the camera lens and the earth surface needs to be as constant as possible to increase the clarity of the images and to have the best possible contrast between the caribou and the background features. The NIR filter bypass filter needs to be as narrow as possible to decrease the environmental light noise

$(\text{Sensor Width}(\text{mm}) \times \text{Height Above the Surface}(\text{m}) \times 100) / (\text{Focal Length}(\text{mm}) \times \text{Pixel Image Width}(\text{pixels})) = (35\text{mm} \times 1524\text{m} \times 100) / (50\text{mm} \times 6576(\text{pixels})) = 16.2\text{cm Pixel at Surface}$

The pixel size needs to be between 6cm and 8cm to allow more of the animal's features to be depicted in the images. Additionally, this pixel resolution should prevent motion blur caused by the airplane's 70mph flight speed.

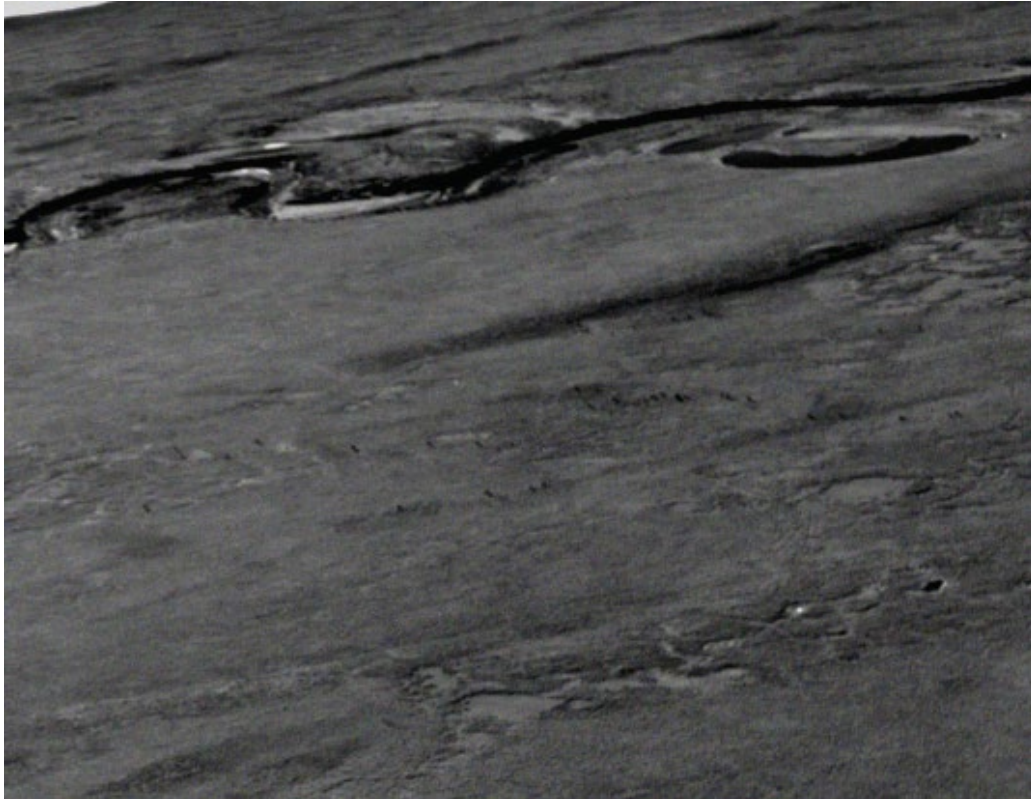


Figure 4 NIR Oblique Image (X20 Zoom) of Caribou taken from 1500' above the ground at a slant range of approximately 1-mile. The pixel resolution is approximately 17cm.

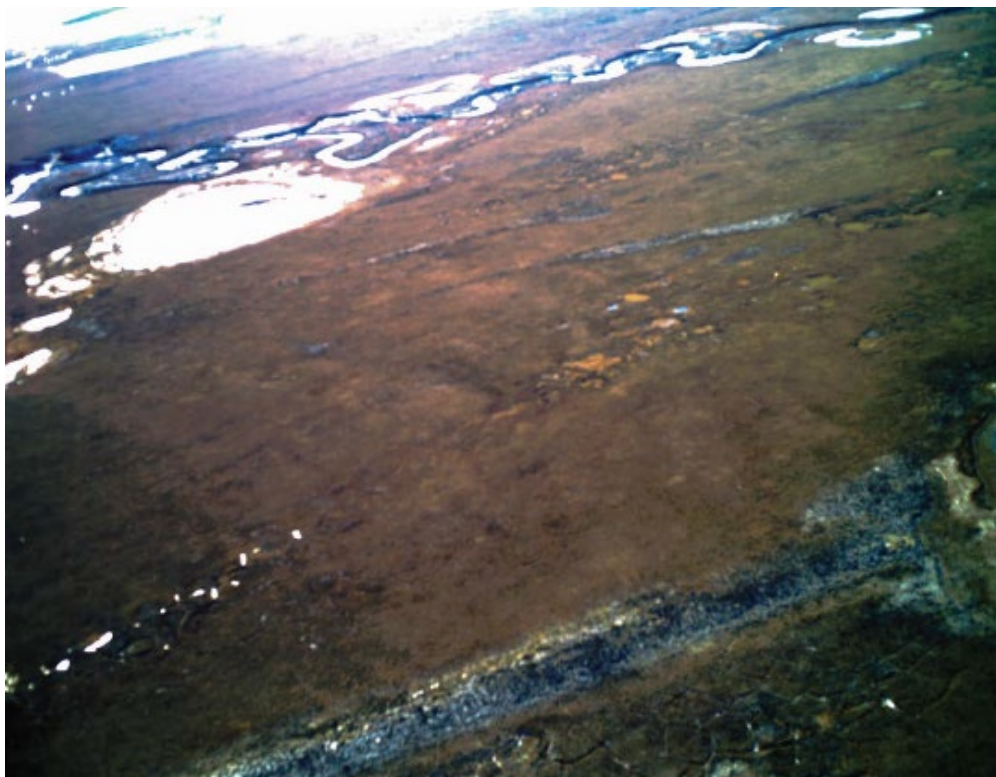


Figure 5 RGB Image of area where caribou are present. The caribou are lost in the tundra background

5 CONCLUSION

This season clearly shows that the NIR camera is a viable approach that should lead to a more automated method of counting caribou. The cameras that were selected for the project appeared to be the right cameras providing the images were taken from a vertical perspective. The prototype camera system that was developed does need some improvements that can easily be done prior to summer 2019. The variables that were outlined in this report have each been explored and it is believed that we may need to continue making small modifications in future work. Except for the NIR filter wavelength and bypass size we have good information that will lead to a successful outcome.

To ultimately acquire a ½ mile swath for an operational mission the system will need to have multiple cameras mounted in an array. While it will take 3 RGB and 3 NIR to achieve the ½ mile swath, we believe that a 2 RGB camera and 2 NIR camera system is more practical and will achieve a reasonable swath. This can be determined in the future. For 2019 testing it is believed that a single RGB and single NIR camera are sufficient to collect the information to make that determination.



Figure 6 Google Image with point of reference overlay to determine the slant range from the Cessna 207 (position reported using WAAS GPS data) and the subject caribou.

6 NEXT STEP

It is believed that it is practical to acquire imagery that can be used for semi-automated and eventually an automated real-time count of caribou over specific transects. Using a single NIR camera mounted vertically to the Cessna 207, at 1500'AGL (+/- 50') with a speed of 70mph (+/- 5 knots) the camera with a 50mm calibrated focus lens should produce crisp NIR images in most summer arctic days with a 7.2cm pixel size. At 70mph the camera lens is traveling across the surface at 36.01m/s, the camera would need a shutter speed of 1/1000th of second to have less than a 50% lens travel forward aircraft travel of 3.6cm during the exposure. This single camera has a swath of ~1200' on the surface. In the future, up to 3 cameras can be placed into an array to produce a collective swath of ~2600' of which most if not all of the swath should

have resolution high enough to be used for counting. The image footprint height would be 800 feet which with a forward flight at 36.01m/s would indicate that the camera could acquire a frame every 4 seconds producing enough overlap to easily mosaic the images for processing. All of this is within the capability of the cameras being used.

This year TerraSond intends to continue prototype camera system development by updating the current system from using a laptop computer connected to each camera to acquire and store the data. This was a very complex installation and led to multiple potential failure points and complexities in operation. Additionally, the operators attempted to focus the lenses based on the range of the oblique imagery which proved to be frustrating with the low sun angles. For future acquisitions, TerraSond plans to use small computers and storage for each of the cameras to allow the control of all the cameras from a single laptop. The lens focusing will be alleviated using laboratory focused lenses with a permanently mounted NIR filter. While there is a cost for this type of lens, we believe it is the best method of producing consistently crisp images at 70 knots at 1650 feet above the ground with a NIR camera.

It is recommended that we schedule 3 flight sessions on the North Slope in 2019 in addition to a series of flight tests in Palmer Alaska to test the system using cattle in lieu of caribou. The flights on the North Slope would be performed over known caribou in different environmental conditions. Obviously, based on the lessons of 2018 this is not always easy.

The camera system should include one 30mp RGB camera and one 30mp NIR camera. The plan will be to begin the tests using the 810nm 5nm bandpass filter that was successful using the small cameras in 2018. Based on the results that filter could be changed over the season to compare results. The 30mp cameras would have 40mm lab focused lenses with the filters permanently mounted. Thus, a change in filter is a change in the lens/filter combination. This combination will not produce the full potential swath but will allow the testing of the system without incurring the cost of two additional cameras and multiple lens combinations.

The aircraft will be operated at altitudes of 1000, 1500, and 2000 feet agl to refine the required GSD required and to determine the effects of motion blur in these conditions. Currently, each camera is connected to a laptop for control and data storage. For 2019, it is planned that each camera would have a small computer located in the camera housing that was developed through the 2018 effort which will increase the reliability of the system. The camera control and storage computers will be connected via ethernet to a laptop that controls and monitors the camera system. finally, in 2019 it is believed that these images should be of such a nature that we can begin examining the algorithms for automated animal counts. In support of this, TerraSond has hired a remote sensing analyst who has a background in mathematically modeling such algorithms.

If 2019 proves to be successful, then it is believed that the cameras can be increased to provide the wider swath. It is conceivable that in 2020 semi-automated counts may be possible.



Figure 7 Second Image of the same caribou group taken from a southern position at 1500' AGL. The slant distance to the caribou was about 4200 feet with a 15cm pixel resolution.

APPENDIX A

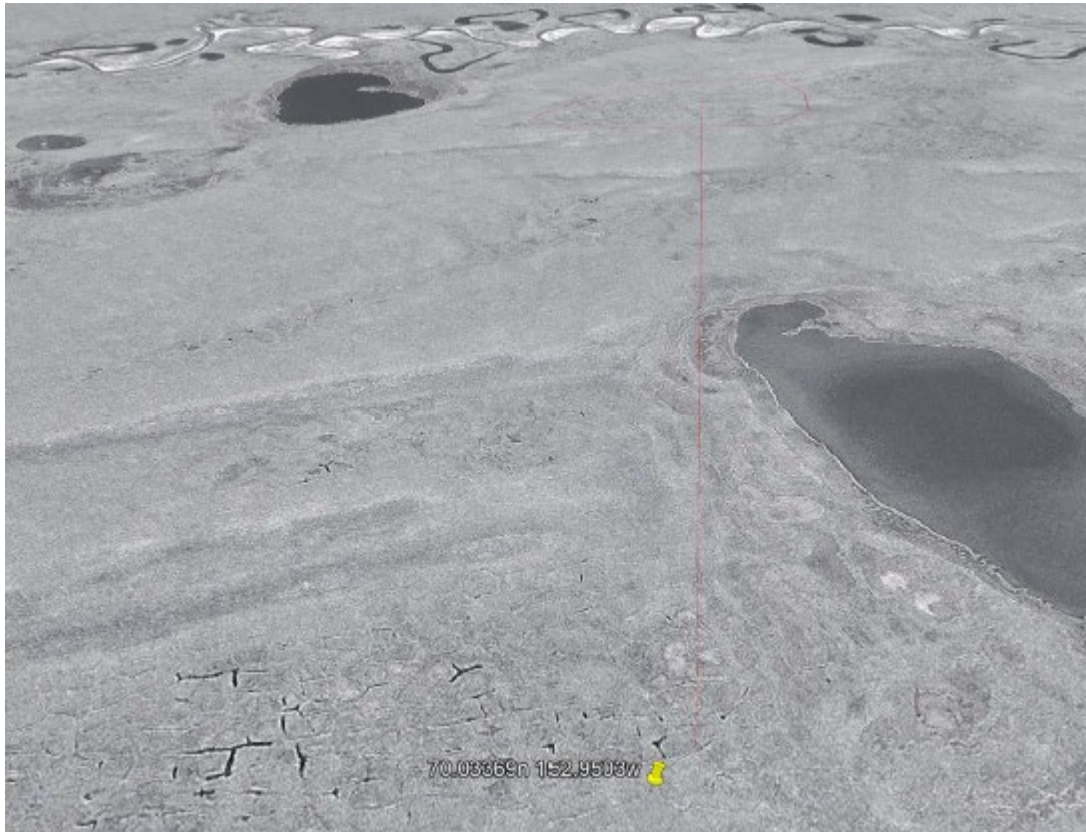


Figure 8. Google Image depicting the approximate slant view from the aircraft taken in the image and the combination of the stream with other water elements clearly depicted in the areas.

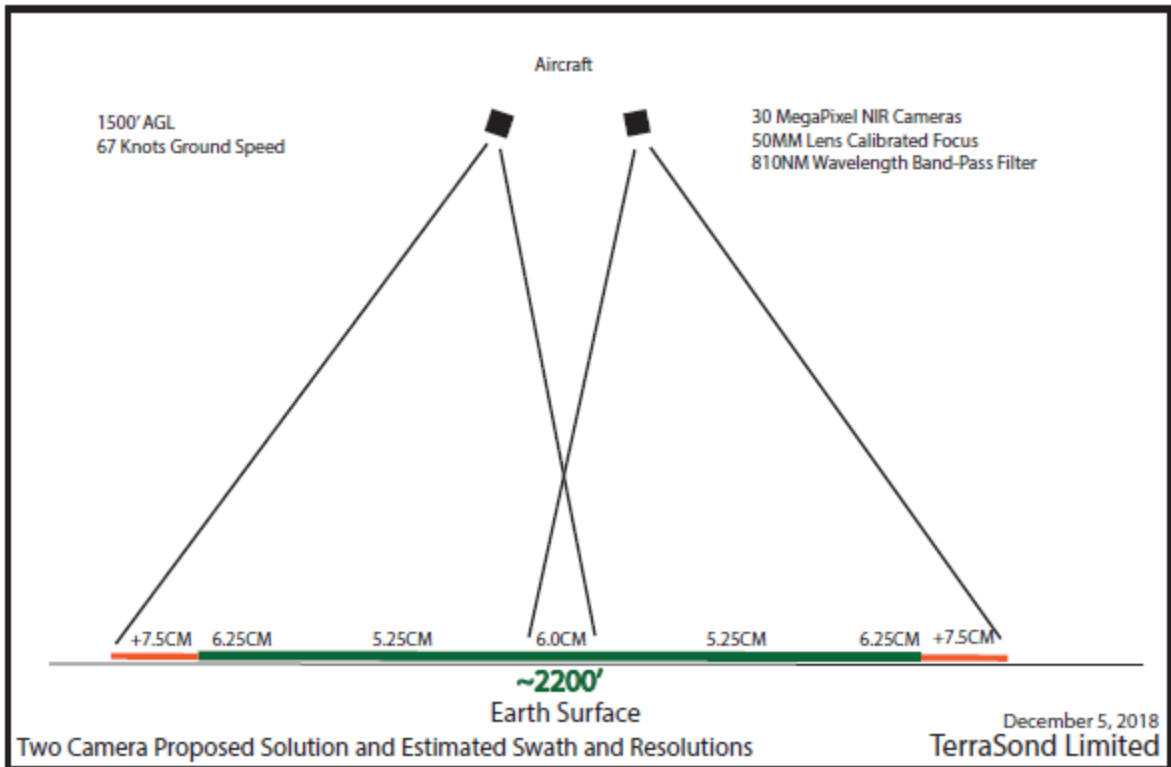
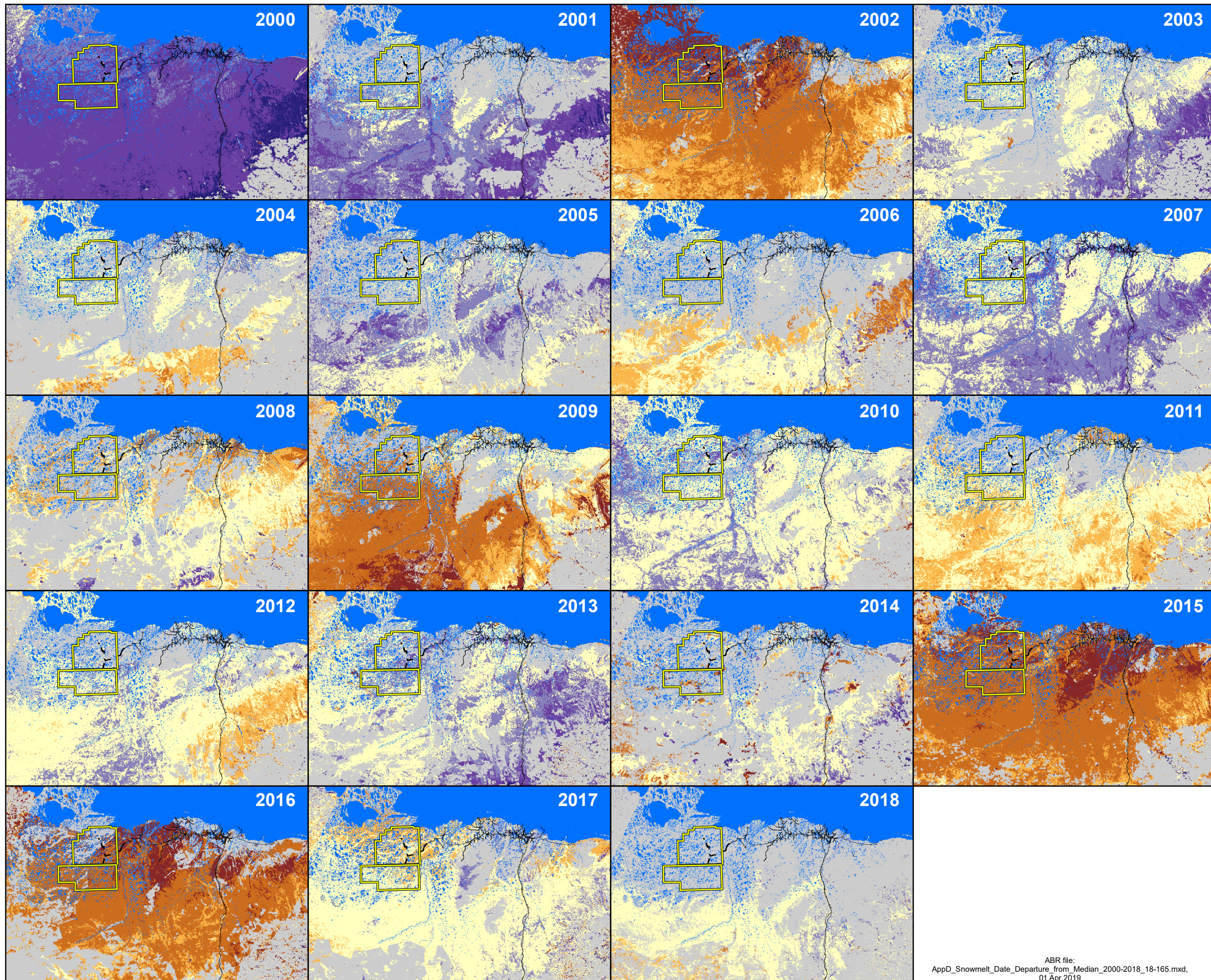


Figure 9. Two RGB and two NIR camera setup with a swath of approximately 2200'.



Timing of Snow Melt

Compared to Median (2000–2018)

- Date not known within one week
- > 14 days earlier than median
- 8–14 days earlier than median
- 4–7 days earlier than median
- Within 3 days of median
- 4–7 days later than median
- 8–14 days later than median
- > 14 days later than median
- >= 50% Water Cover

Aerial Survey Area

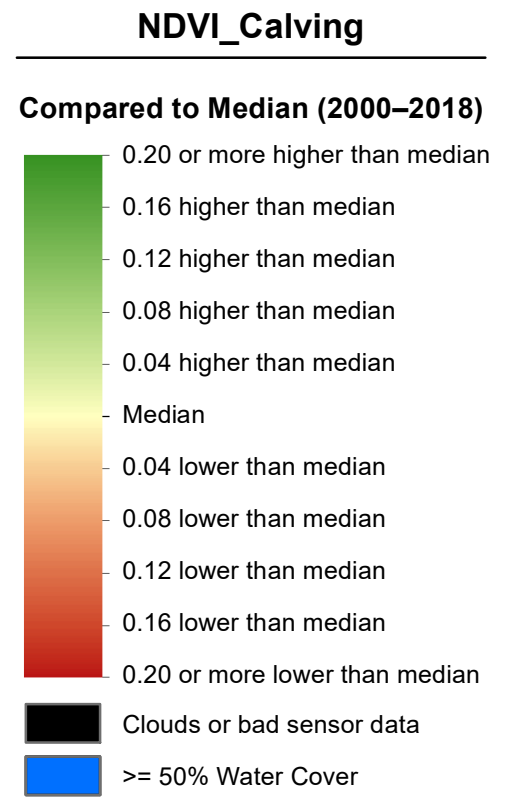
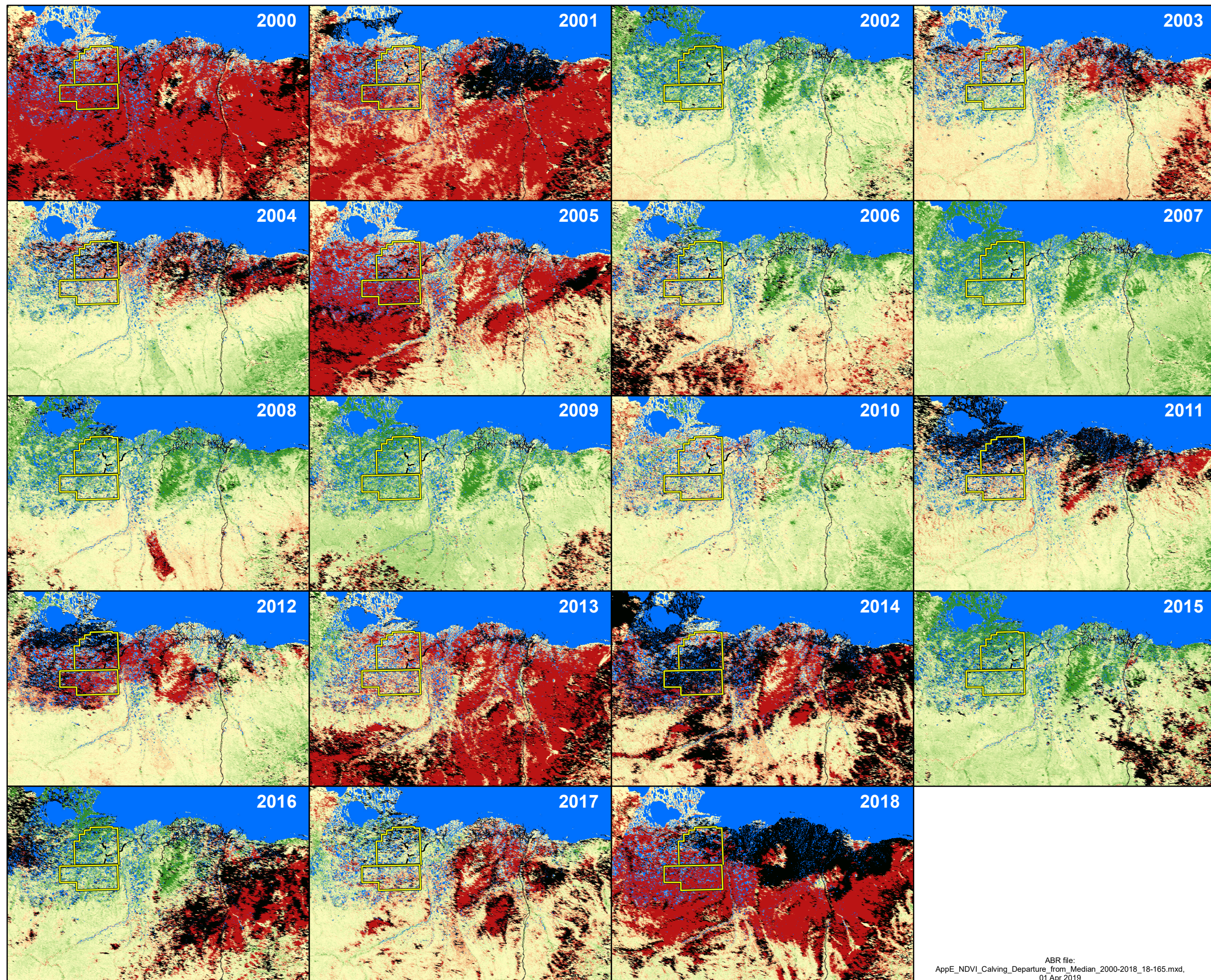



0 20 40 60 80 100 Miles

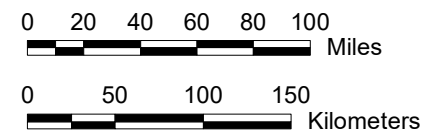
0 50 100 150 Kilometers

Appendix D.
Timing of annual snowmelt (<50% snow cover), compared with median date of snowmelt, on the central North Slope of Alaska during 2000–2018, as estimated from MODIS satellite imagery.

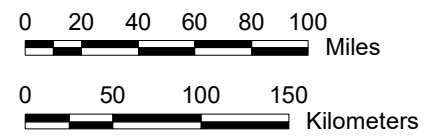
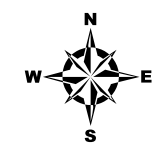
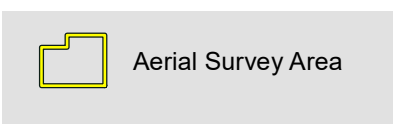
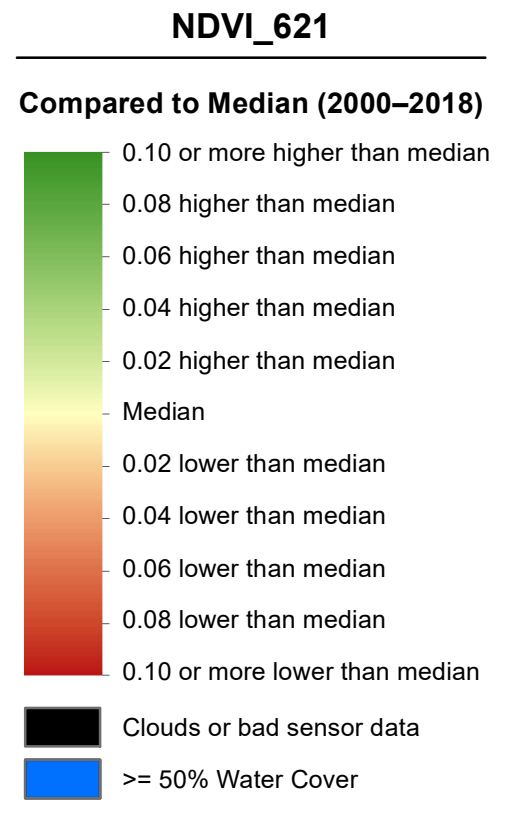
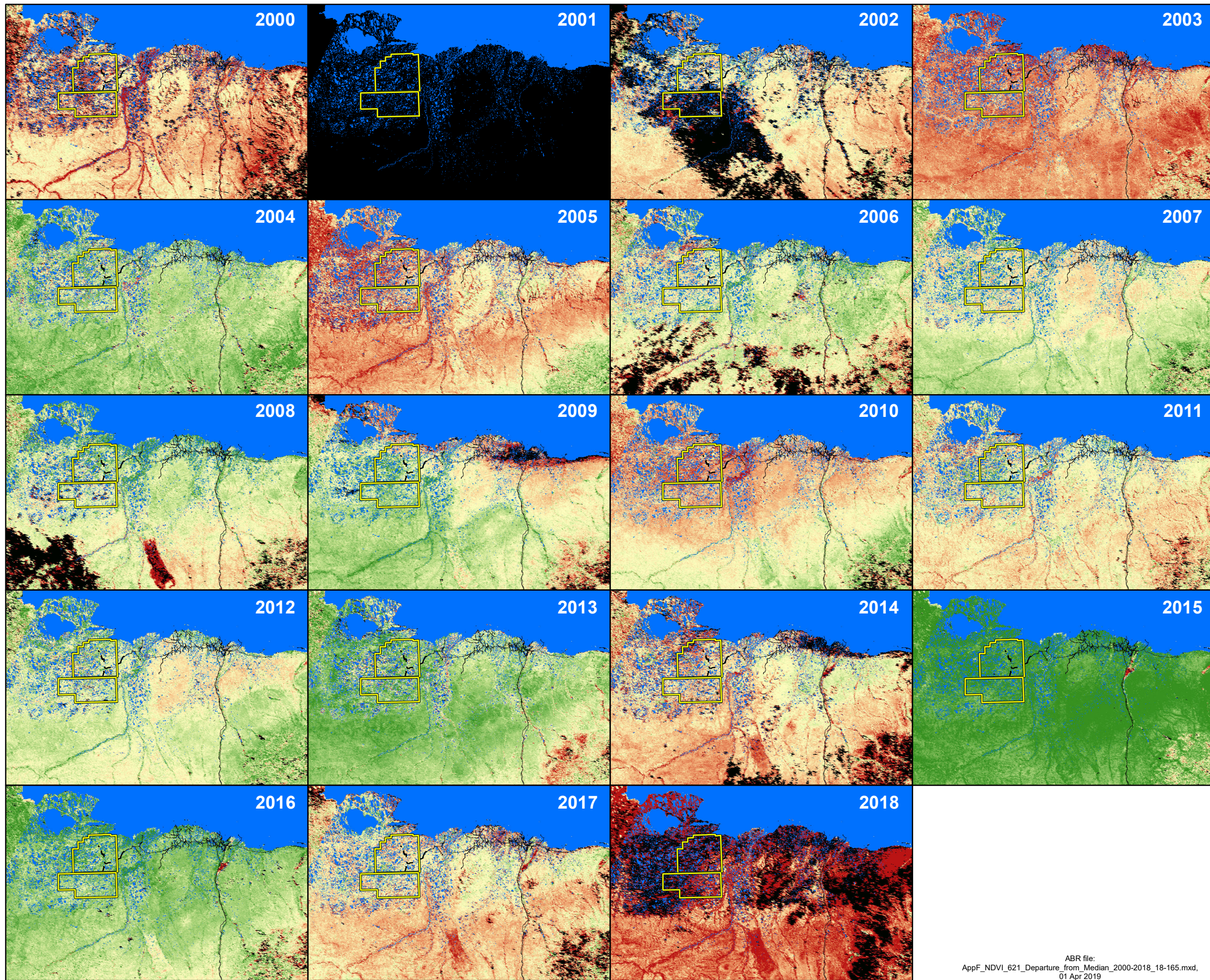
ABR file:
 AppD_Snowmelt_Date_Departure_from_Median_2000-2018_18-165.mxd,
 01 Apr 2019



 Aerial Survey Area

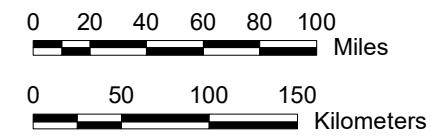
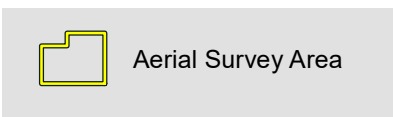
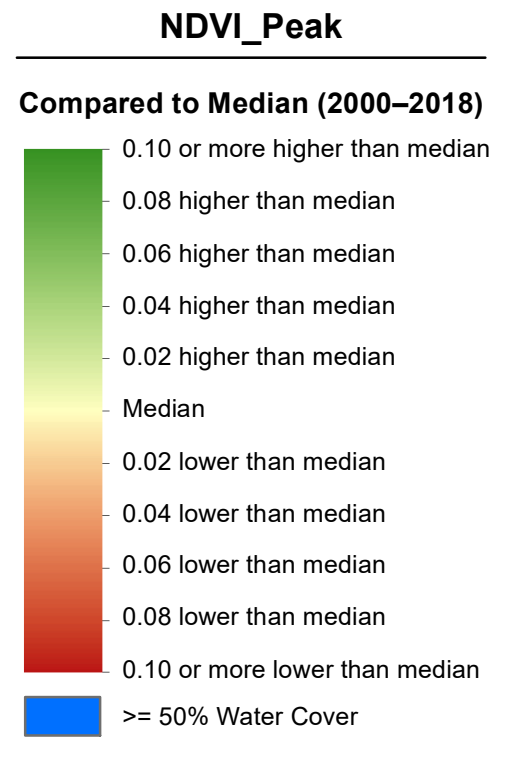
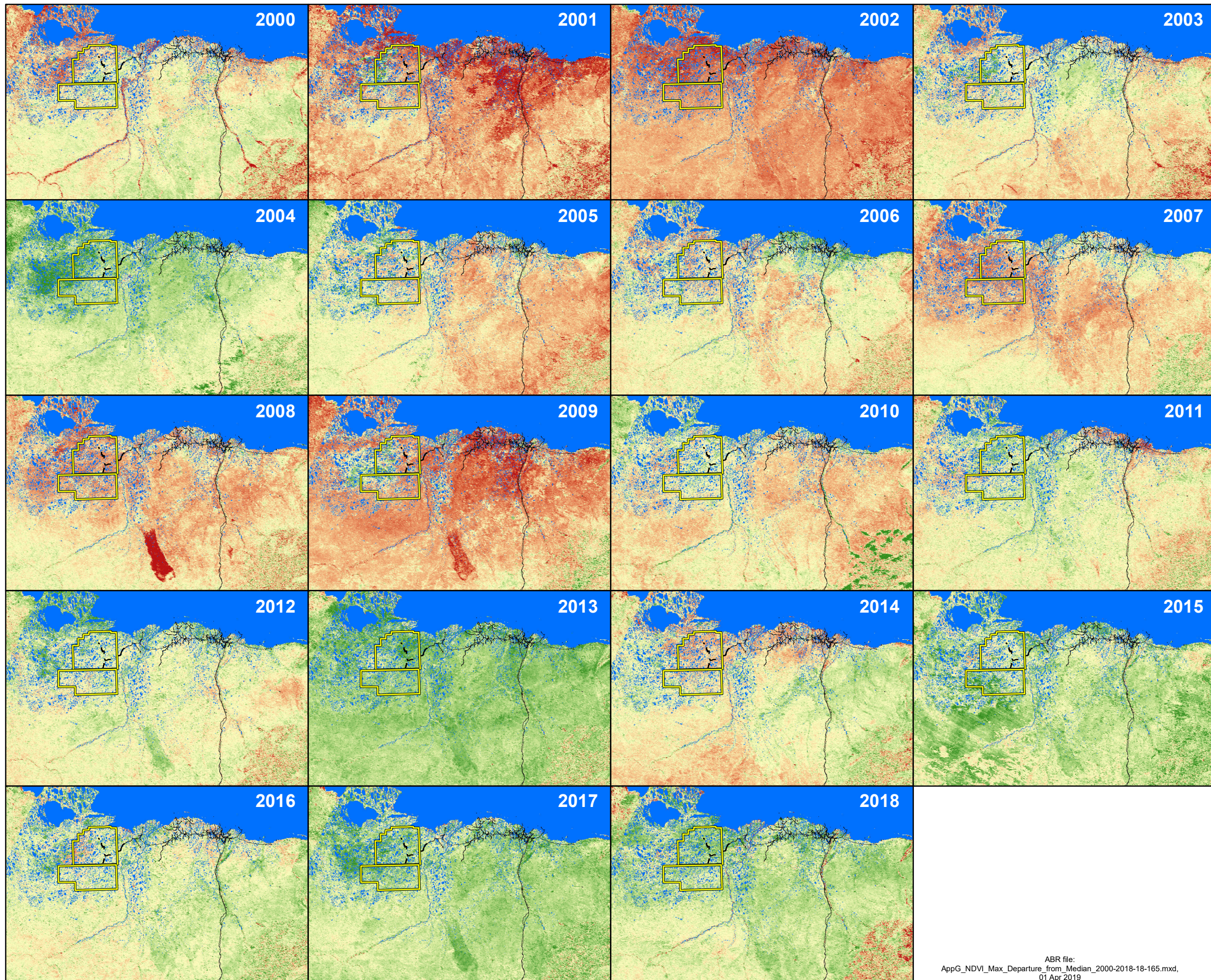


Appendix E.
Differences between annual relative vegetative biomass values and the 2000–2018 median during the caribou calving season (1–10 June) on the central North Slope of Alaska, as estimated from NDVI calculated from MODIS satellite imagery.



Appendix F.
Differences between annual relative vegetative biomass values and the 2000–2018 median at estimated peak lactation for caribou (21 June) on the central North Slope of Alaska, as estimated from NDVI calculated from MODIS satellite imagery.

ABR file:
 AppF_NDVI_621_Departure_from_Median_2000-2018_18-165.mxd,
 01 Apr 2019



Appendix G.
Differences between annual relative vegetative biomass values and the 2000–2018 median for estimated peak biomass on the central North Slope of Alaska, as estimated from NDVI calculated from MODIS satellite imagery.

ABR file:
 AppG_NDVI_Max_Departure_from_Median_2000-2018-18-165.mxd,
 01 Apr 2019